Departamento de Biología Molecular

Facultad de Ciencias

Universidad Autónoma de Madrid

Role of Nrg1 in mouse heart development

Doctoral Thesis

Paula Gómez Apiñániz

Licenciada en Biología, 2013

Universidad Autónoma de Madrid

Director: José Luis de la Pompa Mínguez

Centro Nacional de Investigaciones Cardiovasculares (CNIC)

This work was performed in Dr. José Luis de la Pompa laboratory at the Centro Nacional de Investigaciones Cardiovasculares Carlos III (CNIC) in Madrid.

This study was funded by grants SAF2013-45543-R, SAF2016-78370-R, CB16/11/00399 (CIBER CV) and RD16/0011/0021 (TERCEL) from the Ministerio de Ciencia, Innovación y Universidades, and grants from the Fundación BBVA (Ref.: BIO14_298) and Fundación La Marató (Ref.: 20153431) to JLDLP…

Paula Gómez Apiñániz held a PhD fellowship from MEIC FPI Program with the reference BES-2014-068818.

El éxito es la suma de pequeños esfuerzos que se hacen día tras día

Robert Collier

AGRADECIMIENTOS

Este trabajo no habría sido posible si no hubiera tenido la gran suerte de entrar a formar parte del CNIC, este centro me ha facilitado el acceso a un servicio personal y material de alta calidad que ha sido indispensable para la realización de mi proyecto.

En primer lugar, me quiero dirigir a mi director, **José Luis de la Pompa**, gracias por abrirme las puertas del CNIC. Desde el primer momento que entré a realizar mi proyecto de fin de carrera me has transmitido tu interés y dedicación a la ciencia. Gracias por confiar en mí y hacerme responsable de un proyecto de doctorado tan apasionante. Muchas gracias por tu dedicación durante estos años de doctorado. Gracias por tus consejos de ser crítica y persistente con mi trabajo que, indudablemente, me han ayudado mucho a ir mejorando cada día.

Gracias al programa de doctorado de la UAM que nos ha facilitado poder desarrollar la tesis doctoral en los mejores centros de investigación de Madrid. Gracias a mi tutor Federico Mayor, por mantener el seguimiento de mi trabajo durante estos años de doctorado.

Tuve la enorme suerte de empezar a trabajar en el laboratorio con **Belén Prados**. Gracias Belén por enseñarme tanto, por transmitirme tu criterio y exigencia científica gracias a la cual conseguimos sacar adelante un trabajo estupendo. Aunque nuestros proyectos científicos se separaran, siempre he podido contar contigo para cualquier duda o consejo, e incluso en estos últimos meses de tesis con corrección incluida. Estoy segura de que nos queda mucho por compartir, eres una gran compañera y amiga.

Gracias **Sara,** los lunes eran mucho más fáciles gracias a ti y a todos nuestros cotilleos en el rinconcito. Espero haberte podido ayudar en tu paso por el CNIC y que no olvides todos los momentos tan divertidos que pasamos. Gracias también a **Beatriz Martínez**, ¡mi malagueña preferida! Ha sido un placer coincidir con una persona tan maravillosa como tú, que siempre has querido compartir tu gusto por las manualidades y las plantas con nosotros.

Durante mi primera etapa de estudiante tuve la suerte de tener a los mejores y más divertidos compañeros predoctorales que hicieron que cada día fuera estupendo. Gracias **Guille** porque desde el primer día te preocupaste de que estuviera a gusto y me transmitiste muy buen rollo. Yo creo que mi predilección por los microscopios es gracias a ti. Gracias **Juli** por ser una compañera tan estupenda que nos ha transmitido tanto amor a la ciencia, todos hemos aprendido de tu perseverancia en el trabajo y, a pesar de todo el esfuerzo, siempre estabas preparada para cualquier plan. ¡¡**Gaetanillo**!! ¡Allora! ¡Mi italiano favorito! Desde luego que has sido la alegría de la huerta, cada momento a tu lado me hacía sacar una sonrisa y eso siempre se agradece. Gracias por tantos momentazos inolvidables y por tu enorme apoyo en momentos complicados durante mi proyecto.

Gracias a **Mauro** por enseñarnos el verdadero estilo italiano. Gracias **Lao**, porque también me has hecho pasar momentos muy divertidos. Gracias **Patri** por ayudarme a practicar mi inglés, y por todos los momentos de cotilleo tan divertidos. Gracias a **Ruth**, por tu gran trabajo, has sido una compañera genial con la que he compartido grandes anécdotas, aunque tu estancia fuera cortita. Gracias a nuestros chicos de prácticas **Clara, Diana, Begoña, Paul, Adolfo y Uxue**. ¡Gracias a mi **Bea**! Porque no podríamos compartir más gustos, siempre ha sido un placer compartir el día contigo y mantenernos actualizadas de nuestra vida. Gracias **Tania** por todo lo que he aprendido de ti, por ayudarme a practicar el inglés y aconsejarme sobre cómo debía de explicar mi proyecto y saber interpretar mejor la ciencia.

Y de momento no he hablado de mis actuales compañeros… Gracias **Vane** por tu buen humor y tus ganas de compartir tu día a día con nosotros en las comidas. Gracias **Luis** por preocuparte e interesarte siempre por mi trabajo y por mi vida en general. Siempre me transmites muchos ánimos y estoy encantada de hacerte reír con mis historietas. Gracias **Vanessa Espada** por tu esfuerzo cada día en el laboratorio. Gracias **Vítor** por enseñarnos un poquito de electrofisiología cardiovascular, quizá algún día entendamos todas tus fórmulas. Gracias **Donal** por tus "máster class" de análisis genético de enfermedades valvulares, siempre muy interesantes. Gracias **Quim** por querer volver al labo que te dio las alas en la ciencia, gracias por transmitirme tu entusiasmo por el *live imaging* y querer luchar por conseguir nuevas metas en el laboratorio. Gracias **Abel** porque sin ti ningún proyecto del labo habría sido posible y gracias por ser tan buen compañero. Gracias **Lucía** por compartir con nosotros tu encantadora brujería. Gracias **Ana** por traer tu alegría granaína al laboratorio.

Me quedan mis compis predoctorales a los que deseo mucha suerte en el tiempo que les quede de esta etapa y todo mi ánimo para conseguir sus objetivos. Thanks **Dimitris** because of your amazing knowledge of science and because of transmitting us your huge effort to learn more and improve your research. I am sure you will get it soon and that we will celebrate it together! **Marcos**, siempre has sido un gran apoyo para mí en el laboratorio, quiero agradecerte tu compañerismo y disposición desde el primer día. Sé que siempre puedo contar contigo, sobre todo si es para estar de bares tomando cerves. **Rebe Torregrosa**, la verdad que no tenía yo mucha predilección por Murcia, pero teniendo a murcianas como tú, ¡tiene que ser una ciudad maravillosa! Gracias por dejarme compartir tantos momentos, anécdotas y emociones contigo, ¡gracias por ser una compañera de película! **Ale**, **Ale**, **Ale**, ¡me voy! Jajaja **Ale**, gracias por traer el arte al laboratorio, por ser el alma de El Boss, por compartir momentos tan emocionantes con nosotros y por alegrarnos la vista con tus musculitos. Gracias a **Vera**, por tus estupendas recomendaciones para visitar tus preciosas tierras portuguesas y por la alegría que desprendes a tus compis. Gracias a **Rebe Piñeiro**, porque haces que el acento gallego sea aún más dulce, gracias

por siempre querer compartir conmigo todos tus planes, y gracias por la confianza y cariño que me transmites. Por último, pero no menos importante, gracias a **Tamara**, por lo adorable que eres; me alegro muchísimo de tenerte de compañera ya que siempre encuentro apoyo y risas contigo. ¡Chicos, estoy deseando celebrar vuestras tesis con todos vosotros!

Porque no solo he tenido el privilegio de tener estos grandes compañeros, también quiero acordarme de los demás compis con los que he compartido tantos momentos en el CNIC: Macarena, Brian, Wen, Tania, Noelia, Esther, Jose, Isaac, María, Raquel, Laura, Javi, Carlos…

Además de todos los compañeros del laboratorio, tengo la enorme suerte de que fuera estoy rodeada de las personas más maravillosas e incondicionales que podría soñar.

Gracias a todas mis compis de basket, con las que he compartido tantos momentos durante tantísimos años, siempre tendré un gran recuerdo de esta etapa de equipo tan especial.

Gracias a mis queridísimas "Chicas Marqueríe", porque nuestras quedadas en La Jaima o El 23 (ya que es complicado que lleguemos más lejos…jaja) siempre me alegran el día. Gracias a **Ali**, **Raquel**, **Clea**, **Silvia**, **Noe**, **Patri**, **Aomar** y **Mery**, sois todas maravillosas y gracias a vosotras voy a vivir mucho más por todas las carcajadas que me pego con vosotras. La piscina nos unió y nada nos podrá separar.

Gracias a **Alba**, **Giff**, **Bea**, **Víctor**, **Topi**, **Juan**, **Charlie** y todos los demás pertenecientes al mejor grupo de ingenieros del mundo. Estoy encantada de haberos conocido, de estar cada vez más unidos y de hacer tantos planes "chachis" con vosotros, ¡sois geniales!

Gracias a mis Biólogos Aventureros favoritos: **Jose**, **Pablo**, **Ana** y **María**. Gracias a los 4 por decidir estudiar Biología porque habéis sido los mejores compañeros que haya podido tener. Gracias **Jose** porque siendo más difícil mantener el contacto al salir de la uni, ha sido cuando más nos hemos conocido y más experiencias hemos compartido, sé que he ganado un amigo de verdad contigo. Gracias por tu infinita ayuda, por invitarnos a todos los sitios donde vas, y porque personas como tú hay pocas. **Pablo**, qué suerte de que te cambiaras al turno de mañana porque pude descubrir a un gran amigo. He disfrutado mucho compartiendo contigo todas las fuertes emociones que vivimos con nuestros queridos delfines. Gracias por apreciarme tanto y por hacerme partícipe de cada momento importante de tu vida. "Siempre nos quedará el Zoo". Gracias **Ana**, por ser mi compañera incondicional durante los 5 años de carrera. Gracias porque sé que siempre podré confiar en ti, por mostrarme siempre tu apoyo, por siempre acordarte de mí y por tu entusiasmo para hacer planes juntas. **María**, gracias por ser como eres, por disfrutar tanto de todo lo que tienes, por transmitir toda tu felicidad y hacer que la vida de los que te rodean sea

mejor. Gracias porque siempre puedo contar contigo. Gracias a las dos, por compartir conmigo vuestras vacaciones y habernos hecho unos viajes playeros inolvidables. Quiero que sepáis que nuestras noches de "chicas" son de mis favoritas porque un plan con vosotras siempre es especial.

Gracias a **Laura** y **Javi**, por compartir momentos de pareja tan divertidos y por todos los que nos quedan y que espero que disfrutemos los cuatro juntos. Gracias **Laura** por ser una persona tan especial y por alegrarme las comidas en nuestra vida de laboratorio. ¡Ya queda poquito!

Gracias a mis chicas favoritas, **Ana**, **Laura** y **María**, porque siempre habéis sido especiales, pero en estos últimos años aún más. Todos los recuerdos con vosotras son maravillosos e infinitos. Gracias por hacerme tan feliz, por estar cerca en los buenos y malos momentos, porque siempre puedo contar con vosotras para lo que necesite. Gracias **Laura**, por contar conmigo para noches de terraceo y confidencias, y gracias por redactar las palabras más bonitas del mundo para nosotras cada Nochevieja. Gracias **Ana**, por transmitirme siempre ese buen humor, ese ánimo y esa alegría que me llega nada más verte, gracias por ser como eres y vivir la vida tan intensamente. Gracias **María**, por ser siempre sincera conmigo, por pensar siempre en nosotras para compartir las alegrías y las penas, y porque *FRIENDS* siempre nos una y nos haga las mejores cómplices. Quiero seguir compartiendo todo con vosotras. ¡Sois las mejores amigas que podría tener! Pero no estamos solas las 4 chicas… gracias a esos novios estupendos que habéis encontrado, gracias a **Javi**, **Sergio** y **Fendi**, porque con vosotros los planes son más divertidos. ¡Gracias por cuidar tanto a mis chicas!

Gracias a **Jacoba**, **Daniel**, **Óscar**, **Ana** y **Javier**, por hacerme sentir siempre una más de la familia, por pasar tantos momentos increíbles y por vuestro apoyo incondicional.

GRACIAS a mi **familia** por ser EXTRAORDINARIA.

Gracias a mis abuelos **Mary** e **Hilario**, **Paco** y **Mely** por ser parejas admirables y por crear una familia tan estupenda. Gracias a **Paco**, por querer que consiguiera todo lo que me propusiera. Gracias por querer tanto a tu primera nieta. También quiero compartir esto contigo, como todos mis momentos especiales, porque aún te siento muy cerca. Gracias a yaya **Mely**, por transmitirme tanto entusiasmo por la vida, por ser tan sorprendentemente fuerte y por superarte a ti misma en los peores momentos. ¡Aún nos queda mucho por vivir juntas!

Gracias a mi familia vitoriana, **Javi**, **Natalia**, **Íñigo**, **Irene** e **Íñigo**. Porque desde pequeñita habéis hecho que todos los momentos con vosotros sean especiales y guarde grandes recuerdos, y si algo se me olvidara, estará en algún vídeo. Gracias por querer participar en todos mis momentos

importantes y por todos los que quedan por venir. Gracias por hacer que Vitoria tenga algo tan especial.

Gracias **mami**, por ser desde siempre mi mayor confidente, mi ejemplo a seguir; siempre seré tu gran admiradora. Gracias por todos los planes que son únicamente nuestros, por querer compartir siempre todo conmigo. Gracias por quererme tanto simplemente con tus gestos. Gracias **papi**, por transmitirme desde pequeña todos los valores necesarios para crecer personal y profesionalmente. Gracias por siempre acompañarme en mi etapa "baloncestística", gracias por sacar tiempo para nosotros y por trabajar tanto para conseguir lo mejor para nosotros. Gracias a los dos por organizar tantos viajes inolvidables que nos han permitido empezar a conocer este mundo tan maravilloso y compartir momentos muy especiales en familia. Gracias a los dos por haberos esforzado tanto por querer conseguir siempre lo mejor para mí. Gracias por hacerme sentir la hija más especial y afortunada del mundo por teneros como padres. Os quiero.

Gracias a **Adri** por ser el mejor de los hermanos del mundo. Gracias por haber disfrutado, peleado y reído tanto conmigo desde que llegaste a casa. Gracias por tantas vacaciones fabulosas con una compañía tan divertida e incansable como la tuya. Gracias por estar siempre dispuesto a nuestras charlas de hermanos, de lo mejorcito que se puede pedir. Aunque nuestros caminos se separen y ya no estemos sólo separados por una pared, siempre, y seguro que cada vez más, estaremos unidos. Gracias a **Cris**, por haber entrado a formar parte de nuestra familia y por siempre querer compartir todo con nosotros. Gracias por todos nuestros momentos de confesiones y cotilleos. Gracias por tu enorme ilusión para todo lo bueno que estar por venir y que vamos a vivir juntas.

Y mi mayor GRACIAS a ti, porque has sido la persona más especial para mí en estos últimos 11 años. Gracias por quererme tanto desde el primer minuto, gracias por valorarme tanto y por querer hacerme mejorar cada día. Gracias por tu inmensa ayuda en todo lo que necesite y por tu paciencia hasta que consigo las cosas que más me cuestan. Gracias por todos los momentos inolvidables que hemos compartido, por todas las nuevas experiencias que hemos vivido juntos y por los inconvenientes que siempre vamos a superar. Gracias por querer compartirlo todo conmigo, por ser mi cómplice, y mi mejor compañía. Cada vez tengo más ganas de descubrir todo lo bueno que nos deparará esta vida juntos, pero quiero disfrutarlo todo poco a poco y guardarlo en mi memoria para siempre. Gracias por hacerme sentir la chica más feliz y afortunada del mundo. Porque a cada orilla que llegues, yo seré la ola que llegue detrás.
Te quiero **Sergio**.

SUMMARY/RESUMEN

During embryonic development, cellular interactions are crucial to orchestrate the processes that give rise to the final body plan. The heart is the first organ to form and function during development. The formation of trabeculae, myocardial protrusions covered by endocardium that grow towards the lumen of the ventricles, is the first sign of chamber development, and occurs in response to signals from the endocardium that activate the overlying myocardium. Trabeculae are crucial for increasing the internal ventricular surface, favouring oxygen exchange and nourishment of the cardiomyocytes.

Previous studies in mice have shown that NEUREGULIN1 (NRG1), a ligand belonging to the Epidermal Growth Factor family expressed in the endocardium, and its more widespread receptors -ERBB2,4- are crucial for ventricular trabeculation, but the cellular processes affected by *Nrg1* loss in the heart are not well understood. To gain an insight into the role of NRG1 in heart development, we have used conditional loss- and gain-of-function mouse models. We have found that endothelial-specific, $Tie2^{Cre}$-mediated, *Nrg1* inactivation disrupts trabecular morphology and patterning, and reduces ventricular cardiomyocyte proliferation, while paradoxically, the compact myocardium appeared thickened. Global gene expression analysis in embryonic hearts by RNA-seq revealed a dysregulation of apico-basal polarity marker genes. We thus examined whether cellular polarity and oriented cell division were affected in chamber cardiomyocytes. We observed a loss of polarity (LAMININS-ITGα6, PKC, N-CADHERIN) in cardiomyocytes, and an increase in parallel divisions in chamber cardiomyocytes of $Nrg1^{flox};Tie2^{Cre}$ mutants. This finding would explain the thickened compact myocardium and the impaired trabeculation of these mice. In addition to trabeculation defects, $Nrg1^{flox};Tie2^{Cre}$ mutant hearts show hypoplastic valves, due to impaired epithelial-mesenchyme transition (EMT) of presumptive valve endocardial cells, presumably because binding and activation of the receptor ERBB2,3 by NRG1 in this region is impaired.

To study the function of NRG1 signalling at later stages of ventricular chamber development, we have induced *Nrg1* deletion during compaction, using the $Cdh5^{CreERT2}$ driver. Late *Nrg1* inactivation in cardiac endothelium leads to a thinner compact myocardium, and defective myocardial patterning and coronary vessel morphogenesis. We have also generated a conditional gain-of-function transgenic line for NRG1. $Tie2^{Cre}$-mediated *Nrg1* overexpression lead to thickened valves, and $Nkx2.5^{Cre}$-mediated *Nrg1* lead also to thickened valves, ventricular septal defect and ventricular chamber dilation.

Our results indicate that NRG1 is essential from early to late stages of ventricular wall development. NRG1 is required for cardiomyocyte polarization and oriented cell division during trabeculation, for endocardial cushion formation during valve development, and for chamber maturation and coronary vessel formation during compaction.

Las interacciones celulares son cruciales para el desarrollo del corazón, que es el primer órgano que se forma y funciona durante la embriogénesis. La formación de las trabéculas ventriculares, protuberancias miocárdicas recubiertas por el endocardio que crecen hacia el lumen ventricular, es el primer signo de desarrollo de las cámaras, y se produce en respuesta a señales del endocardio que activan el miocardio. Las trabéculas son cruciales para aumentar la superficie ventricular interna, favoreciendo el intercambio de oxígeno y la nutrición de los cardiomiocitos.

Estudios previos en ratones han demostrado que NEOREGULIN 1 (NRG1), un ligando que pertenece a la familia del Factor de Crecimiento Epidérmico expresado en el endocardio, y sus receptores -ERBB2,4- son cruciales para la trabeculación ventricular, pero los procesos celulares afectados por la pérdida de *Nrg1* en el corazón no se conocen bien. Para avanzar en el conocimiento del papel de NRG1 en el desarrollo cardíaco, hemos utilizado modelos condicionales de pérdida y ganancia de función. Hemos encontrado que la inactivación de *Nrg1* en el endotelio cardíaco, mediada por $Tie2^{Cre}$, altera la morfología y el patrón trabecular, y reduce la proliferación de cardiomiocitos ventriculares, mientras que, paradójicamente, el miocardio compacto está engrosado. El análisis de la expresión génica global en corazones embrionarios mediante RNA-seq mostró una expresión alterada de genes marcadores de polaridad ápico-basal. Por lo tanto, examinamos si la polaridad celular y, en consecuencia, la división celular orientada, estaban afectadas en estos mutantes. Observamos una pérdida de polaridad (LAMININAS-ITGα6, PKC, N-CADHERINA), y un aumento en las divisiones paralelas de los cardiomiocitos ventriculares de los mutantes $Nrg1^{flox};Tie2^{Cre}$. Este resultado explicaría el engrosamiento del miocardio compacto y el defecto en trabeculación observado. Los mutantes $Nrg1^{flox};Tie2^{Cre}$ muestran además válvulas hipoplásicas, debido a la alteración de la transición epitelial-mesénquima (EMT) de las células endocárdicas que darán lugar a la válvula, probablemente porque la unión de NRG1 a los receptores ERBB2,3 en esta región está afectada.

Para estudiar la función de NRG1 en etapas posteriores del desarrollo ventricular, hemos inducido la inactivación de *Nrg1* durante la compactación, utilizando la línea $Cdh5^{CreERT2}$. La inactivación tardía de *Nrg1* en el endotelio cardíaco conduce a un miocardio compacto más fino, un patrón defectuoso del miocardio y un desarrollo de la vasculatura coronaria alterado. Hemos generado también una línea transgénica de ganancia de función condicional para NRG1. La sobreexpresión de *Nrg1* mediada por $Tie2^{Cre}$ o $Nkx2.5^{Cre}$ da lugar al engrosamiento valvular, septación ventricular defectuosa, y dilatación de la cavidad ventricular.

Nuestros resultados indican que NRG1 es esencial para la polarización de los cardiomiocitos y la división celular orientada durante la trabeculación, para la formación de los primordios valvulares durante el desarrollo de la válvula, y para la maduración de la cámara y la formación de vasos coronarios durante la compactación.

Index of contents

Index of figures, schemes and tables

Figures

Schemes

Tables

RNA-seq data and videos are provided in the digital format of the Thesis.

Abbreviations

AV: Atrioventricular
AVC: Atrioventricular canal
AVM: Arterio-venous malformations
CM: Compact myocardium
CV: Coronary vessels
CX40: Connexin 40
E: Embryonic day
ECD: Extracellular domain
ECM: Extracellular matrix
EMT: Epithelial-mesenchymal transition
ENCs: endocardial cells
HA: Hyaluronic acid
H&E: Hematoxylin & Eosin
IB4: Isolectin B4
IF: Immunofluorescence
ISH*: In situ* hybridization
lv: left ventricle
LVNC: Left ventricular non-compaction
mv: mitral valve
N1ICD: Notch1 intracellular domain
NuMa: Nuclear mitotic apparatus
NRG1: Neuregulin 1
OCD: Oriented cell division
OFT: Outflow tract
PCP: Planar cell polarity
PFA: Paraformaldehyde
RTKs: Receptor tyrosine kinase
rv: right ventricle
s: somites
slv: semilunar valve
SMA: smooth muscle actin
SMC: smooth muscle cells
TM: trabecular myocardium
TSA: tyramide signal amplified
tv: tricuspid valve
VM: venous malformations
WGA: wheat germ agglutinin

INTRODUCTION

Early heart development

The heart is the first organ to form and function during vertebrate embryogenesis. At around mouse embryonic day 7.0 (E7.0), bilateral progenitors of the cardiac mesoderm, specified after gastrulation, migrate rostrally to form the cardiac crescent (Abu-Issa and Kirby, 2007; Evans *et al.*, 2010) (Figure 1a). The first cardiac mesoderm marker described is *Mesp1* (Saga *et al.*, 1996). All cardiovascular lineages: myocardium, endocardium, endothelium and epicardium, segregate from progenitors cells expressing *Mesp1* (Lescroart *et al.*, 2018).

The initial cardiac progenitors located in the cardiac crescent constitute the first heart field (FHF), that will give rise to the endocardium and myocardium of the primitive heart tube, left ventricle, and part of the ventricular septum (Figure 1a). There is a second source of cardiac progenitors, called the second heart field (SHF), which is more proliferative and is incorporated as a late addition into the arterial and venous poles of the heart tube (Dyer and Kirby, 2009) (Figure 1a). The SHF contributes to myocardial, endocardial, and mesenchymal cells that give rise to the right ventricle, outflow tract (OFT), branchial arches, atria, and sinus venosus (Zaffran *et al.*, 2004; Verzi *et al.*, 2005).

The SHF progenitors interact with other cell lineages, including cardiac neural crest cells (NCCs), which are ectoderm-derived mesenchymal cells that originate from the dorsal neural tube, through cellular interactions mediated by numerous signalling pathways including NOTCH, WNT, fibroblast growth factor (FGF), BMP, and HEDGEHOG (Rochais, Mesbah and Kelly, 2009).

The primitive heart tube consists of an inner endocardial layer and an outer myocardial layer separated by an extracellular matrix (ECM) termed cardiac jelly (Figure 1b). The heart tube grows at both ends by addition of SHF progenitors into its anterior (arterial) and posterior (venous) poles and, at the same time, undergoes rightward looping morphogenesis (Männer, 2009) (Figure 1c). The endocardium is a specialized endothelial subpopulation originated by vasculogenesis from progenitor cells in the cardiac crescent (Grieskamp *et al.*, 2011).

At E9.5, a mass of progenitors located at the venous pole of the heart, the proepicardium, undergoes epithelial to mesenchymal transition (EMT) and mesenchymal cells spread over the myocardium to form the primitive epicardial epithelium that covers the outer side of the heart (von Gise, 2013) (Figure 1d).

Valve formation begins at mouse E9.5 in the atrioventricular canal (AVC) and one day later in the OFT (Figure 1d), when endocardial-derived mesenchymal cells invade the cardiac jelly by

EMT, in response to NOTCH signalling from the endocardium (Timmerman *et al.*, 2008; MacGrogan *et al.*, 2016) and to BMP2 and/or BMP4 signalling in the myocardium (Shirai *et al.*, 2009) (Figure 1d). The cardiac jelly is ECM composed of proteoglycans and hyaluronan acid (HA) (Day and Prestwich, 2002). HAS2 appears to be the major enzyme responsible for HA synthesis (Weigel, Hascall and Tammi, 1997). In the absence of the cardiac jelly, the endocardial cushions are unable to form (Camenisch *et al.*, 2000). Cardiac valves are populated by smooth muscle cells, fibroblasts and myofibroblasts intercalated between the ECM layers (Taylor *et al.*, 2003).

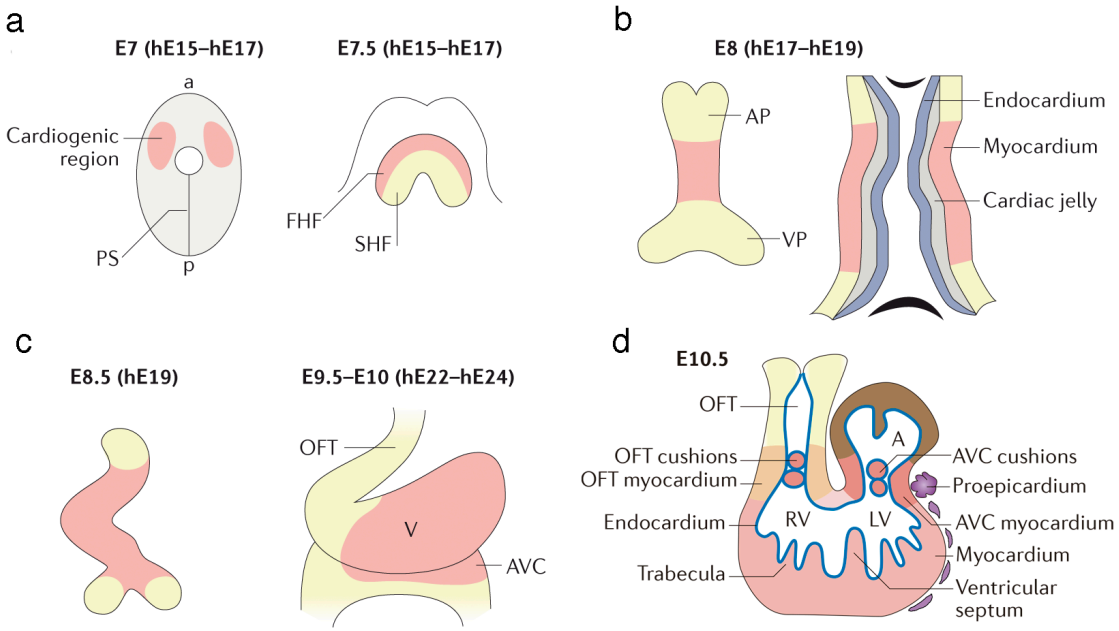

Figure 1. Heart development: Initiation

a) Cardiac progenitors migrate antero-laterally in the embryo after emerging from the primitive streak (PS) at approximately embryonic day 7 (E7.0) in mice and at embryonic day 15–17 in humans (hE15.0–hE17.0). Cardiogenic regions of the lateral plate mesoderm fuse at the embryo ventral midline and form the cardiac crescent (E7.5), containing first heart field (FHF) and second heart field (SHF) progenitors. b) The primitive heart is a linear myocardial tube lined by endothelial cells (endocardium) and with cardiac jelly between them. The heart tube expands by addition of SHF cardiac progenitors to arterial pole (AP) and venous pole (VP). c) As the heart tube elongates, it undergoes rightward looping (E8.5). The outflow tract (OFT) is formed at the AP (E9.5–10), and regions at the outer curvatures of the heart tube proliferate extensively to form the future atrial (A) and ventricular (V) chambers, which are separated by the atrioventricular canal (AVC). d) Cardiac chambers expand by proliferation of cardiomyocytes and trabeculae meshwork is well formed. Proepicardium-derived cells contribute to atrioventricular canal (AVC) cushion mesenchyme and will form the epicardium through epithelial to mesenchymal transition (EMT) (From: MacGrogan, Münch and de la Pompa, 2018)

Trabeculation

At around E9.0, trabeculation begins in mice, when cardiomyocytes form myocardial protrusions towards the ventricular lumen that ultimately will give rise to a complex meshwork (Phillips *et al.*, 2013) (Figure 2). Trabeculae are the first sign of chamber differentiation and are formed by endocardial cells which overlie the myocardium, both cell types are separated by ECM. Trabecular cardiomyocytes and endocardium are close to each other, especially at the base of the forming trabecula, and the crosstalk between both tissue layers regulates trabecular growth and patterning (Sedmera *et al.*, 2000; Moorman and Christoffels, 2003).

The function of trabeculae is to increase the myocardial mass, facilitating oxygen and nutrients exchange in the embryonic myocardium before coronary vascularisation (Sedmera *et al.*, 2000; Phillips *et al.*, 2013). Failure in trabeculae formation is embryonic lethal (H. Chen, 2004; Gassmann et al., 1995). Cells at the tip of the trabeculae are more differentiated than those at the base (Sedmera and Thompson, 2011). Consequently, cardiomyocytes from the trabecular region (inner layer) proliferate very little and show a mature sarcomere structure in comparison with the compact myocardium cardiomyocytes (outer layer), which facilitates ventricular contractility (Phillips *et al.*, 2013).

The heart beats from the early heart tube stage, and cardiac rhythm and electrical propagation are regulated by the cardiac conduction system (CCS). The ventricular conduction system (VCS) forms on the subendocardial surface of the ventricular myocardium. The entire VCS is derived from common myogenic progenitor cells, with cardiomyocytes in the FHF and SHF contributing to it (Miquerol *et al.*, 2013). A biphasic mode of development, lineage restriction followed by limited outgrowth, underlies establishment of the mammalian VCS (Miquerol *et al.*, 2010). Rapid transmission of electrical impulse is favoured by CONNEXIN 40 (CX40, also known as GJA5) and CONNEXIN 43 (CX43, also known as GJA1) gap-junctions channels or connexons, which are strongly expressed in the trabecular myocardium, and will give rise to the Purkinje fibre network (Christoffels & Moorman, 2009; Moorman & Christoffels, 2003; Stacey Rentschler *et al.*, 2001).

BRG1, a chromatin remodelling protein, is essential for ECM establishment and for trabeculation. BRG1 repress ADAMTS1, a secreted matrix metalloproteinase, in the endocardium which controls the degradation of the cardiac jelly and prevents excessive trabeculation (Stankunas *et al.*, 2008). Recently, the HAND2 transcription factor has been shown to be an important downstream regulator of NOTCH-dependent endocardium-myocardium signalling mechanism active in trabeculation, and a direct regulator of *Nrg1* (VanDusen *et al.*, 2014).

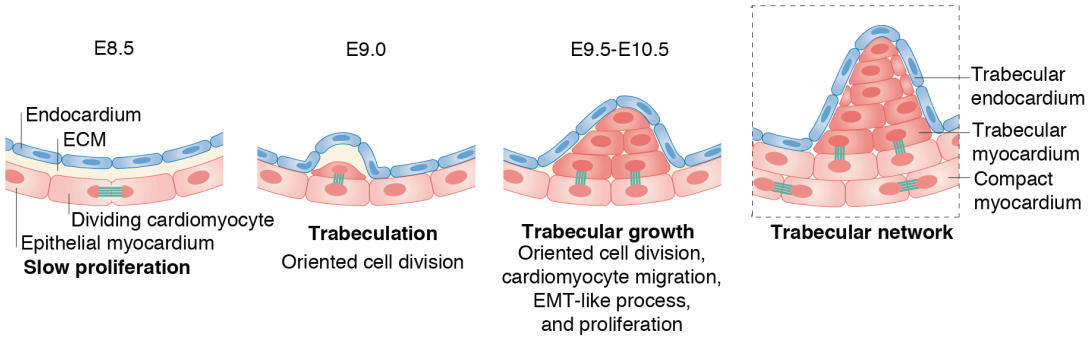

Figure 2. Heart development: Trabeculation

Cartoons depicting the initial stages of trabeculation beginning at E8.5, when the heart tube is formed by an inner endocardium and a slowly proliferative epithelial myocardium. At E9.0, the first myocardial protrusions covered by endocardium, growing towards the ventricular lumen, appear. At E9.5–E10.5, a growing trabecular network is formed by oriented cell division, cardiomyocyte migration, EMT-like process, and proliferation. A rapidly dividing outer layer of compact myocardium and a slowly dividing inner trabecular myocardium are defined at this stage. (From: MacGrogan, Münch and de la Pompa, 2018)

Compaction and coronary vessels development

Trabeculae gradually become part of papillary muscles, the interventricular septum, and cardiac conductions system cells (Sedmera *et al.*, 1997). At around E13.5 in mice, trabeculae compressed within the ventricular wall through the process of compaction, contributing to the thickness of the myocardium (Sedmera *et al.*, 2000) (Figure 3). The compacting ventricular wall is formed by the subendocardial inner myocardial wall or trabecular myocardium (TM), a medial hybrid myocardial zone or intermediate myocardium (IM) (D'Amato *et al.*, 2016a; Zhang *et al.*, 2016) and an outer compact myocardium (CM), or outer myocardial wall (Figure 3).

As the ventricular wall expands by proliferation of the compact myocardium, and the trabeculae coalesce during compaction, an hypoxic environment facilitates the invasion of coronary vessels to nourish the increasingly thickened compact myocardium of the ventricular wall. At the same time, trapped endocardial cells transform into vascular endothelial cells to form the vascular supply for the newly compacted myocardium (Tian *et al.*, 2014) (Figure 3).

At around E11.5 in mouse, the primitive coronary plexus giving rise to the coronary vessels invades the subepicardial layer on the heart surface by angiogenic sprouting from the sinus venosus (Tian *et al.*, 2014), and enters the myocardium to differentiate into coronary arteries, whereas few of the remaining subepicardial vessels differentiate into coronary veins at the heart surface (Red-Horse *et al.*, 2010; Tian *et al.*, 2013). The sinus venosus sprouting model proposed

that coronary arteries are re-specified from subepicardial veins (Tian *et al.*, 2014). It has been demonstrated that subepicardial endothelial precursors form most coronary arteries (Tian *et al.*, 2013).

The epicardium has a minimal contribution of endothelial cells to the coronaries, and does not appear to be the primary source of the coronary endothelial cell layer, but rather it gives rise to most coronary smooth muscle cells and provides trophic factors that support coronary growth (Zhou *et al.*, 2010; S. P. Wu *et al.*, 2013).

Ventricular wall endocardium constitutes a third source of coronary endothelium and contributes to most ventricular septum arteries (Wu *et al.*, 2012; Tian *et al.*, 2014). Endocardium is incorporated into the myocardial wall during compaction by trabecular coalescence (Tian *et al.*, 2014) and it was originally said that these endocardial cells contribute to the majority of the intramyocardial coronary arteries (Leslie *et al.*, 2012).

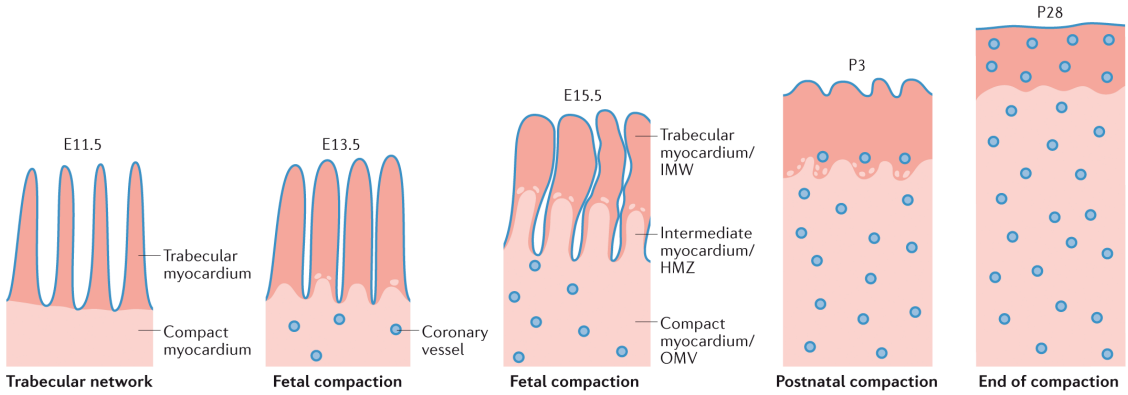

Figure 3. Heart development: Compaction

At E11.5, trabeculae form a complex network, and at around E13.5, compaction begins and trabeculae integrate into the CM. In parallel, coronary vessels begin to form to nourish the thickening CM. At E15.5, the TM or inner myocardial wall (IMW), the intermediate myocardium (IM) or hybrid myocardial zone (HMZ), and the CM or outer myocardial wall (OMW) can be distinguished. Compaction continues postnatally, and approximately concludes at P28 in mice. (From: MacGrogan, Münch and de la Pompa, 2018)

Oriented cell division and polarity during trabeculation

Clonal analysis has shown that during ventricular chamber development, myocardial cells undergo two growth phases. One with cell dispersion, leading to the separation of clonally-related cell clusters, and another in which cells remain close after division, thus favouring the formation of a cluster (Meilhac, 2003). Later studies in the embryonic heart, showed that the growth of the

myocardium is oriented in a planar or transmural shape (Meilhac *et al.*, 2004). Image analysis of 3D confocal scans show that neighbouring cells are already locally coordinated in the mouse embryonic myocardium. The myocardium grows in a plane parallel to the outer surface of the heart and also thickens transmurally, which contributes to trabeculae formation (Le Garrec *et al.*, 2013).

The early chamber myocardium has apico-basal polarity in both mice and zebrafish. Cell polarity is essential for oriented cell division to occur during chamber development and trabeculae formation (J. Li *et al.*, 2016; Jiménez-Amilburu *et al.*, 2016; Passer *et al.*, 2016) (Figure 4).

Previous studies have shown that in the mouse heart, cardiomyocytes undergo oriented cell division (OCD) and directional migration during cardiac trabeculation in a N-CADHERIN-regulated manner. The geometric location of the different signals involved may cause asymmetric distribution of "patterning" mRNAs (*Hey2* and *Bmp10*) in perpendicular divisions, that contribute to cardiomyocyte regional specification towards trabeculae (J. Li *et al.*, 2016) (Figure 4).

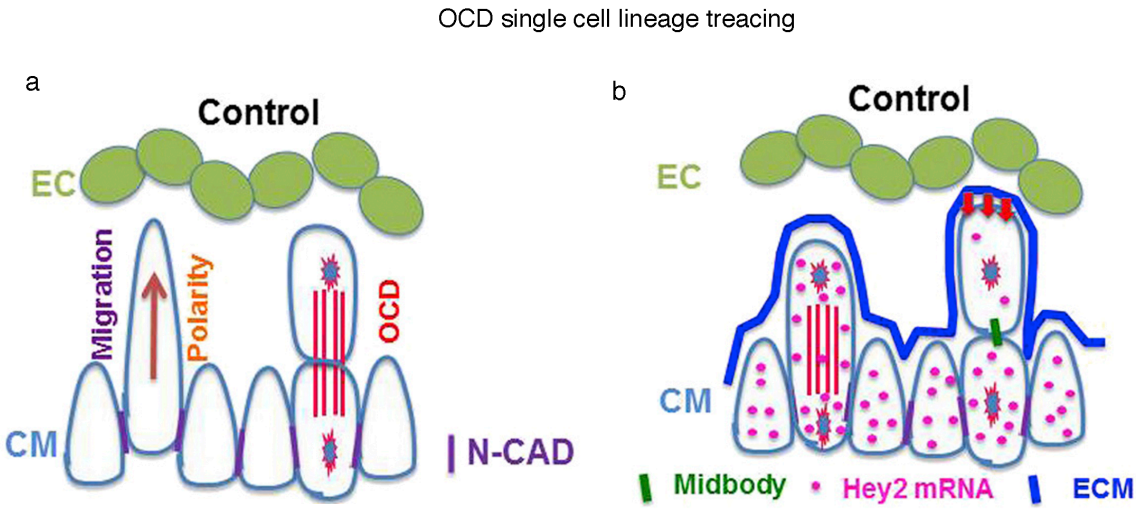

Figure 4. Oriented cell division contributes to trabecular morphogenesis

a) Both oriented cell division (OCD) and directional migration contribute to cardiac trabecular initiation from compact myocardium (CM). N-CADHERIN regulates these processes in a cell-autonomous manner. b) Perpendicular OCD is an extrinsic asymmetric cell division and contributes to trabecular regional specification (differential *Hey2* mRNA distribution). Cardiac jelly (ECM) and endocardium (EC) might provide instructive cues for trabecular cardiomyocyte regional specification. (From: J. Li *et al.*, 2016)

Passer et al 2016 described that the PAR polarity complex machinery (PAR3, PAR6 and PRKCi -protein kinase C iota-) coordinates normal cellular differentiation by facilitating perpendicular

cell division and promoting the differentiation of trabecular myocardium from compact myocardium in mice. NuMA (Nuclear Mitotic Apparatus) directs trabecular formation by orienting the mitotic spindle, so that the cell division plane is perpendicular to the heart´s lumen. Disruption of the polarity complex or its downstream interacting partner NuMA, results in aberrant mitotic spindle alignment, loss of polarized cardiomyocyte division and lack of trabeculation in mice (Passer *et al.*, 2016). These studies use SURVIVIN to analyse OCD. SURVIVIN is essential for mitotic spindle establishment and localizes to different components of the mitotic apparatus, including centromeres in prophase, kinetochores of the metaphase and anaphase spindle, and the midbody during cytokinesis (Uren *et al.*, 2000; Caldas *et al.*, 2005).

Ventricular trabeculation in zebrafish

Image analysis of fixed and live zebrafish samples during trabecular morphogenesis in zebrafish has shown that nrg signalling from the endocardium is required for trabeculation (Peshkovsky, Totong and Yelon, 2011). Qian et al 2015 have shown that cardiac contraction is required for trabeculation and for *notch1b* transcription in ventricular endocardium. These authors propose a model in which cardiac contraction initiates flow, which is detected by primary cilia on endocardial cells to activate the regulatory *notch1-efnb2a-nrg1* pathway and promote cardiac trabeculation (Qian *et al.*, 2015). In zebrafish cardiomyocytes, erbB2 contributes to both proliferation and migration of cardiomyocytes, to form a relatively thin layer of myocardium and to initiate cardiac trabeculation (Liu *et al.*, 2010).

A combination of clonal analysis and live cell imaging showed that zebrafish heart cardiomyocytes first extend luminal protrusions, then constrict their abluminal surface and move their cell body into the trabecular layer. The neighbouring cardiomyocytes move into the space left behind to maintain a cohesive compact layer (Staudt *et al.*, 2014). This view has been refined to suggest that cardiomyocytes undergo apical constriction before depolarization in order to delaminate in a nrg1-erbb2-dependent manner, suggesting that trabeculation is an EMT-like process (Jiménez-Amilburu *et al.*, 2016). They postulate that the “basal” region of cardiomyocytes faces the cardiac jelly, and the “apical” represents the abluminal side of cardiomyocytes close to the epicardium. Later *in vivo* imaging experiments, demonstrated that is nrg2a, and not nrg1, the one essential for trabeculation in zebrafish heart (Rasouli and Stainier, 2017).

Initially, cdh2 (n-cadherin) was observed to be expressed along the lateral sides of embryonic cardiomyocytes, in an evenly distributed pattern, and with the occasional appearance of punctate signal. Delaminating cardiomyocytes accumulate cdh2 on the surface facing the basal side of

compact layer cardiomyocytes, thereby allowing tight adhesion between these layers. ErbB2 signalling is required for the re-colocalization of cdh2 from the lateral to the basal side of cardiomyocytes along the membrane (Cherian *et al.*, 2016).

Time-lapse imaging analysis showed that cardiomyocyte proliferation in zebrafish is essential for trabecular growth, but not initiation. Cardiomyocytes mostly divide in parallel to the myocardial wall. This proliferation relies on nrg-erbb signalling and is more frequent in the trabecular layer. In contrast, tgfβ signalling functions to inhibit cardiomyocyte division in both layers (Uribe *et al.*, 2018).

Recent *in vivo* imaging studies shows that cardiomyocyte polarity regulation is essential for trabeculation in zebrafish heart. Crb2a is expressed in all ventricular cardiomyocytes in tight and *adherens* junctions, and re-localizes to the apical side of compact layer cardiomyocytes before cardiomyocyte delamination on a nrg-erbb2 dependent manner (Jiménez-Amilburu and Stainier, 2019).

The NRG1-ERBB signalling pathway

The NEUREGULINS (NRGS) are cell-cell signalling proteins that are ligands for receptor tyrosine kinases of the ERBB family. NRG1 proteins are released from the endocardium into the extracellular space and, then, bind to their ERBB2,4 receptors in the myocardium, acting as paracrine signals (Falls, 2003; Parodi and Kuhn, 2014).

The *Nrg1* gene expands 1400 Kb and is located in chromosome 8p12. It has various promoter sequences and undergoes alternative splicing that produces several NRG1s isoforms (Holmes *et al.*, 1992; Chen *et al.*, 1994; Meyer and Birchmeier, 1995; Falls, 2003) (Figure 5a). The differences in the biological functions of NRG1 isoforms are determined by the type of EGF-like domain (α- or β), which is common for all isoforms and binds to the ERBB receptor, the N-terminal sequence and the transmembrane (TM) or non-membrane localization signal of the protein (Falls, 2003) (Figure 5a, b). The active form of NRG1 is released after proteolytic cleavage at the juxta membrane (JM) region lying on the carboxy-terminal side of the EGF-like domain previous to the TM domain (Fleck *et al.*, 2013) (Figure 5a, b).

Type I isoforms contain an Ig-like domain, an EGF-like domain (α- and β-), a proteolysis site (black arrows, Figure 5b), a hydrophobic domain suggested to act as internal signal sequence for secretion of the factor and additional C-terminal sequences (Meyer *et al.*, 1997) (Figure 5b).

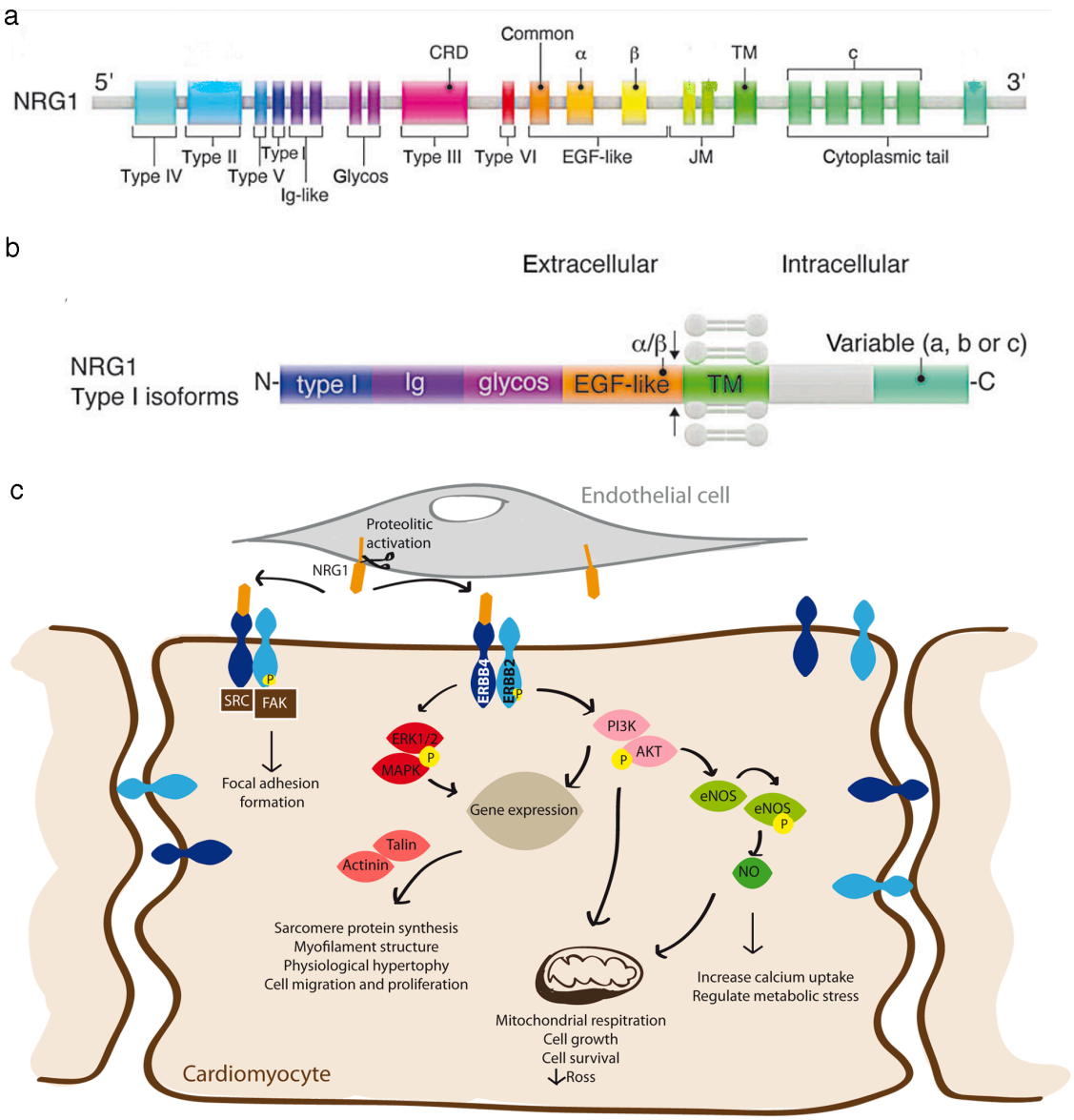

Figure 5. NRG1 molecular structure and signalling pathway

a) NRG1 genetic loci. b) NRG1 protein isoform composition, with the extracellular (N-terminal), the transmembrane (TM) and the intracellular domains (C-terminal). Arrows indicate proteolytic sites. (From: Parodi and Kuhn, 2014) c) In cardiomyocytes, NRG1 stimulates the activation of MAPK/ERK 1/2 that may induce myofilament organization and hypertrophy in adult cardiomyocytes. NRG1 regulates PI3-KINASE/AKT pathway, which protects cardiac myocytes against cell death and regulates metabolism and growth. AKT is implicated in cell survival, enhances glucose uptake and AKT-dependent activation of eNOS (endothelial Nitric Oxide Synthase), triggering changes in mitochondrial respiration, which may also regulate cell survival in the setting of metabolic stress. FAK is critical for the formation of focal adhesion complexes. FAK is a substrate for the adaptor protein SRC and is involved in the maintenance of sarcomeres and cell survival. (modified from Pentassuglia and Sawyer, 2009 and Odiete, Hill and Sawyer, 2012)

Type I NRG1 is the predominant isoform expressed in early embryogenesis. Type I NRG1 is essential for development of neural crest-derived sensory neurons in cranial ganglia as well as for trabeculation of the cardiac ventricles (Meyer *et al.*, 1997).

The ERBB family of receptor tyrosine kinases (RTKs) consists of four receptors: ERBB1-4. These receptors are composed with an extracellular ligand-binding domain (ECD), a transmembrane domain and a cytoplasmic tyrosine kinase domain (Odiete, Hill and Sawyer, 2012). ERBB signal transduction occurs upon binding of a ligand to the ECD, promoting hetero- or homodimerization, which results in activation of their cytoplasmic tyrosine kinase domain (ERBB2 and ERBB4), and transphosphorylation of intracellular tyrosine residues (Riese and Stern, 1998). NRG1 binds to ERBB3 and ERBB4. ERBB2 acts as a co-receptor which enhances and stabilizes dimerization with other ERBB receptor to initiate signal transduction, but does not have a direct ligand itself (Horan *et al.*, 1995).

Receptor transphosphorylation favours the recruitment of signalling proteins leading to activation of different downstream pathways: the extracellular signal-regulated kinase 1/2 (ERK1/2), and phosphoinositide 3-kinase (PI3K)/protein kinase B (AKT) pathways (Sanchez-Soria and Camenisch, 2010) (Figure 5c). These pathways are implicated in the regulation of cell proliferation, differentiation, migration, survival and death (Iwamoto and Mekada, 2006). The mitogen-activated protein kinase (MAPK)/ ERK1/2 is a multi-kinase cassette which acts as a transcription factor promoting cell growth and cardiac hypertrophy (Heineke and Molkentin, 2006; Wang, 2007) (Figure 5c). Ras-MAPK pathway is also important during valve development because it regulates differentiation, migration and proliferation of cells during EMT. The activation of the PI3-kinase/AKT pathway is involved in the protection of cardiomyocytes against cell death, as well as in the regulation of metabolism and growth (Pentassuglia and Sawyer, 2009) (Figure 5c). ERBB also interacts with the SRC-FAK signalling pathway, implicated in focal adhesion contact and lamellipodia formation (Figure 5c). These interactions are crucial for maintenance of electrical coupling (Kuramochi, Guo and Sawyer, 2006).

NRG1 signalling in mouse heart development

Mice deficient for NRG1, expressed in the endocardium, or mutant for ERBB2 and ERBB4, expressed in myocardium, die at around E10.5 due to severe defects in trabeculation (Gassmann *et al.*, 1995; Lee *et al.*, 1995; Meyer and Birchmeier, 1995). Embryos deficient for ERBB2 or NRG1 also exhibit underdeveloped cushion and valve tissue.

ERBB2 is expressed in the myocardium and endocardium of the AVC region, and in the invading mesenchymal cells within the cushion matrix. ERBB3 is expressed in endocardial cells that undergo EMT but its phosphorylation is predominantly detected in the invading mesenchymal cells. HA interacts with and activates ERBB2-ERBB3 receptors, initially, to promote EMT and then to limit the extent of endocardial cell delamination and transformation. *In vitro* studies suggest that ERBB3 is specifically required for transformation and not activation of the AVC endocardium (Camenisch *et al.*, 2002). *ErbB3*$^{-/-}$ mice die by E13.5, and have hypoplastic cardiac cushions (Erickson *et al.*, 1997).

As described before, the CCS is a complex network of cells within the heart that generates and conducts electrical impulses to coordinate heart contraction. NRG1 are ligands responsible for inducing murine embryonic cardiomyocytes to differentiate into cells of the conduction system (Rentschler *et al.*, 2002). NRG1 induces expression of several conduction specific markers such us *Cx40* and Cx*45* (Patel and Kos, 2005). NRG1 is required to maintain the cardiac transcription factor program in both trabecular and non-trabecular myocardium (Lai *et al.*, 2010).

NRG1 and NOTCH signalling interact during trabeculation. Targeted mutants for the NOTCH1 receptor or the effector transcription factor RBPJ show defective trabeculation, while expression and epistasis analysis showed that *Nrg1* transcription depends at least in part on NOTCH activity (Grego-Bessa *et al.*, 2007) (Figure 6a). Recently, knowledge about the interplay between NRG1 and NOTCH signalling during trabeculation has been refined. It has been suggested that NOTCH signalling promotes ECM degradation, whereas NRG1 promotes ECM synthesis necessary for trabecular rearrangement and growth (del Monte-Nieto *et al.*, 2018) (Figure 6b). This confirms that ECM dynamics are necessary for individualization and organization of trabecular units (del Monte-Nieto *et al.*, 2018).

Later in development, pERBB2 is activated in coronary endothelium. ERBB2 partners with NEUROPILIN 1 (NRP1) to form a functional receptor for the vascular guidance molecule SEMA3d; NRP1 loss leads to abnormal patterning of the coronary veins, a phenotype recapitulated by endothelial loss of ERBB2 (Aghajanian *et al.*, 2016).

Nrg1 expression is variable from early stages of development until adulthood. It is shown that *Nrg1* expression is restricted to the endocardial endothelium and the cardiac microvascular endothelium (CMVE), but it is absent in larger coronary arteries and veins and in aortic endothelium in adult heart (Lemmens *et al.*, 2006).

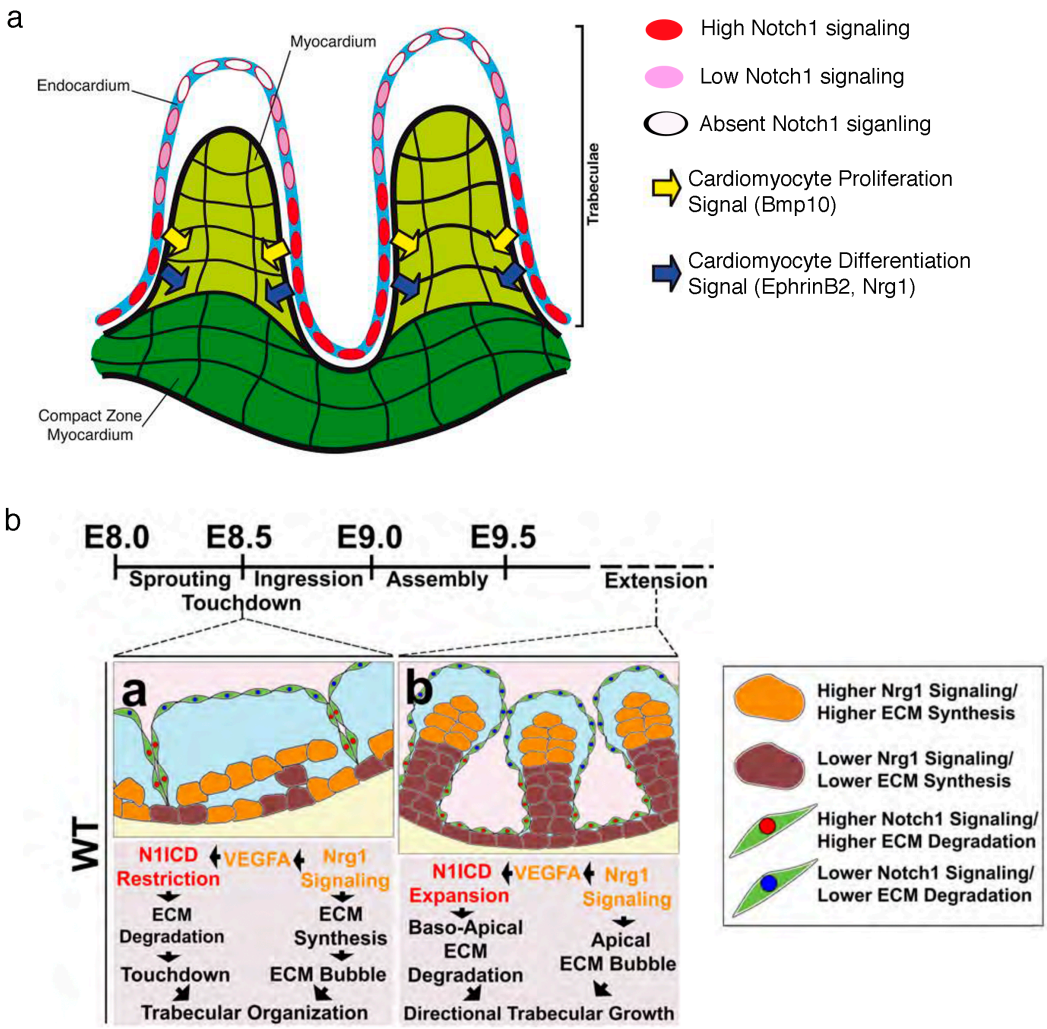

Figure 6. Structural and molecular basis underlying trabeculation

a) Scheme of the molecular pathway downstream of NOTCH signalling during trabeculation. The inner layer of endocardium (blue) produces signals that induce myocardium (green) development. N1ICD signalling is stronger in the endocardial cells (red nuclei) close to the base of the growing trabeculae (light green), but N1ICD signalling decays towards the tip (pink-white nuclei). N1ICD signals to the trabecular myocardium to promote proliferation (yellow arrow) through BMP10, and differentiation (black arrow) through EPHRINB2 and NRG1 activation in the endocardium. (modified from Grego-Bessa *et al.*, 2007) b) Cartoon with morphology and pathway changes during early trabeculation. Touchdowns occur at E8.0–E8.5 as endocardial projections progress through cardiac jelly and establish the first anchor points with CM. Endocardial ridges then form between touchdowns, creating endocardial domes that segment the ventricular chamber into multiple matrix-rich areas (ECM bubbles), thus encapsulating the TM and defining the initial trabecular architectural units. Lateral ingression occurs from E8.5 as endocardial touchdowns expand laterally, isolating trabecular units. Trabecular assembly occurs at E8.5–E9.0 as trabecular cardiomyocytes rearrange into a radial disposition. Finally, trabecular extension occurs from E9.5 when trabeculae undergo radially oriented cardiomyocyte growth and ECM bubbles are progressively reduced in a basal-to-apical manner. (From: del Monte-Nieto *et al.*, 2018)

Both NRG1 and ERBB receptors are expressed in vascular endothelial cells, and stimulation of endothelial cells in vitro or in vivo induces an angiogenic response similar to and independent of VEGF (vascular endothelial growth factor) (Strong Russell *et al.*, 1999). NRG1 also can induce angiogenesis via enhanced expression of *Vegf* (Bagheri-Yarmand *et al.*, 2000).

NRG1-ERBB signalling in cardiovascular disease

The NRG1-ERBB signalling cascade has also been described to be involved in adult heart homeostasis. Cardiac AKT can activate the mammalian target of rapamycin (mTOR), promoting protein synthesis and hypertrophy (Kemi *et al.*, 2008). MAPK/ERK1/2 is implicated in cellular proliferation and hypertrophy in cardiomyocytes (Ueyama *et al.*, 2000) (Figure 5c).

NRG1-ERBB activity is implied in myocardial metabolism, inducing cardiac myocyte glucose uptake in a PI3K-dependent manner (Cote *et al.*, 2005). Metabolic stress, as seen in ischemic heart disease and chronic heart failure, also disrupts NRG1-ERBB signalling via effects on heat shock protein 90 chaperone activity (Chiosis *et al.*, 2001).

Cardiac myocytes from conditional *ErbB4* deletion mice exhibit both delayed conduction and impaired contractility (Garcia-Rivello, 2005). Intravenous administration of recombinant NRG1 improved cardiac function and prolonged survival in animal models of ischemic, dilated and viral cardiomyopathy (Wadugu and Kuhn, 2012).

ERBB2 is necessary for NRG1 induced cardiomyocyte proliferation during embryonic/fetal and neonatal stages (D'Uva *et al.*, 2015). ERBB2-deficient mutant mice show dilated cardiomyopathy, including wall thinning and decrease contractility. Transient reactivation of ERBB2 signalling facilitates heart regeneration after myocardial infarction as a result of cardiomyocyte dedifferentiation and proliferation with neovascularization, followed by re-differentiation, tissue replacement with reduced scar formation and repair of left ventricle function (D'Uva *et al.*, 2015). ERBB2 signalling in cardiomyocytes is therefore essential for the prevention of dilated cardiomyopathy (Crone *et al.*, 2002; D'Uva *et al.*, 2015).

The importance of ERBB signalling in heart is highlighted by the associated cardiotoxicity in cancer patients treated with Trastuzumab (Herceptin). The monoclonal antibody trastuzumab targets ERBB2 receptor, as it is overexpressed in several breast cancer patients. Trastuzumab has been a successful therapy in reducing mortality rates for breast cancer patients (Romond *et al.*, 2005). The inhibition of ERBB2 pro-survival signal has a detrimental effect on myofibrils

structure and cardiomyocyte viability, leading to dilated cardiomyopathy, left ventricular systolic dysfunction and heart failure (Rohrbach *et al.*, 1999).

The finding that expression of one component of the NRG1 signalling system is increased in cancers suggest that the therapeutic application of recombinant NRG1 for cardiac therapy may unintentionally stimulate proliferation of non-cardiac cells (Parodi and Kuhn, 2014).

These studies collectively demonstrate the importance of an intact NRG1-ERBB signalling axis in adult cardiomyocytes for adaptation of cardiac structure and function.

OBJECTIVES

Heart development is essential for embryonic viability. Several studies describe the importance of a high number of signalling pathways implicated in heart development, whose function is also required in adulthood and necessary to prevent heart diseases.

Previous studies in our laboratory showed that NRG1 signalling is downregulated in NOTCH targeted mutants with defective ventricular trabeculation. Likewise, NRG1-ERBB signalling inactivation disrupts trabeculation, but the molecular mechanisms and cellular processes involved are poorly understood.

The objectives of this thesis were:

1) To study the role of NRG1-ERBB2,4 signalling in cardiac development, identifying the affected molecular mechanisms and cellular processes.
2) To study the role of NRG1-ERBB2,4 signalling in compaction and coronary vessel development.
3) To study the effect of *Nrg1* overexpression in heart development, to better understand its normal function.

In this thesis we have used targeted mutant and transgenic NRG1 mouse lines to study NRG1 function during trabeculation and compaction. We have observed alterations in cardiomyocyte polarity and OCD, defective coronary vessel morphogenesis, and affected myocardial patterning and metabolism.

MATERIALS AND METHODS

Mouse strains and genotyping

Nrg1 mutant mouse was obtained from Carmen Birchmeier laboratory (Cheret *et al.*, 2013). $Nrg1^{flox}$: *LoxP* sequences (green arrowheads) are located upstream and downstream of exons encoding the α, β and isotype 3 of the EGF domain of *Nrg1* gene (Scheme 1). CRE-mediated recombination prevents transcription of the complete EGF common domain, and introduces frameshifts that result in the early termination of all *Nrg1* transcripts.

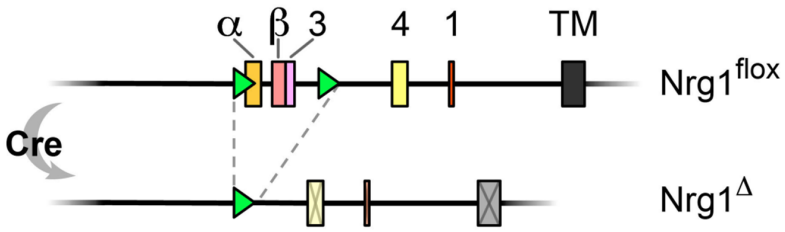

Scheme 1. Scheme of *Nrg1* conditional knockout gene and deletion of *Nrg1* domains after CRE recombination. (Cheret *et al.*, 2013)

We used the following CRE driver mouse strains: $Tie2^{Cre}$ (Kisanuki *et al.*, 2001), $Mesp1^{Cre}$ (Y Saga *et al.*, 1999), $Cdh5^{Cre\ ERT2}$ (Wang *et al.*, 2010) and $Nkx2.5^{Cre}$ (Stanley *et al.*, 2002).

In order to early (E7.5) conditional deletion of *Nrg1* in the endothelium/endocardium, we crossed the $Nrg1^{flox}$ line with the $Tie2^{Cre}$ driver line to generated the double heterozygous $Nrg^{flox/+};Tie2^{Cre/+}$, and then, crossed it with a $Nrg1^{flox/flox}$ mouse with the aim of analysing the phenotype during early embryonic development of the $Nrg1^{flox/flox};Tie2^{Cre/+}$ embryos (from now on, $Nrg1^{flox};Tie2^{Cre}$). To further confirmed the effect of *Nrg1* deletion in heart development, we generated a double heterozygous for $Nrg1^{flox/+};Mesp^{Cre/+}$ and crossed it with a $Nrg1^{flox/flox}$ mouse to analyse the phenotype of $Nrg1^{flox/flox};Mesp1^{Cre/+}$ embryos (from now on, $Nrg1^{flox};Mesp1^{Cre}$). To avoid the lethal effect of *Nrg1* deletion during trabeculation, we used the inducible $Cadherin5^{CreERT2}$ ($Cdh5^{Cre}$) line, which is active in the endocardium and coronary vessels (Luna-zurita *et al.*, 2010; Wang *et al.*, 2010). We generated a double heterozygous for $Nrg1^{flox/+};Cdh5^{Cre/+}$ and crossed it with a $Nrg1^{flox/flox}$ mouse. After 4-hidroxitamoxifen (H6278, Sigma) administration at E10.5 and E11.5, we induce *Nrg1* deletion in the endothelium during compaction. Then, we examined the phenotype of $Nrg1^{flox/flox};Cdh5^{CreERT2/+}$ embryos (from now on, $Nrg1^{flox};Cdh5^{Cre}$) at E16.5.

For the generation of *R26PA-Nrg1-iresGFP* transgenic line a complete cDNA from mouse *Nrg1* (2103 bp) was obtained from clone IMAGE 100064088. The sequence was PCR-amplified with

Phusion High-Fidelity DNA Polymerase (NEB). The product of the PCR was digested with *Nhe*I and was cloned into a *pBigT-IRESeGFP* plasmid previously generated by cloning a *Sal*I *IRES-eGFP* fragment into the *Xho*I site of *pBigT*. The *loxP-PGK-Neo*-3X-STOP-*loxP-Nrg1-IRES-eGFP* fragment obtained from the ligation of the digested *Nrg1* cDNA and the *pBigT-IRESeGFP* plasmid was cloned into *Pac*I and *Asc*I sites of *pROSA26PA* plasmid (Soriano, 1999) (Figure 28a). The final construct was linearized with *Pvu*I and electroporated into G4 mESCs derived from a cross of 129S6/SvEvTac and C57BL/6Ncr mice (Vintersten, Testa and Stewart, 2004). After G418 (200 μg/ml) selection for 7 days, 168 clones were picked. Homologous recombination was identified by Southern blot of *Eco*RV-digested DNA and hybridized with 5' and 3' probes (Figure 28b).

About 6 % of the clones were positive, and we selected three clones to confirm karyotype. One positive clone was injected into C57/BL6C blastocysts to generate chimaeras that transmitted the transgene to their offspring. The resulting founders were genotyped by PCR of tail genomic DNA samples using primers in the *R26* locus before and after the cloning site and in the polyA signal of the transgene.

We crossed this new line with the endothelial driver $Tie2^{Cre}$ to analyse the phenotype of the $R26PA\text{-}Nrg1\text{-}iresGFP^{-/+};Tie2^{Cre/+}$(from now on, $R26Nrg1GFP;Tie2^{Cre}$) or with the endocardial/myocardial driver $Nkx2.5^{Cre}$ to analyse the phenotype of the $R26PA\text{-}Nrg1\text{-}iresGFP^{-/+};Nkx2.5^{Cre/+}$(from now on, $R26Nrg1GFP;Nkx2.5^{Cre}$).

Genotyping of the different genes was performed using the primers listed in Table 1.

Table 1. PCR primers and conditions for genotyping

Gene	Oligos 5´to 3´	Annealing Temperature (Cº)	Product
$Nrg1^{flox/flox}$	5´ TCC TTT TGT GTG TGT TCA GCA CCG G 3´ 5´ GCA CCA AGT GGT TGC GAT TGT TGC T 3´	68º	400 bp mutant 250 bp WT
$Tie2^{Cre}$	5´ GGG AAG TCG CAA AGT TGT GAG TT 3´ 5´ CTA GAG CCT GTT TTG CAC GTT C 3´	60º	500 bp
$Mesp1^{Cre}$	5'-TGA CG GTG GGA GAA TGT TAA T-3' 5'-GCC GTA AAT CAA TCG ATG AGT-3'	57º	286 bp (CRE)
$Cdh5^{CreERT2}$	5´CTG GGA TGC TGA AGG CAT CAG 3´ 5´ TTG CGA ACC TCA TCA CTC GTT 3	55º	760 bp
R26Nrg1-iresGFP	5´AAA GTC GCT CTG AGT TGT TAT 3´ 5´GGA GCG GGA GAA ATG GAT ATG 3´ 5' TGC CCG ACA ACC ACT ACC TGA G 3'	62º	585 bp WT 853 Tg
$Nkx2.5^{Cre}$	5´ GCG CAC TCA CTT TAA TGG GAA GAG 3´ 5´ GAT GAC TCT GGT CAG AGA TAC CTG 3´	60º	583 bp

(WT) While Type; (Tg) Transgenic; (bp) base pairs.

Tissue processing

Dissected early embryos (E8.0-E10.5) were selected depending on number of somites to perform all the experiments in control and mutant embryos with a comparable developmental stage. Embryos were fixed in 4% paraformaldehyde (PFA) at 4ºC. For immunostaining, early embryos (E8.5 and E9.5) were fixed for 2 hours at 4ºC, E10.5 embryos were fixed 4h at 4ºC and older embryos were fixed overnight (O/N) at 4ºC. For *in situ* hybridization (ISH), Hematoxylin and Eosin (H&E) and Alcian blue studies all embryos were fixed O/N. Embedding was performed following a dehydration using a graded ethanol series, xylene washes and a final paraffin-embedding step at 65ºC. For cryosections, embryos were fixed in 4% PFA for 1h on ice, then washed in sucrose 30% and embedded in Optimal Cutting Temperature (OCT) medium at -80ºC.

Immunofluorescence in sections

Paraffin-embedded 7 μm-sections or OCT-embedded 10 μm-sections of embryonic hearts were blocked in histoblock solution or in 5% FBS in PBS 0.3% triton, respectively, and incubated O/N with primary antibodies, followed by 1h incubation with a fluorescent-dye-conjugated secondary antibody. NFATC1, CD31, NRG1 and pERBB2 immunostainings were performed using tyramide signal amplified (TSA) coupled to Cy3 or to fluorescein (NEL744 or NEL741 Perkin Elmer; 1:100) (Del Monte *et al.*, 2011). N1ICD- and BrdU- immunostainings were amplified with biotinilated secondary antibody, ABC (Vectastain Kit) and TSA. Nuclei were counterstained with DAPI. Cryosections samples were used to perform immunofluorescence (IF) for NRG1, pERBB2, PRKCi, ITGα6, and SURVIVIN. All the primary and secondary antibodies used are listed in Table 2 and 3, respectively.

Histology, Alcian blue and *in situ* hybridization

H&E and Alcian blue staining's were performed on sections according to standard protocols. ISH was performed as described (de la Pompa *et al.*, 1997; Kanzler *et al.*, 1998).

Whole-mount immunofluorescence

Embryos were fixed for 2 hours (E10.5) or O/N (E16.5) at 4ºC in PFA 4% and, then kept in PBS at 4ºC. Permeabilization was performed for 1h in 0.5% Triton X-100/PBS and subsequently embryos were blocked for 1h in 10% FBS in 0.5% Triton X-100/PBS. E10.5 embryos were stained with the following primary antibodies: anti-alpha smooth muscle actin-Cy3 (SMA-Cy3) and Isolectin-B4-AlexaFluor647 (IB4-647).

Table 2. List of primary antibodies used for IF

Antibody	Cardiac expression	Dilution	Source Ig	Company	Reference
α-smooth muscle actin-Cy3	CM/SMc	1:200	mouse	Sigma Aldrich	C6198
Isolectin-B4-AlexaFluor647	Endo/CV	1:200		Invitrogen	I32450
Nfatc1	Endo	1:250	mouse	Enzo	ALX-804-022
Anti-CD31 (PECAM)	Endo/CV	1:100	rat	BD Bioscience	550274
BrdU	BrdU	1:100	rat	Abcam	ab6326
N1ICD	Endo	1:100	rabbit	Cell signaling	4147S
Laminin	BM	1:300	rat	Sigma Aldrich	L9393
N-Cadherin	CM	1:100	mouse	Invitrogen	333900
WGA-Rhodamine	All cells	1:100		Vector Laboratories	RL-1022
cTnT1	CM	1:50	rabbit	Abcam	Ab58544
Endomucin	Endo/Veins	1:200	rat	Santa Cruz Biotechnology	Sc-65495
Glut1	CM	1:100	rabbit	Merck Millipore	07-1401
MF20	CM	1:20	mouse	DSHB	
Neuregulin 1	Endo/CV	1:100	mouse	Santa Cruz Biotechnology	sc-393006
pErbB2	CM/Endo/CV	1:100	rabbit	Cell signaling	2247
Prkci/aPKC	CM	1:100	mouse	Santa Cruz Biotechnology	sc-17804
Itgα6	TM	1:500	rat	Invitrogen	14-0495-82
Survivin	PC	1:300	rabbit	Cell signaling	2808P
DAPI	All cells	1:1.000		Sigma Aldrich	D9542

(CM) cardiomyocytes; (SMc) smooth muscle cells; (Endo) endocardium; (CV) coronary vessels; (Mc) mesenchymal cells; (BM) basement membrane; (TM) trabecular myocardium; (PC) proliferating cells.

E16.5 hearts were stained with the following primary antibodies: MF20, anti-CD31 (PECAM), ENDOMUCIN and IB4. The secondary antibodies used are listed in Table 3. After several washes in PBS-T (PBS, 0.1% Tween-20) embryos were mounted on a slide with the following procedure (Scheme 2): in order to image the inside of the chamber, E10.5 and E16.5 hearts were dissected and placed on a petri dish with PBS, then a piece of the ventricular wall was cut to visualize the trabecular network inside the ventricle. The cut heart was mounted on a slide with 2 or 3 small glasses, respectively, in each side of the tissue to keep it immobile. Fluoromount medium was used to mount the tissue and a cover slide was placed on the top. Additionally, to visualize the

coronary vasculature of the E16.5 hearts the procedure was similar but with the dorsal or ventral side of the heart facing up, so the coronary vessel plexus could be scanned. 3 glasses were used to make the reservoir a bit deeper. For details of the procedure see the material and methods sections in (Mukouyama *et al.*, 2012).

Table 3. List of secondary antibodies used for IF

Antibody	Dilution	Company	Reference
anti mouse-HRP	1:100	DakoCytomation	P0447
anti rabbit-HRP	1:100	DakoCytomation	P0448
anti rat-HRP	1:100	Thermo Fisher Scientific	31470
anti rabbit-AlexaFluor488	1:100	Thermo Fisher Scientific	A-11034
anti rat-AlexaFluor488	1:100	Thermo Fisher Scientific	A-11006
anti mouse-alexaFluor488	1:100	Thermo Fisher Scientific	A-11029
anti rabbit-alexaFluor647	1:100	Invitrogen	A-21245
anti mouse-alexaFluor594	1:100	Thermo Fisher Scientific	A-21203
anti rat-AlexaFluor555	1:200	Invitrogen	A-21434
anti rabbit-biotinilated	1:100	Jackson ImmunoResearch	111-066-003
anti rat-biotinilated	1:100	Vector Laboratories	BA-4001

Proliferation analysis and quantification

Cell proliferation in the developing heart was evaluated by 5-bromo-2'-deoxyuridine (BrdU) incorporation. Pregnant females were intraperitoneally injected with 300 µl of BrdU (10 mg/ml). Two hours later control and $Nrg1^{flox};Tie2^{Cre}$ embryos (E8.5, E9.5 and E10.5) were collected in PBS and processed for IF. BrdU was detected by staining with a rat anti-BrdU monoclonal antibody (1:100, abcam, ab6326) followed by anti-rat-biotinilated secondary antibody (1:100, Biotin-SP-AffiniPure F(ab')2 Fragment Rabbit Anti-rat IgG, Vector laboratories, BA-4001). The signal was amplified with tyramide coupled with Flourescein (E8.5, E9.5, E10.5). Sections were then stained with α-SMA-Cy3 (1:200, Sigma-Aldrich, C6198) and IB4-647 (1:200, Invitrogen, I32450). Total cells (DAPI) and BrdU-positive cells in the myocardium or in the endocardium of developing hearts were counted on non-consecutive sections (≥ 3) in 4-5 control and 4-5 $Nrg1^{flox};Tie2^{Cre}$ embryos using Fiji (Image J plugging). Statistical analyses were performed using unpaired two-tailed Student´s *t*-test. Data are presented as means ± SD. Differences were considered statistically significant at $P < 0.05$.

Quantification of compact myocardium thickness and trabecular length

We analysed 7 µm paraffin sections from E9.5 (n=4) and E10.5 (n=5) control and *Nrg1^{flox};Tie2^{Cre}* hearts were stained with α-SMA-Cy3 and IB4-647 to allow identification of ventricular structures. In E16.5 (n=5) control and *Nrg1^{flox};Cdh5^{Cre}* hearts, endocardial cells were stained with anti-ENDOMUCIN and myocardial cells with anti-cTNT. Quantification of the compact myocardium thickness was performed using Fiji (ImageJ plugging). Right and left ventricles were quantified separately. 4 regions of each ventricle (at E9.5 and E10.5) were counted in 3 non-consecutive sections for control and *Nrg1^{flox};Tie2^{Cre}* hearts. For E16.5 control and *Nrg1^{flox};Cdh5^{Cre}* embryos, 6 regions of each ventricle were counted. The mean was expressed in µm. The quantification of the trabecular length was done at E9.5 and E10.5 in 3 non-consecutive sections for control and *Nrg1^{flox};Tie2^{Cre}* mutants of the same embryos. Data are presented as mean ± SD. A *P* value of <0.05 was considered significant.

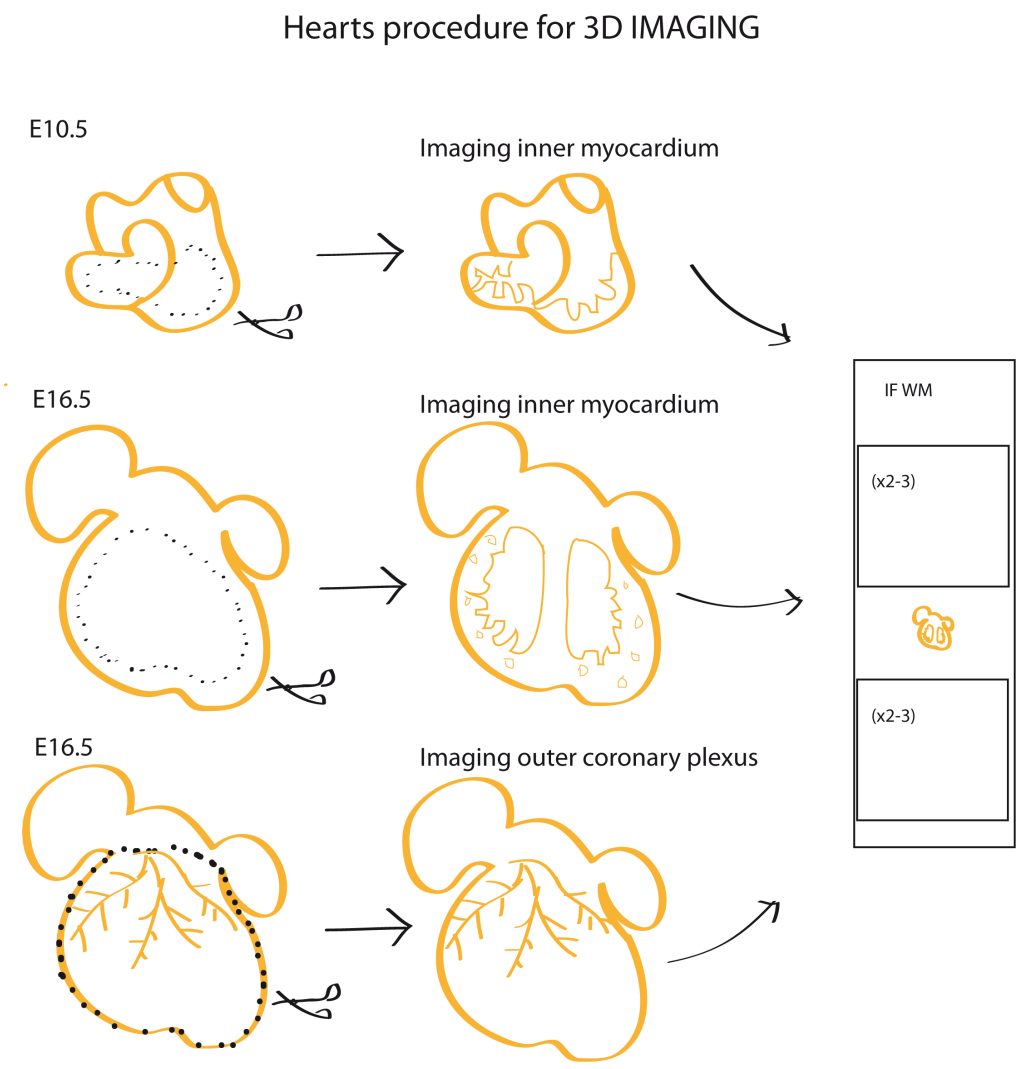

Scheme 2. Hearts procedure for 3D imaging

AVC area quantification

With Alcian blue staining we were able to distinguish the area of mesenchymal cells that form the endocardial cushions of the heart valves. We performed the quantification of 4 control and 4 *Nrg1^{flox};Tie2^{Cre}* embryos at E9.5 and E10.5 analysis. We quantified 3 non-consecutive sections in each heart using Fiji (ImageJ pluggin). The final results are shown in area (mm^2). Data are presented as mean ± SD. A *P* value of <0.05 was considered significant.

ITGα6 quantification

We used the IF of ITGα6, α-SMA, IB4 and DAPI at E9.5 control and *Nrg1^{flox};Tie2^{Cre}* embryos to do the quantification. The area of ITGα6 was measured using Fiji (ImageJ plugging). The region of interest was selected considering the area with myocardial marker staining (α-SMA), a threshold was stablished to select the area to measure the signal of ITGα6 (positive green signal in the myocardial region). This was done in 3 embryos per genotype, in 3 non-consecutive sections, and in 3 comparative myocardial regions per section (from right, medium and left regions of the ventricle). The final results are shown in area (mm^2). Data are presented as mean ± SD. A *P* value of <0.05 was considered significant.

N-CADHERIN quantification

We used the IF of N-CADHERIN, WGA, IB4 and DAPI at E8.5 and E9.0 control and *Nrg1^{flox};Tie2^{Cre}* embryos to do the quantification. We quantified the area of N-CADHERIN signal in the basal region of cardiomyocytes compared with the total basal section of cardiomyocytes. We use WGA signal to have a reference of the cardiomyocyte membrane along the basal region of each section. This was done in 3 control and 4 *Nrg1^{flox};Tie2^{Cre}* embryos, in 3 non-consecutive sections, and in 3 comparative compact myocardium regions per section (from right, medium and left regions of the ventricle). The area was measured using Fiji (ImageJ plugging). The final results are shown in percentage. Data are presented as mean ± SD. A *P* value of <0.05 was considered significant.

OCD quantification

We used the IF of SURVIVIN (a marker of the mitotic plate), SMA, IB4 and DAPI at E8.5 and E9.5 control and *Nrg1^{flox};Tie2^{Cre}* embryos to do the quantification. To better show the mitotic cells, a discontinuous white line surrounds each cardiomyocyte in mitotic phase. A yellow line

indicates the orientation of the cardiomyocyte division, and a white line indicates the basal surface of cardiomyocyte to the lumen. The measurement of the angle between both lines will indicate the OCD type. Division plane oriented between angles of 70-90º to the basement membrane were classified as perpendicular, those between 20-70º as oblique, and those between 0-20º as parallel. The software used for measuring was Fiji (ImageJ plugging). Cardiomyocytes (α-SMA) in mitosis were carefully analysed in all epithelial myocardium at E8.5 or in the compact myocardium at E9.5. We quantified all cardiomyocytes in anaphase, telophase or cytokinesis, as it was easy to identify the orientation of the division. The final results are shown as percentage of each type of divisions (parallel, oblique and perpendicular) both at E8.5 and E9.5.

RNA-Seq

Embryos were dissected in PBS and rapidly kept in ice-cold. Hearts of E9.5 control and *Nrg1*^{flox}*;Tie2*^{Cre} embryos were separated from the rest of the body. Then RNA was extracted using the PicoPure RNA isolation kit (Thermofisher). We compared 4 pools of 6 hearts each pool. Libraries were sequenced in an Illumina HiSeq 2500 System sequencer using a 75bp single end elongation protocol. Sequenced reads were QC and pre-processed using Cutadapt v1.6 (Martin, 2011) to remove adaptor contaminants. Resulting reads were aligned against a mouse reference transcriptome, and gene expression quantified, using RSEM v1.2.3 (Li and Dewey, 2011). The reference transcriptome was based on release 91 of Ensemble gene annotations for genome assembly GRCm38. Differential gene expression was evaluated with the EdgeR package from Bioconductor (Robinson, McCarthy and Smyth, 2009). Genes showing altered expression with Benjamini-Hochberg adjusted *P* value <0.05 were considered to be differentially expressed. For the sets of differentially expressed genes, functional analyses were performed using Ingenuity Pathway Analysis software (Li and Dewey, 2011) and interested significantly enriched processes were selected according to their relevance for the biological processes under study. The R package GOPlot (Walter, Sánchez-Cabo and Ricote, 2015), was used to generate circular plots representing the relationships between genes and selected enriched processes.

Quantitative RT-PCR of E9.5 hearts

E9.5 control and *Nrg1*^{flox}*;Tie2*^{Cre} hearts were isolated and pooled into 3 replicates containing 6 hearts each replicate. RNA-seq samples were used to synthesize the cDNAs. First-strand cDNAs were synthesized using the High Capacity cDNA Reverse Transcription Kit (Applied Biosystems); each reaction was conducted with 0.5 μg total RNA per replicates and per genotype. Quantitative PCR was performed with Power SYBR Green Master Mix (Applied Biosystems,

4367659). Oligonucleotide sequences of Mouse-*Nrg1* are the following: GCCAGAGAAACCCCTGACTC (forward primer) and ATTTCCGAAGGGGGCGATTT (reverse primer). We used Mouse-*β-actin* as a housekeeping gene and the oligonucleotide sequences are the following: CTAAGGCCAACCGTGAAAG (forward primer) and ACCAGAGGCATACAGGGAC (reverse primer). Experiments were performed with triplicate samples. Statistical analyses were performed using unpaired two-tailed t-test to assess differences between two groups. Data are presented as mean ± SD. A *P* value of <0.05 was considered significant.

Confocal imaging

Confocal images of whole-embryos and tissue sections were acquired with a Nikon A1R laser scanning confocal microscope with a 10X, 20X and 60X objectives, and with a Zeiss 780 confocal microscope fitted with a 20X objective with a dipping lens with a NIS-Element SD Image Software. Images of N-CADHERIN, SURVIVIN, ITGα6 and the whole mounts (WM) were collected as Z-stacks. Z-stacks of WM were taken every 2 μm (E10.5 hearts) or every 1-10 μm (E16.5 hearts). Z-projections and 3D images were assembled using Fiji (ImageJ plugging) and with IMARIS software (Bitplane Scientific Software). Images were processed in Adobe Photoshop Creative Suit 5.1 and Fiji (ImageJ plugging).

Bright field images

Images of the H&E, Alcian blue and ISH staining's were acquired with an Olympus BX51 coupled to a Nikon DP71 camera and cellSens software.

Statistics

Statistical analyses were performed using Student´s t test inGraph Pad (Prism 5.0). Data are presented as mean ± S.D., unless otherwise indicated. Differences were considered statistically significant at P value of <0.05.

RESULTS

Endothelial *Nrg1* deletion disrupts trabeculation

NRG1 is essential for trabeculation (Gassmann *et al.*, 1995; Lee *et al.*, 1995; Meyer and Birchmeier, 1995). We have used a conditional knock-out mouse line for *Nrg1* that harbours *loxP* sites flanking exons 9-11 of the *Nrg1* gene (Cheret *et al.*, 2013). To study the biological function of NRG1, we have disrupted *Nrg1* in the endocardium and vascular endothelium using the $Tie2^{Cre}$ driver line (Kisanuki *et al.*, 2001). We have analysed the viability of the $Nrg1^{flox};Tie2^{Cre}$ embryos and found that this genotype is embryonic lethal at E11.5 (Table 4).

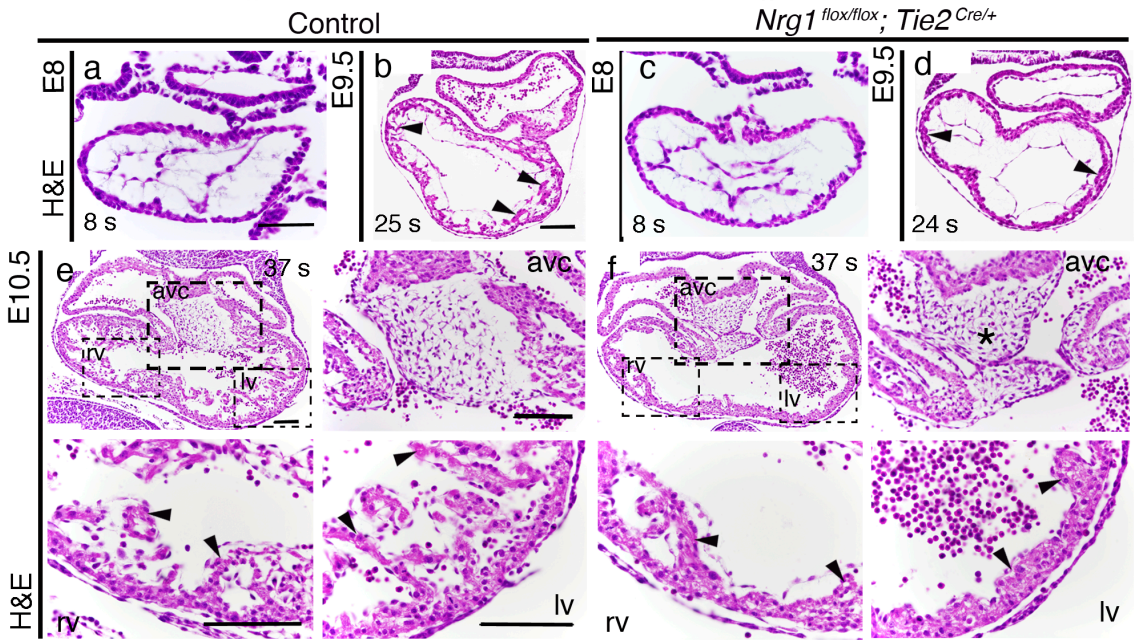

Figure 7. After *Nrg1* deletion, the ventricular myocardium is underdeveloped

a-f) H&E staining in transversal paraffin sections. a and b) E8.0 and E9.5 control hearts. c and d) E8.0 and E9.5 $Nrg1^{flox};Tie2^{Cre}$ mutant hearts, with no trabeculae in the ventricle at E9.5. e and f) E10.5 control and $Nrg1^{flox};Tie2^{Cre}$ hearts, insets are magnifications of avc, rv and lv. Asterisk in avc inset indicates shorter area of endocardial cushions. Arrowheads in the magnifications indicate the prominent trabeculae in control heart and the small myocardial protrusions in $Nrg1^{flox};Tie2^{Cre}$ ventricle. s, somites; H&E, Hematoxylin & Eosin; lv, left ventricle; rv, right ventricle; avc, atrioventricular canal. Scale bars: 100 µm (a-f and insets).

Histological analysis by H&E staining at E8.0 showed no obvious abnormalities in the myocardium or in the endocardium (Figure 7a and c). At E9.5, trabeculae were poorly developed in the $Nrg1^{flox};Tie2^{Cre}$ mutant heart (Figure 7d) compared with the control (Figure 7b). At E10.5, developing trabeculae were evident in the control heart (Figure 7e, rv and lv insets), but trabeculation defects were clear in $Nrg1^{flox};Tie2^{Cre}$ mutants (Figure 7f, rv and lv insets).

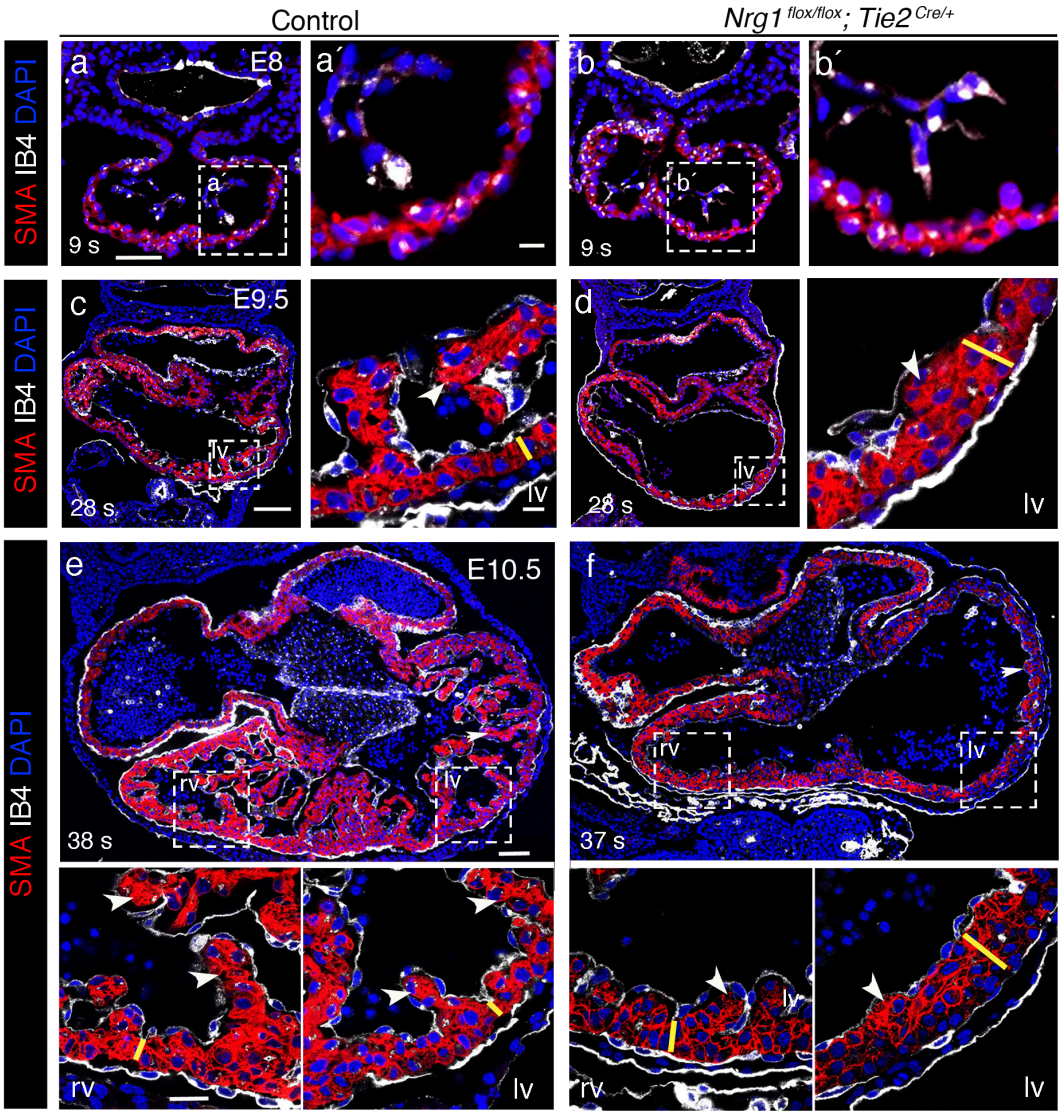
Control
Nrg1 flox/flox; Tie2 Cre/+
SMA IB4 DAPI
a
E8
a´
b
b´
9 s
c
E9.5
d
28 s
lv
e
E10.5
f
38 s
37 s
rv
lv

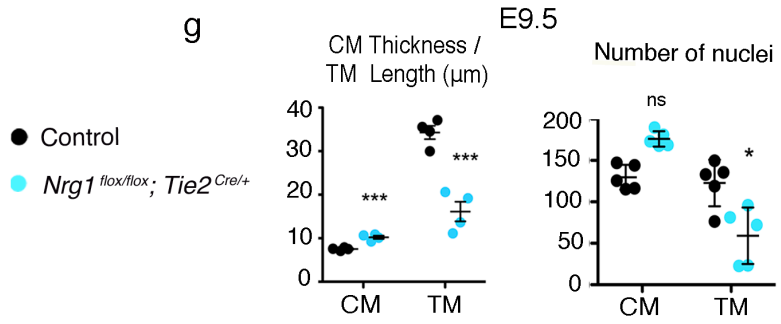
g
E9.5
Control
Nrg1 flox/flox; Tie2 Cre/+
CM Thickness / TM Length (µm)
Number of nuclei
ns
***
*
CM
TM

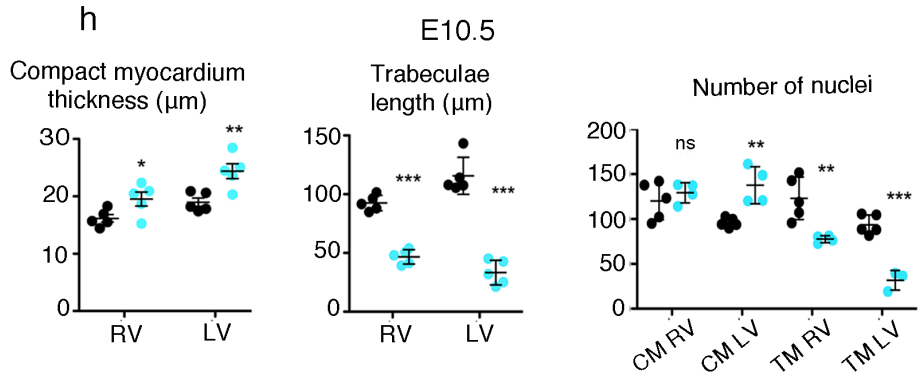
h
E10.5
Compact myocardium thickness (µm)
Trabeculae length (µm)
Number of nuclei
RV
LV
CM RV
CM LV
TM RV
TM LV

Figure 8. *Nrg1* deletion in the endocardium impairs trabeculation and compact myocardium appears thicker

a-f) Immunofluorescence (IF) in heart paraffin sections of SMA to detect myocardium (red), IB4 for endocardium (white) and DAPI for nuclei (blue). Control and *Nrg1^{flox};Tie2^{Cre}* mutant hearts at E8.5 (a and b), E9.5 (c and d) and E10.5 (e and f). Insets shows magnification of the myocardium at E8.5 (a´ and b´), of lv at E9.5 and of the rv and lv at E10.5. Arrowheads indicate the trabeculae in the ventricles. Yellow line represents the thickness of the CM region. g and h) Quantification of the thickness of the CM, the length of the trabeculae and the number of nuclei in control and *Nrg1^{flox};Tie2^{Cre}* mutant hearts at E9.5 and E10.5, respectively. Asterixs indicate significant result (*, P<0.05; **, P<0.01; ***, P<0.0001). SMA, smooth muscle actin; IB4, Isolectin B4; s, somites; lv/LV, left ventricle; rv/RV, right ventricle; CM, compact myocardium; TM, trabecular myocardium; ns, no significant. Scale bars: 50 μm (a, b), 10 μm (a´, b´, and c and d insets), 100 μm (c, d, e, f), 25μm (insets of e, f).

We observed less cellularized AVC cushion mesenchyme in E10.5 *Nrg1^{flox};Tie2^{Cre}* hearts (Figure 7f, avc inset) compared with AVC region in control hearts (Figure 7e, avc inset).

In order to examine if the myocardium and endocardium of *Nrg1^{flox};Tie2^{Cre}* mutant embryos express tissue identity markers, we performed IF for the myocardium marker alpha-smooth muscle actin (α-SMA) and the endothelial marker Isolectin B4 (IB4) during early embryonic stages. At E8.5, *Nrg1^{flox};Tie2^{Cre}* mutant embryos showed no apparent malformations in the myocardium or the endocardium (Figure 8b and b´) compared with control embryos (Figure 8a and a´). In contrast, at E9.5 ventricular chamber in *Nrg1^{flox};Tie2^{Cre}* mutants showed very small or collapsed trabeculae (Figure 8d and lv inset), compared with the growing trabeculae in control ventricles (Figure 8c and lv inset). Myocardium thickness was significantly increased in E9.5 *Nrg1^{flox};Tie2^{Cre}* mutant hearts and presented significantly shorter trabeculae (Figure 8g). This phenotype was even more evident at E10.5, when a trabecular network was well developed in control ventricles (Figure 8e and insets), but *Nrg1^{flox};Tie2^{Cre}* mutants showed severely reduced trabeculation (Figure 8f and insets). At this stage, the compact myocardium in *Nrg1^{flox};Tie2^{Cre}* embryos was significantly thicker in mutant ventricles, that also showed significantly reduced trabecular length (Figure 8h). The quantification of the number of nuclei tended to be increased in the mutant compact myocardium at E9.5, and was significantly reduced in trabecular cardiomyocytes, which was consistent with the shortened trabeculae (Figure 8g). At E10.5, the number of nuclei was significantly increased in the left compact myocardium, which normally presents a stronger phenotype, and was significantly reduced in both right and left trabecular myocardium (Figure 8h).

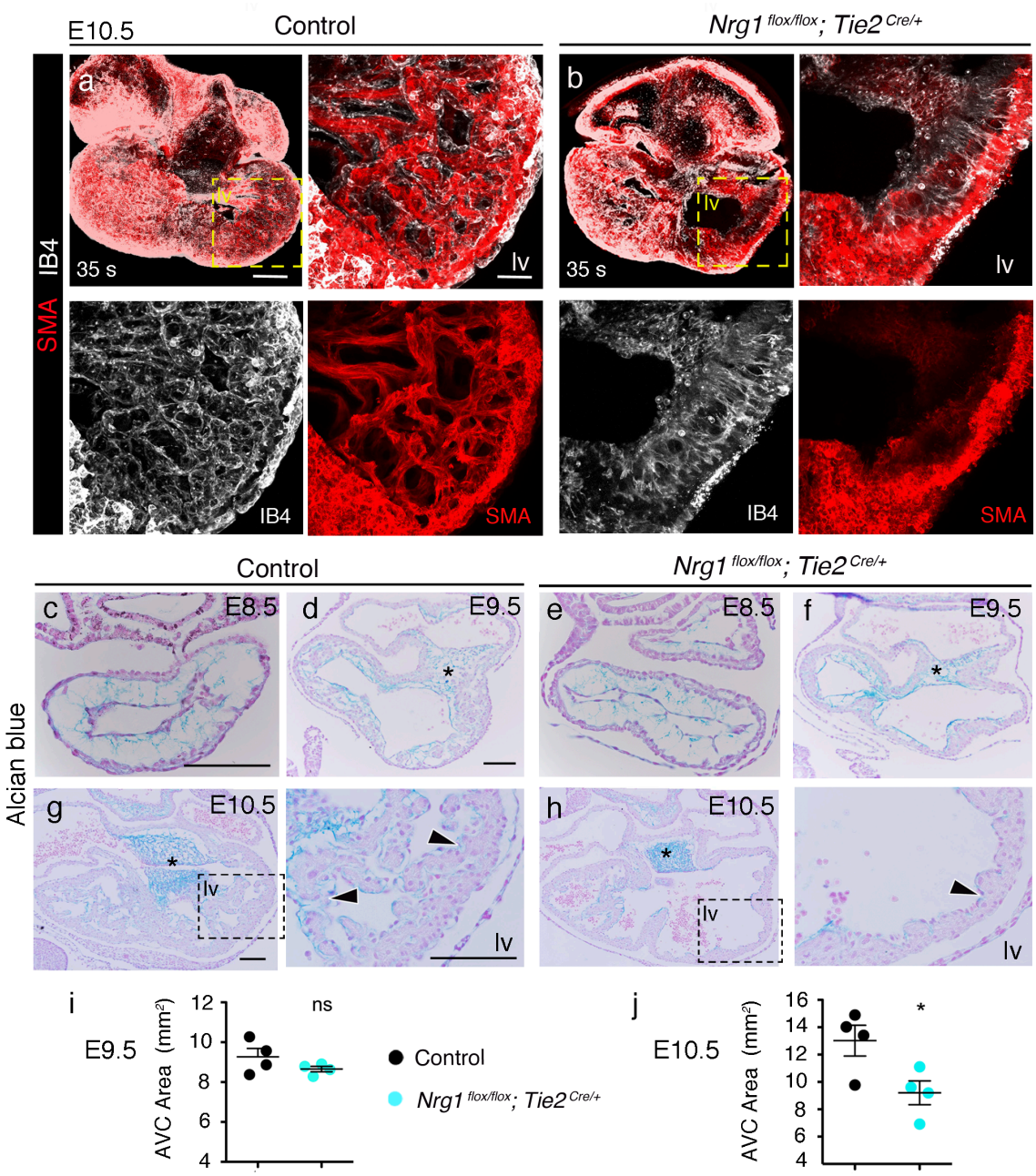

We then performed IF of the myocardium and endothelial markers SMA and IB4 in WM embryos at E10.5, to get a better impression of the chamber phenotype of mutant hearts. Control hearts showed a well-developed trabecular meshwork (Figure 9a and lv insets). In contrast, trabeculae were underdeveloped and the ventricular lumen was almost devoid of trabeculae in *Nrg1*^{flox};*Tie2*^{Cre} mutant hearts (Figure 9b and lv insets).

NRG1 is implicated in extracellular matrix (ECM) secretion (del Monte-Nieto *et al.*, 2018). Based on the important role of ECM in the trabeculation process, we analysed the cardiac jelly, predicting a decrease in ECM region in *Nrg1*^{flox};*Tie2*^{Cre} mutants.

Figure 9. *Nrg1* deletion affects ECM secretion

a-b) Whole mount (WM) IF at E10.5 (35ps) with SMA for myocardium (red) and IB4 for endocardial cells (white). a) Control heart is a Z-projection of 114 µm, region of lv is a Z-stack of 204 µm. b) E10.5 *Nrg1^{flox};Tie2^{Cre}* mutant heart is a Z-projection of 126 µm, region of lv is the Z-stack of 176 µm. The different channels are shown separately. c-h) Alcian blue staining in paraffin sections. c) E8.5 control heart with the ECM similar to *Nrg1^{flox};Tie2^{Cre}* mutant heart (e). d and f) E9.5 control and *Nrg1^{flox};Tie2^{Cre}* mutant heart, asterix indicates the AVC region. g and h) E10.5 control and *Nrg1^{flox};Tie2^{Cre}* mutant hearts, the inset shows a magnification of the lv. Arrowheads indicate the ECM of the trabeculae, very reduced in *Nrg1^{flox};Tie2^{Cre}* mutant. i and j) Graphs representing the area of the AVC of the E9.5 and E10.5 hearts. Asterixs indicate significant result (*, P<0.05). s, somites; lv, left ventricle; SMA, smooth muscle actin; IB4, Isolectin B4; ns, no significant. Scale bars: 100 µm (lv insets of a and b, images c-h), 200 µm (a and b).

Alcian blue staining showed that ECM appeared normal at E8.5 in control and *Nrg1^{flox};Tie2^{Cre}* embryos (Figure 9c and e, respectively). At E9.5-E10.5, the ECM in the AVC region was reduced in *Nrg1^{flox};Tie2^{Cre}* hearts (Figure 9f, h) compared with control hearts (Figure 9d, g), being significantly reduced at E10.5 (Figure 9j) but not at E9.5 (Figure 9i). Alcian blue staining revealed a difference in the ECM distribution in the ventricles beginning at E9.5 (Figure 9d and f), that was more evident at E10.5 (Figure 9g, h and insets). These data indicate that *Nrg1* inactivation in the endocardium cause defective trabeculation and reduced ECM secretion.

NRG1-ERBB2 signalling pathway activation is disrupted in *Nrg1^{flox};Tie2^{Cre}* embryos

To confirm that *Nrg1* deletion was effective we examined NRG1 expression in *Nrg1^{flox};Tie2^{Cre}* mutant embryos. We first showed by qRT-PCR that *Nrg1* transcription was markedly reduced in mutant hearts (Figure 10a). Immunostaining revealed that NRG1 was expressed in the endocardium of control hearts (Figure 10b and lv insets), and was almost lost in *Nrg1^{flox};Tie2^{Cre}* mutants (Figure 10c and lv insets). NRG1 pathway activation occurs via the phosphorylation of the ERBB2 receptors in the myocardium after NRG1 release from the endocardium, and subsequent ERBB2-ERBB4 receptors dimerization (Riese and Stern, 1998). Immunostaining showed pERBB2 expression in the myocardium of E9.5 control hearts, as revealed by colocalization with the SMA myocardium marker (Figure 10d and lv insets). Expression was severely reduced in *Nrg1^{flox};Tie2^{Cre}* mutant hearts (Figure 10e and lv insets). These data confirmed that ERBB2 signalling activation in the myocardium was disrupted after *Nrg1* deletion in the endocardium.

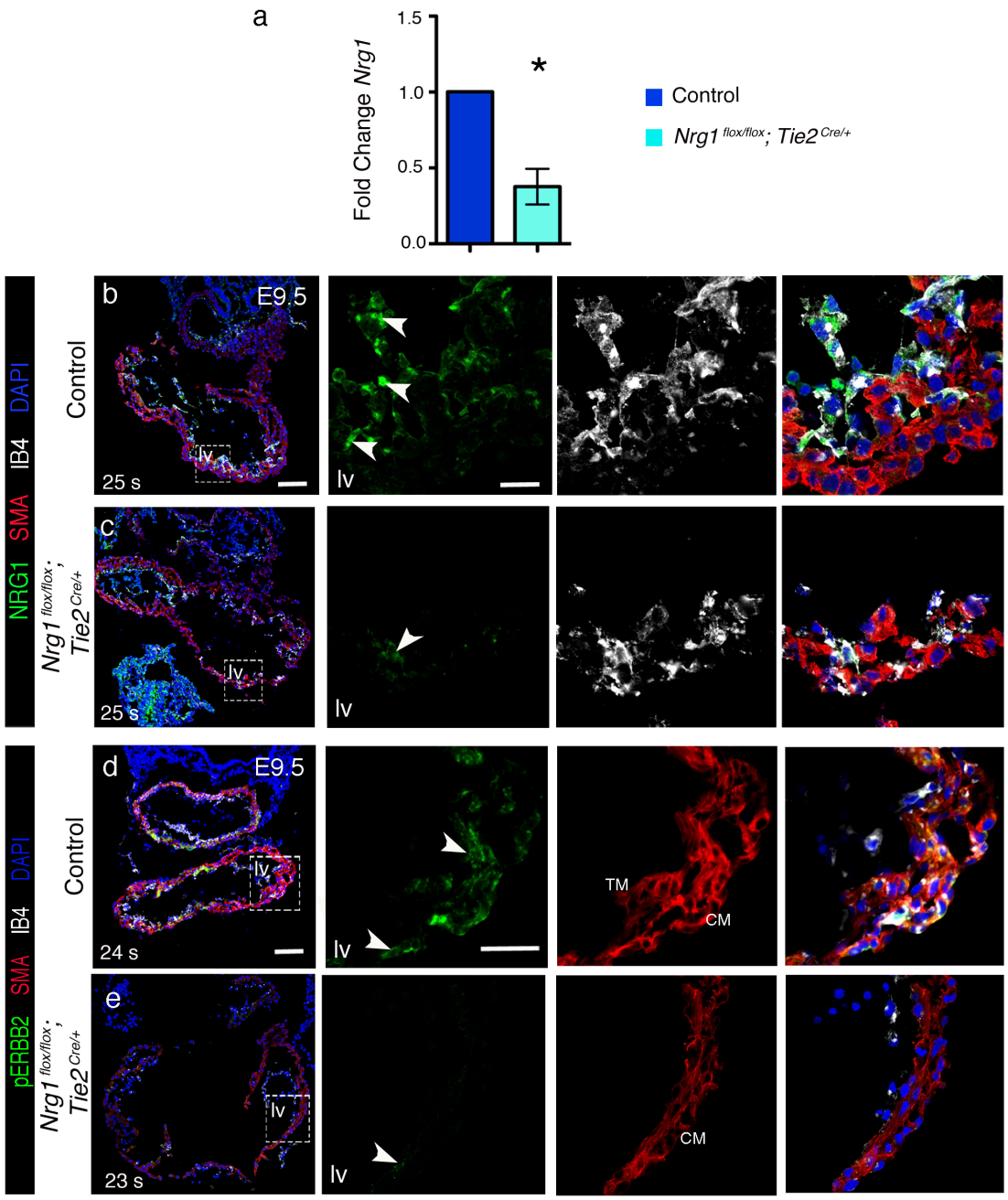

Figure 10. NRG1 signalling pathway is inactivated in *Nrg1^{flox};Tie2^{Cre}* mutants

a) Graph representing the RNA relative expression of *Nrg1* in E9.5 *Nrg1^{flox};Tie2^{Cre}* mutant hearts measured by qPCR. Asterix indicates significant result (*, P<0.05). b and c) NRG1 IF on cryosections in control and *Nrg1^{flox};Tie2^{Cre}* hearts at E9.5. Insets are magnifications of lv, and the different channels are shown separately, NRG1 (green), IB4 (white) and merge with SMA (red) and DAPI (blue). White arrowheads indicate NRG1 signal in the endocardium. d and e) pERBB2 signal in control and *Nrg1^{flox};Tie2^{Cre}* mutant hearts at E9.5. Insets are magnifications of lv, pERBB2 (green), SMA (red) and merge with IB4 (white) and DAPI (blue). White arrowheads indicate ERBB2 activation the myocardium. SMA, smooth muscle actin; IB4, Isolectin B4; s, somites; lv, left ventricle; NRG1, NEUREGULIN1. Scale bar: 100 µm (b, c, d and e), 50 µm (all insets).

Myocardial patterning is lost after *Nrg1* deletion in the endocardium

We then examined whether endocardial identity was affected after *Nrg1* deletion in the endocardium.

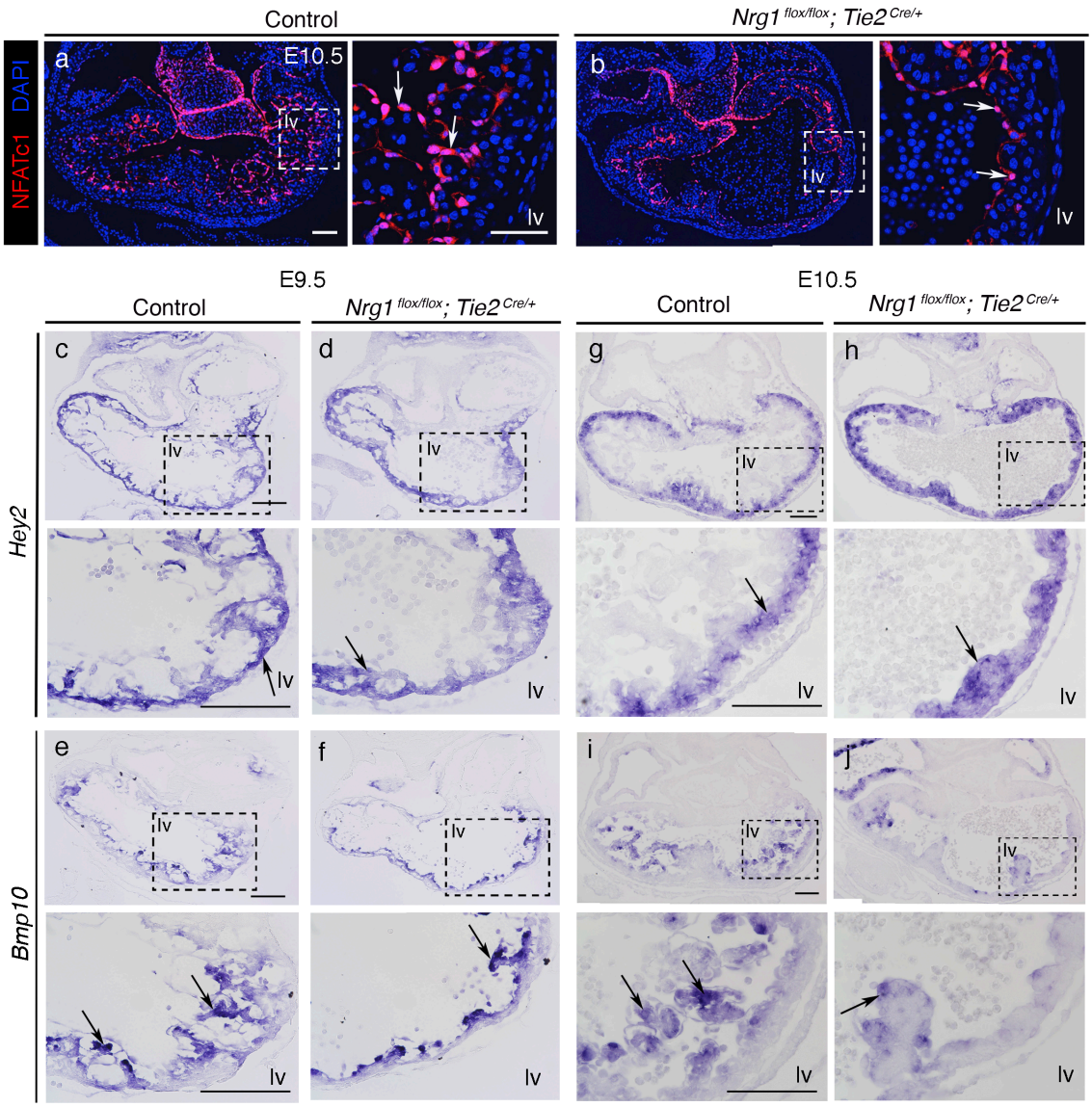

Figure 11. Myocardial patterning is disrupted after *Nrg1* deletion in the endocardium

a and b) NFATc1 IF at E10.5 in control and *Nrg1^{flox};*Tie2Cr paraffin sections. White arrows indicate nuclear signal. Insets are magnifications of lv. c-f) E9.5 and (g-j) E10.5 *in situ* hybridization (ISH) on paraffin sections. Insets are magnifications of lv. *Hey2* in control hearts (c, g and insets), arrow indicates the signal restricted to the CM. Arrows in *Nrg1^{flox};Tie2^{Cre}* mutant embryos (d, h and insets), show *Hey2* expression in the small projection in mutant ventricle. *Bmp10* signal in TM in control (e, i and insets) and *Nrg1^{flox};Tie2^{Cre}* mutant (f, j and insets) hearts. Arrows indicate trabecular signal in control hearts and signal in the tip of the trabeculae in mutants. lv, left ventricle. Scale bars: 100 µm (a-j), and 50 µm (all insets).

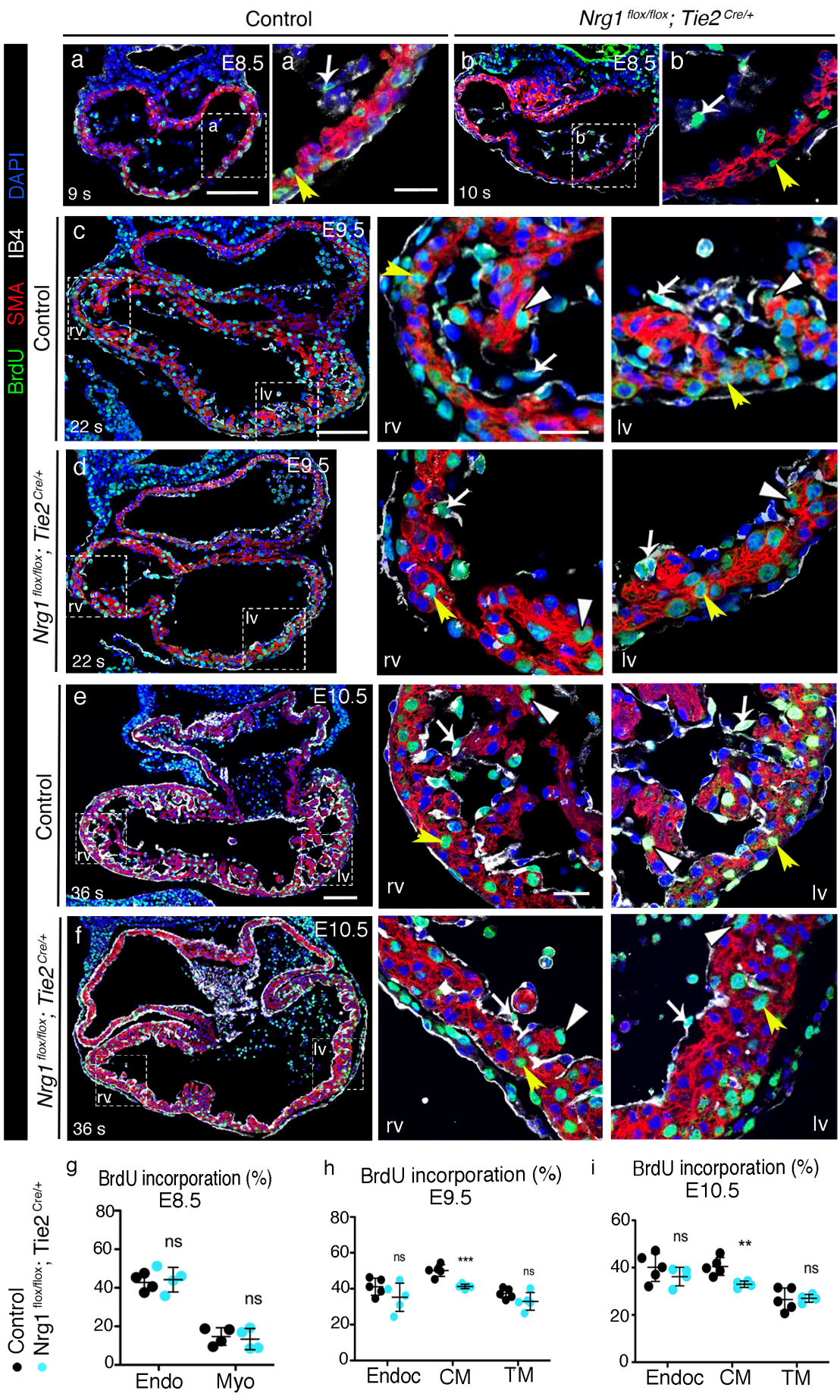
Control
Nrg1 flox/flox; Tie2 Cre/+
BrdU SMA IB4 DAPI
Control
Nrg1 flox/flox; Tie2 Cre/+
Control
Nrg1 flox/flox; Tie2 Cre/+
a
E8.5
a´
9 s
b
E8.5
b´
10 s
c
E9.5
rv
lv
22 s
d
E9.5
22 s
e
E10.5
36 s
f
E10.5
36 s
rv
lv
g
BrdU incorporation (%)
E8.5
ns
ns
Endo
Myo
h
BrdU incorporation (%)
E9.5
ns
***
ns
Endoc
CM
TM
i
BrdU incorporation (%)
E10.5
ns
**
ns
Endoc
CM
TM
Control
Nrg1 flox/flox; Tie2 Cre/+

Figure 12. Compact myocardium proliferation is reduced in *Nrg1^{flox};Tie2^{Cre}* mutants

a-f) IF of BrdU (green), SMA (red), IB4 (white), and DAPI (blue) in control and *Nrg1^{flox};Tie2^{Cre}* mutant hearts paraffin sections at E8.5 (a and b), E9.5 (c and d) and E10.5 (e and f). Insets show ventricle magnification in a´ and b´ or rv and lv magnifications in c-f. White arrows indicate proliferating endocardial cells, yellow arrowheads indicate proliferating CM cells and white arrowheads indicate proliferating TM cells. g-i) Quantification of the BrdU incorporation % in endocardium and myocardium are represented in g (E8.5), h (E9.5) and i (E10.5). Asterixs indicate significant result (**, P<0.01; ***, P<0.0001). SMA, smooth muscle actin; IB4, Isolectin B4; rv, right ventricle; lv, left ventricle; s, somites; ns, no significant. Scale bars: 100 µm (a, b, c, d, e and f), 25 µm (all insets).

We performed IF for NFATc1, that is the earliest endocardial differentiation marker (De La Pompa *et al.*, 1998; Ranger *et al.*, 1998) and we noticed similar nuclear distribution throughout both chamber and valve endocardium, both in control and *Nrg1^{flox};Tie2^{Cre}* hearts at E10.5 (Figure 11a and b and insets), indicating that endocardial identity is unaffected in *Nrg1^{flox};Tie2^{Cre}* mutants.

To analyse whether myocardial patterning was affected in *Nrg1^{flox};Tie2^{Cre}* embryos, we examined by *in situ* hybridization (ISH) the expression of early compact and trabecular markers. *Hey2*, a compact myocardium marker (Koibuchi and Chin, 2007) was expanded into the small trabecular projections of *Nrg1^{flox};Tie2^{Cre}* mutant embryos, both at E9.5 and E10.5 (Figure 11d, h and insets), compared to control embryos (Figure 11c and g). In contrast, expression of the trabecular marker *Bmp10* (Chen, 2004) was limited to the tip of the few trabeculae present in E9.5-10.5 *Nrg1^{flox};Tie2^{Cre}* mutants (Figure 11f, j and insets) compared to its strong trabecular expression in control hearts (Figure 11e and i and insets). These changes suggest that NRG1-ERBB2 signalling inactivation disrupts myocardial patterning during trabeculation.

As trabecular development and compact myocardium thickness were altered, we examined cardiac proliferation during trabeculation (E8.5-10.5) in *Nrg1^{flox};Tie2^{Cre}* mutant embryos. 5-bromo-2'-deoxyuridine (BrdU) incorporation analysis showed that endocardial and myocardial proliferation was relatively normal in E8.5 embryos (Figure 12a, a´, b, b´ and g). At E9.5, proliferation in the compact myocardium was reduced in *Nrg1^{flox};Tie2^{Cre}* mutant hearts (Figure 12d, insets and h) compared with control hearts (Figure 12c, insets and h). At E9.5-E10.5, we did not detect significant changes in proliferation of the endocardium, nor in the trabecular myocardium (Figure 12h and i). By E10.5, we detected significantly reduced proliferation in *Nrg1^{flox};Tie2^{Cre}* mutant compact myocardium (Figure 12f, insets and i) compared with the compact myocardium in control embryos (Figure 12e, insets and i). In these images of the proliferative ventricle, it can also be detected the increased thickness of the compact myocardium in *Nrg1^{flox};Tie2^{Cre}* mutants (Figure 12f, rv and lv insets). Thus, the diminished proliferation in the

compact myocardium of the *Nrg1*^{flox};*Tie2*^{Cre} mutant embryos could be involved in the defective trabeculation of these mice.

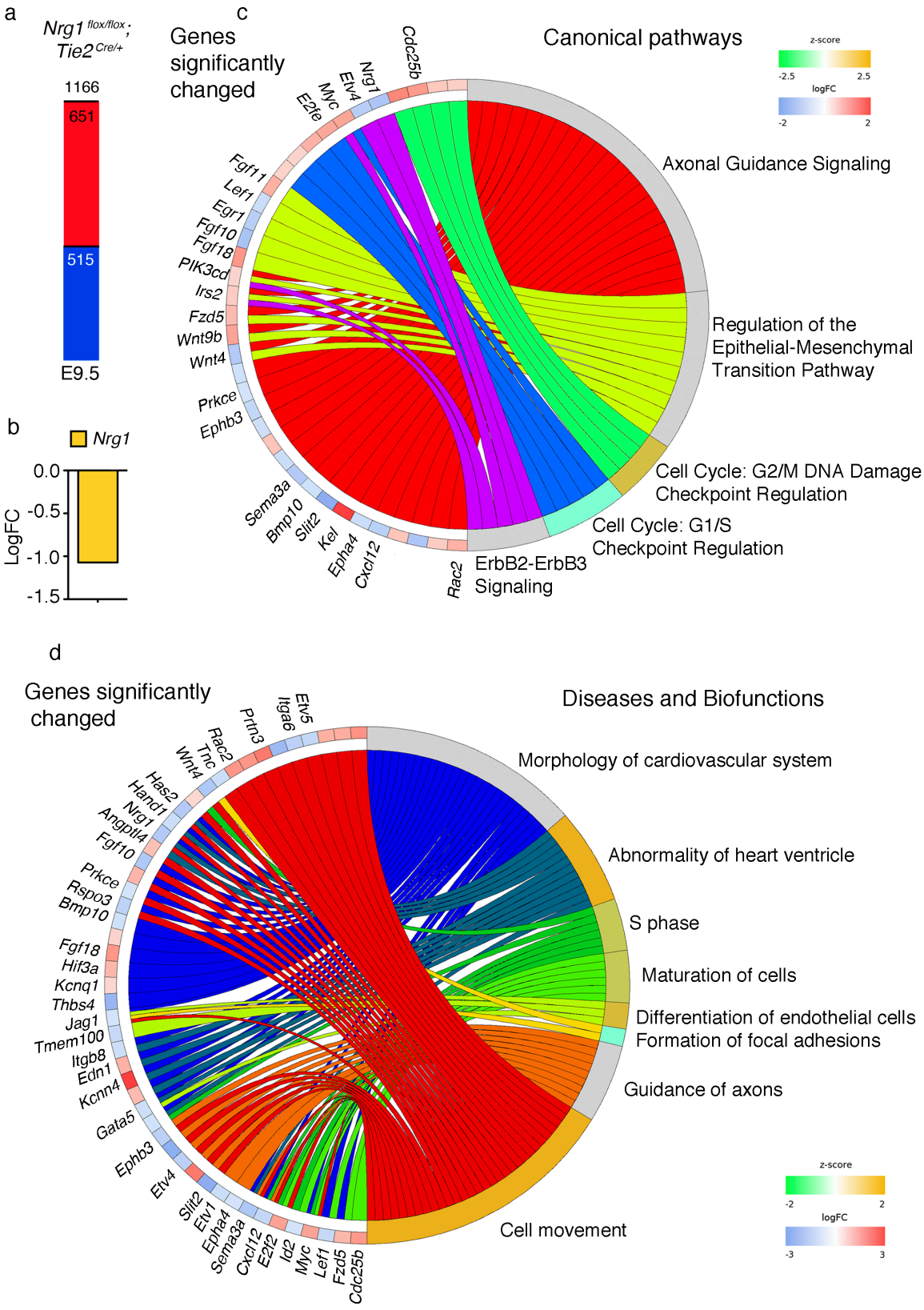

Transcriptome analysis of E9.5 control and *Nrg1^{flox};Tie2^{Cre}* hearts indicates that NRG1-ERBB signalling is implicated in EMT, proliferation and migration

To identify the genes whose expression depends on NRG1-ERBB signalling during cardiac development, we carried out a RNA sequencing experiment (RNA-seq) with E9.5 control and *Nrg1^{flox};Tie2^{Cre}* mutant hearts. We found 1,166 differentially expressed genes in *Nrg1^{flox};Tie2^{Cre}* mutants (651 upregulated, 515 downregulated; $P < 0.05$, Figure 13a). Ingenuity Pathway Analysis (IPA) revealed that several genes whose expression was significantly altered belonged to the NRG1-ERBB signalling pathway, including *Nrg1* (Figure 13b, c). Other affected pathways were involved in cell cycle regulation, EMT and axonal guidance (Figure 13c). In addition, IPA analysis revealed that several genes involved in functions such as cardiovascular system development, heart ventricle, S phase of cell cycle, maturation of cells, differentiation of endothelial cells, formation of focal adhesions, guidance of axons and cell movements, were altered in *Nrg1^{flox};Tie2^{Cre}* mutant embryos (Figure 13d). Interestingly, the dysregulation of molecules implicated in cell cycle is compatible with our previous results showing reduced proliferation of the compact myocardium in *Nrg1^{flox};Tie2^{Cre}* mutants (Figure 12).

Endocardium-myocardium communication involves the ECM (Camenisch *et al.*, 2002; del Monte-Nieto *et al.*, 2018) and several ECM markers were downregulated in *Nrg1^{flox};Tie2^{Cre}* mutant hearts (Figure 14a). We validated by ISH the expression of *Has2*, whose expression was reduced in the endocardium and myocardium of *Nrg1^{flox};Tie2^{Cre}* mutants (Figure 14d, e and insets). We confirmed that specific markers for trabeculae were diminished in *Nrg1^{flox};Tie2^{Cre}* mutant hearts in the RNA-seq, such as *Bmp10*, *Hand1*, *Itgα6*, *Irx3*, *Thbs4* and *Slit2* (Figure 14b). We have previously observed the downregulation of *Bmp10* by ISH (Figure 11f, j and insets). In addition, *Irx3* expression was nearly absent in trabecular myocardium in *Nrg1^{flox};Tie2^{Cre}* mutants compared with control hearts (Figure 14f, g).

Figure 13. Global gene expression analysis by RNA-seq shows that affected genes are implicated in ERBB2-ERBB3 signalling, EMT, cell cycle, and axonal guidance

a) Chart showing the number of deregulated genes ($P<0.05$) in E9.5 *Nrg1^{flox};Tie2^{Cre}* hearts; red, UP and blue, DOWN. b) RNA-seq data graph showing *Nrg1* downregulation in *Nrg1^{flox};Tie2^{Cre}* mutants at E9.5. c) Circular plot of 24 differentially expressed genes, simultaneously representing a detailed view of the relationships between expression changes (left semicircle perimeter) and canonical pathways (right semicircle perimeter). d) Circular plot of 37 differentially expressed genes, simultaneously presenting a detailed view of the relationships between expression changes (left semicircle perimeter) and diseases and biofunctions (right semicircle perimeter).

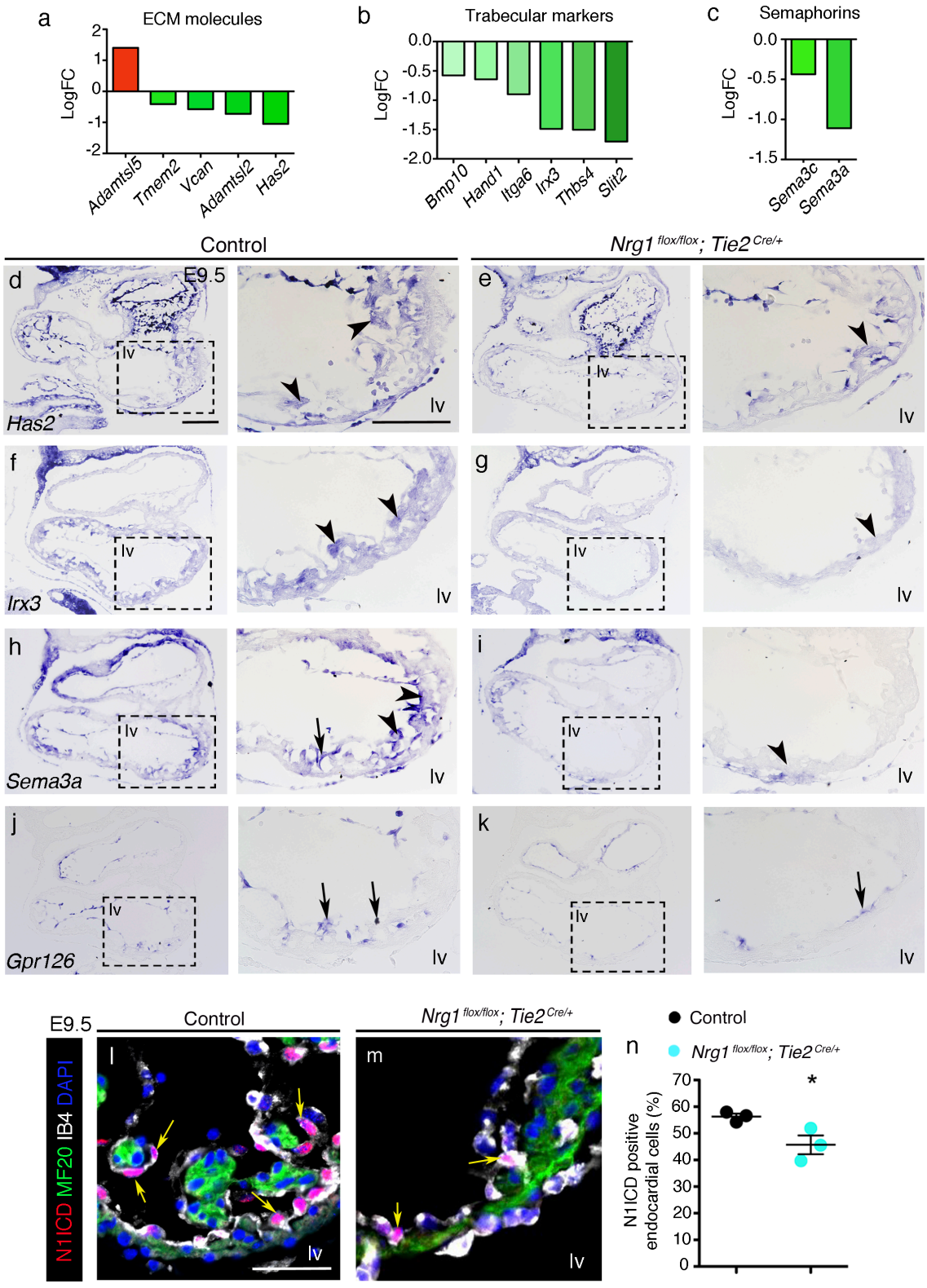

RNA-seq data showed downregulation of *Sema3a* and Sema*3c* in *Nrg1*^{flox};*Tie2*^{Cre} mutants (Figure 14c). By ISH, we confirmed that *Sema3a* was expressed in the endocardium and myocardium in E9.5 control ventricles (Figure 14h and inset), by contrast expression was almost lost in

Figure 14. Extracellular matrix molecules, chambers markers and N1ICD signalling are downregulated in *Nrg1^{flox};Tie2^{Cre}* mutants

a-c) Graphs representing several markers dysregulated in the RNA-seq data from E9.5 hearts. ECM molecules (a) and trabecular markers (b and c) are downregulated in *Nrg1^{flox};Tie2^{Cre}* embryos. d-k) ISH in E9.5 paraffin sections in controls and *Nrg1^{flox};Tie2^{Cre}* mutants of *Has2* (d and e), *Irx3* (f and g), *Sema3a* (h and i), and *Gpr126* (j and k). The insets show a magnification of the lv. Black arrowheads indicate the signal in the myocardium and black arrows in the endocardium. l and m) IF of N1ICD (red), MF20 (green), IB4 (white) and DAPI (blue) at E9.5 in control and *Nrg1^{flox};Tie2^{Cre}* mutant paraffin sections, region of the lv is represented. Yellow arrows indicate the signal in the endocardium. n) Quantification of N1ICD in the endocardium at E9.5. Asterix indicates significant result (*, P<0.05). lv, left ventricle; IB4, Isolectin B4. Scale bar: 100 µm (d-k and insets), 50 µm (l and m)

Nrg1^{flox};Tie2^{Cre} mutant ventricle (Figure 14i and inset), suggesting a crosstalk between NRG1-ERBB and SEMAPHORINS signalling during trabeculation.

RNA-seq data also showed that *Jag1*, a ligand for NOTCH, was downregulated in *Nrg1^{flox};Tie2^{Cre}* mutant hearts (Figure 13d), thus we stained for NOTCH signalling activity, using an antibody against the activated NOTCH1 receptor (N1ICD). We performed IF for N1ICD at E9.5, and we observed a significant downregulation of N1ICD in the endocardium of *Nrg1^{flox};Tie2^{Cre}* mutant hearts (Figure 14l, m and n). In addition, the G protein coupled receptor *Gpr126*, expressed in chamber endocardium (Waller-Evans *et al.*, 2010), functions downstream of NOTCH signalling during trabeculation (D'Amato *et al.*, 2016). We analysed whether *Gpr126* expression was affected after *Nrg1* deletion. ISH of *Gpr126* at E9.5 showed a weak signal in *Nrg1^{flox};Tie2^{Cre}* mutant endocardium (Figure 14k and inset) compared to the control (Figure 14j and inset). These data suggest that NRG1, signalling to the myocardium, affects NOTCH signalling activity in the endocardium.

Cardiomyocyte polarity is disrupted after *Nrg1* deletion

Planar cell polarity (PCP) is the mechanism by which epithelial tissues become polarized in planes orthogonal to the apical-basal axis, and the PCP pathway is required for heart morphogenesis (Henderson and Chaudhry, 2011). E9.5 RNA-seq data provided us the intriguing result that the expression of PCP and cell polarity markers was deregulated in *Nrg1^{flox};Tie2^{Cre}* mutants (Figure 15a and a´). *Fzd5, Vangl1* and *Dvl1*, involved in the PCP pathway, were upregulated in *Nrg1^{flox};Tie2^{Cre}* mutant hearts (Figure 15a). On the contrary, expression of the PCP members *Wnt11*, *Rspo3* and *Wnt4*, was downregulated in *Nrg1^{flox};Tie2^{Cre}* mutants (Figure 15a). These results suggest that NRG1-ERBB signalling may regulate PCP molecules during trabeculation.

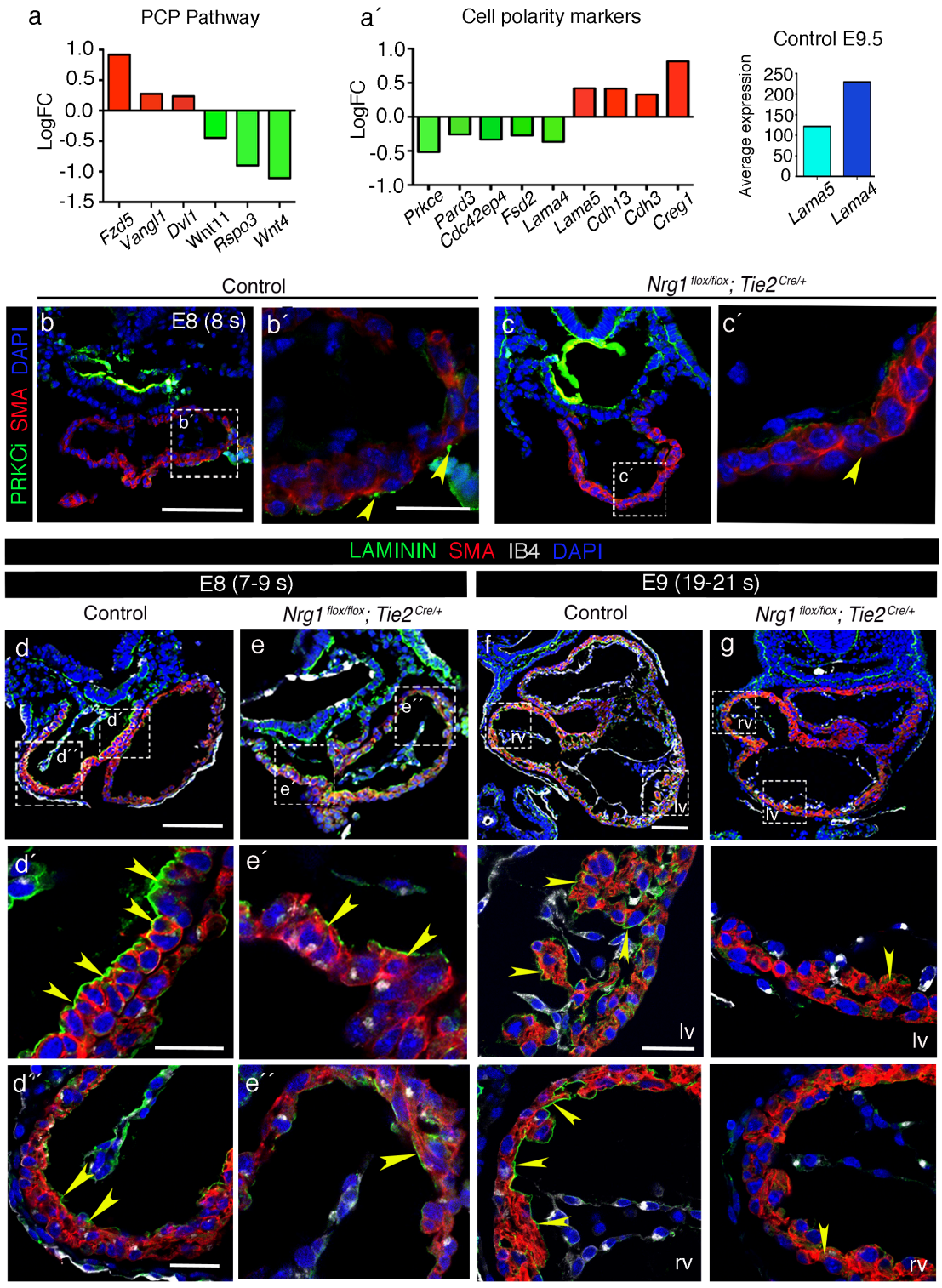

The PAR complex genes, *Pard3* and *Prkce*, involved in the establishment of cell polarity necessary for normal tissue generation and morphogenesis (Watts *et al.*, 1996), were downregulated in $Nrg1^{flox};Tie2^{Cre}$ mutant hearts (Figure 15a´), suggesting defective polarity in the heart of $Nrg1^{flox};Tie2^{Cre}$ mutant embryos. PKC is one of the components of the PAR Complex that orchestrate cell polarity (Watts *et al.*, 1996).

Figure 15. Cell polarity is affected in cardiomyocytes of *Nrg1^{flox};Tie2^{Cre}* mutant hearts

a and a´) Graphs from RNA-seq data analysis that show components of the PCP Pathway and cell polarity markers dysregulated in *Nrg1^{flox};Tie2^{Cre}* mutants. b and c) PRKCi expression in control and *Nrg1^{flox};Tie2^{Cre}* mutant heart cryosections at E8.5. Insets show a magnification of the ventricle (b´ and c´), yellow arrowheads indicate the expression of PRKCi. d-g) LAMININ IF (green) in paraffin sections, SMA (red), IB4 (white) and DAPI (blue). d-d´´ and e-e´´) Basal LAMININ staining in a 7-9 s control and *Nrg1^{flox};Tie2^{Cre}* mutant embryo. f and g) 19-21 s control and *Nrg1^{flox};Tie2^{Cre}* mutant embryo. Yellow arrowheads indicate LAMININ signal in the rv and lv magnification (insets of f and g). SMA, smooth muscle actin; IB4, Isolectin B4; rv, right ventricle; lv, left ventricle. Scale bars: 100 µm (b, c, d, e, f and g), 25 µm (b´, c´, d´, e´, d´´, e´´, insets f and g).

Interestingly, expression of *Cdc42*, target protein of PKC proteins (Macara, 2004), was also downregulated in *Nrg1^{flox};Tie2^{Cre}* mutants (Figure 15a´). It is described that the PAR complex localizes to the apical cortex in invertebrate and vertebrate epithelial cells (Doe and Siller, 2009). Then, we examined the distribution of PRKCi in the E8.0 heart, and found that was localized to the apical region of cardiomyocytes (facing the epicardium) in control hearts as expected (Figure 15b and b´). By contrast, PRKCi was absent in *Nrg1^{flox};Tie2^{Cre}* mutant hearts, consistent with the RNA-seq data (Figure 15c and c'), suggesting polarity defects.

Other molecules of interest were Cadherins (*Cadh13* and *Cdh3*) and *Creg1* (cellular repressor of E1A-stimulated genes 1) that are involved in *adherent* junction formation between cardiomyocytes (Liu *et al.*, 2016) and were found upregulated in *Nrg1^{flox};Tie2^{Cre}* embryos (Figure 15a´). These results suggest that the adherent junctions between cardiomyocyte were not well established in mutant ventricles and, as a consequence, cardiomyocyte movement during trabeculation was affected.

LAMININS are major components of basement membranes, that are essential for embryonic implantation, induction and maintenance of cell polarity, tissue morphogenesis, and organogenesis (Miner and Yurchenco, 2004). We also observed a dysregulation of *Laminins* expression in the RNA-seq data, as *Lama4* was downregulated, while *Lama5* was upregulated in *Nrg1^{flox};Tie2^{Cre}* mutant hearts (Figure 15a´). In contrast, *Lama4* was highly expressed in relation to *Lama5* in E9.5 control hearts (Figure 15a´). We carried out LAMININ IF and detected protein staining in the basement membrane of cardiomyocytes in E8.0 control hearts (Figure 15d, d´ and d´´). In contrast, LAMININ staining was patchy in *Nrg1^{flox};Tie2^{Cre}* mutants (Figure 15e, e´ and e´´). At E9.0, LAMININ expression was localized to the basement membrane of cardiomyocytes in control hearts (Figure 15f, lv and rv insets) but it was almost absent in *Nrg1^{flox};Tie2^{Cre}* mutant cardiomyocytes (Figure 15g, lv and rv insets).

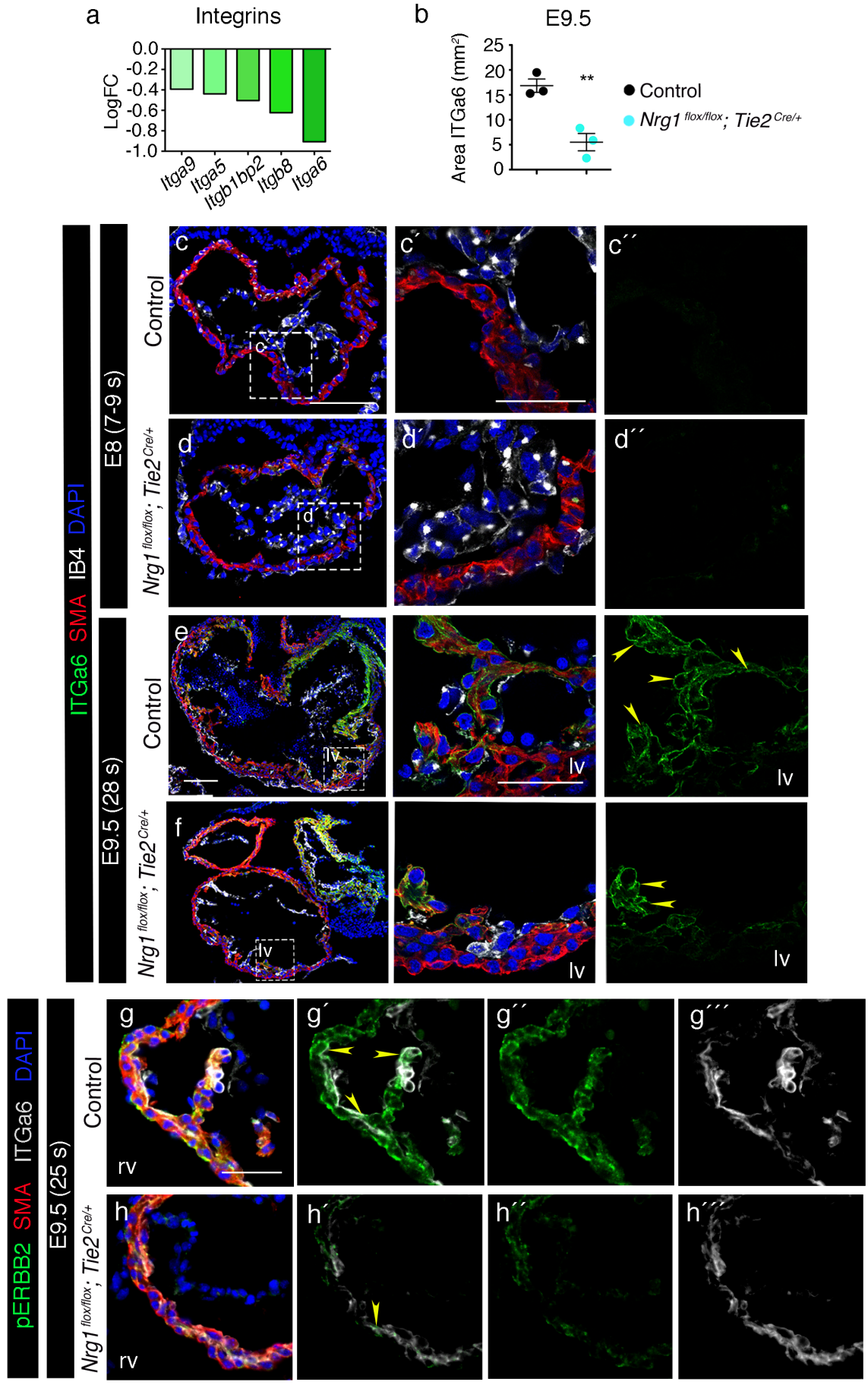
a
Integrins
LogFC
0.0
-0.2
-0.4
-0.6
-0.8
-1.0
Itga9
Itga5
Itgb1bp2
Itgb8
Itga6
b
E9.5
Area ITGa6 (mm²)
25
20
15
10
5
0
**
Control
Nrg1 flox/flox; Tie2 Cre/+
ITGa6 SMA IB4 DAPI
E8 (7-9 s)
E9.5 (28 s)
Control
Nrg1 flox/flox; Tie2 Cre/+
c
c´
c´´
d
d´
d´´
e
f
lv
pERBB2 SMA ITGa6 DAPI
E9.5 (25 s)
Control
Nrg1 flox/flox; Tie2 Cre/+
g
g´
g´´
g´´´
h
h´
h´´
h´´´
rv

Figure 16. ITGα6 positive area is reduced in trabecular myocardium of *Nrg1^{flox};Tie2^{Cre}* mutant hearts

a) Integrin membrane receptors changed in RNA-seq at E9.5 ventricles. b) Quantification of the area of ITGα6 in E9.5 hearts. Asterixs indicate significant result (**, P<0.01). c-f) IF in cryosections of ITGα6 IF (green), SMA (red), IB4 (white) and DAPI (blue) in 7-9 s (E8.0) (c and d) and 28s (E9.5) (e and f) in control and *Nrg1^{flox};Tie2^{Cre}* mutant hearts. Magnification of c and d shows a region of the ventricle (c´, d´, c´´ and d´´) and magnification of e and f shows a region of the lv, with a merge of ITGa6, SMA, IB4 and DAPI, or ITGa6 alone. Yellow arrowheads indicate ITGα6 signal. g and h) IF of ITGα6 (white), pERBB2 (green), SMA for myocardium (red) and DAPI for nuclei (blue) in 25s (E9.5) control and *Nrg1^{flox};Tie2^{Cre}* mutant cryosections, rv region is represented. The different channels are shown separately. ITGα6 and pERBB2 merge in g´(control) and h´(*Nrg1^{flox};Tie2^{Cre}*). Yellow arrowheads indicate double staining for both ITGα6 and pERBB2. pERBB2 in control (g´´) and *Nrg1^{flox};Tie2^{Cre}* (h´´). ITGα6 in control (g´´´) and *Nrg1^{flox};Tie2^{Cre}* (h´´´). SMA, smooth muscle actin; IB4, Isolectin B4; s, somites; lv, left ventricle; rv, right ventricle. Scale bars: 100 μm (c, d, e, f, g and h), 50 μm (c´, c´´, d´, d´´, insets of e, f, g and h).

These observations indicate that *Laminin* mRNA expression and LAMININ protein distribution in the cardiomyocytes of *Nrg1^{flox};Tie2^{Cre}* mutant embryos was impaired.

The INTEGRINS, the LAMININ receptors, are transmembrane receptors that promote the attachment and migration of cells on the surrounding ECM through cytoskeleton regulation (Ahmed *et al.*, 2005; Arnaout, Mahalingam and Xiong, 2005). Several integrins were downregulated in the RNA-seq (Figure 16a). We analysed ITGα6 because it is specific for trabecular cardiomyocytes (G. Li et al., 2016) and it colocalizes with ERBB2 (Pentassuglia and Sawyer, 2013). We performed ITGα6 IF with the myocardium marker SMA, and the endothelial marker IB4 in E8.0-E9.5 control and mutant embryos. ITGα6 was not detectable at E8.0 (7-9 s) both in control and *Nrg1^{flox};Tie2^{Cre}* mutant hearts, as trabeculation has not yet started (Figure 16c, c´, c´´ for control and d, d´, d´´ for *Nrg1^{flox};Tie2^{Cre}*). When trabeculae have already emerged (E9.5, 28 s), ITGα6 expression was clear in control trabecular cardiomyocytes, especially in the membrane where receptors for ECM molecules are located (Figure 16e and lv inset). In contrast, in *Nrg1^{flox};Tie2^{Cre}* mutants at E9.5, ITGα6 distribution was restricted to the membrane of the few cardiomyocytes that were forming short projections to the lumen (Figure 16f and lv inset). Overall, there was a significant decrease of ITGα6 signal at E9.5 in the ventricular myocardium of *Nrg1^{flox};Tie2^{Cre}* mutant hearts compared with control embryos (Figure 16b).

We were able to show ITGα6 and pERBB2 co-staining in trabecular cardiomyocytes that were positive for both markers in E9.5 control hearts (Figure 16g, g´). This colocalization was not

obvious in *Nrg1^{flox};Tie2^{Cre}* mutant hearts (Figure 16h, h´), suggesting impaired interaction between both receptors, ITGα6 and pERBB2, in mutant cardiomyocytes.

These results suggest that NRG1-ERBB2,4, INTEGRINS and PKC pathways interact to coordinate trabeculation. These data also indicate that NRG1-ERBB2,4 signalling may control cell polarity and OCD.

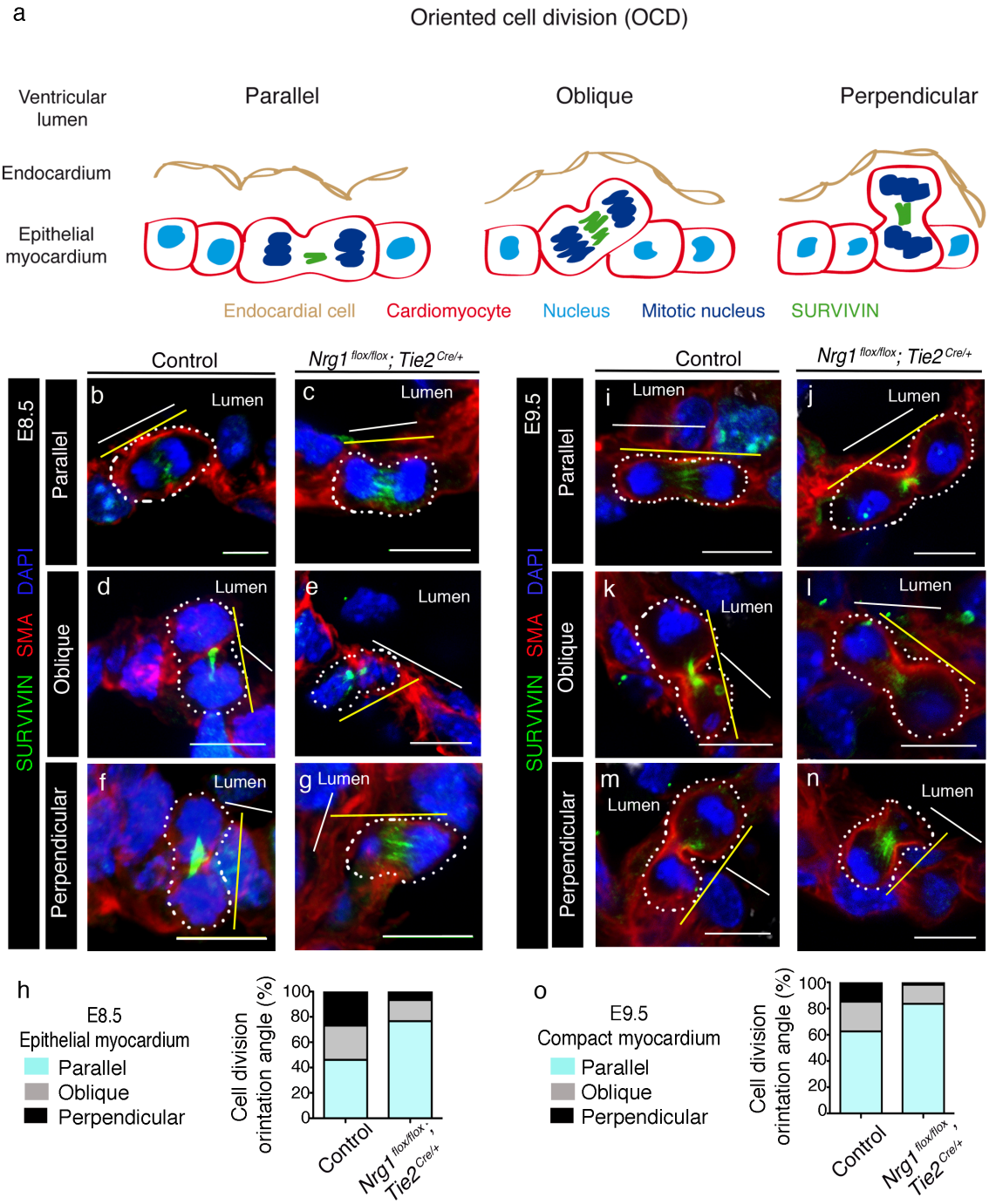

Perpendicular cardiomyocyte division is reduced in *Nrg1^{flox};Tie2^{Cre}* mutants

Regulation of OCD is crucial for trabeculation, as oblique and perpendicular cell division leads to trabecular growth towards the ventricular lumen (J. Li *et al.*, 2016; Jiménez-Amilburu *et al.*, 2016; Passer *et al.*, 2016) (Figure 17a). When cardiomyocytes divide in parallel to the ventricular lumen, this promotes growth of the compact layer (Passer *et al.*, 2016) (Figure 17a). We used a SURVIVIN antibody to analyse OCD in developing chambers, as we wanted to examine whether OCD was altered in cardiomyocytes of *Nrg1^{flox};Tie2^{Cre}* mutant embryos. SURVIVIN co-localizes with the mitotic spindle of dividing cardiomyocytes at E8.5 (Passer *et al.*, 2016) (Figure 17a).

In E8.5 control hearts, we found cardiomyocytes dividing in parallel (Figure 17b), obliquely (Figure 17d), or perpendicularly (Figure 17f) with respect to the ventricular lumen. In *Nrg1^{flox};Tie2^{Cre}* mutant hearts, we found cardiomyocytes dividing in parallel (Figure 17c), obliquely (Figure 17e), and perpendicularly (Figure 17g) towards the ventricular lumen. Quantification at E8.5 showed that parallel cardiomyocyte division was increased in *Nrg1^{flox};Tie2^{Cre}* mutant hearts (Figure 17h, light blue bar). In contrast, oblique cardiomyocyte division was reduced in *Nrg1^{flox};Tie2^{Cre}* mutants compared with control (Figure 17h, grey bar). Furthermore, perpendicular cardiomyocyte division was dramatically diminished in *Nrg1^{flox};Tie2^{Cre}* mutants compared with control hearts (Figure 17 h, black bar).

We performed a similar analysis at E9.5, when trabeculation is well in progress. We analysed dividing cardiomyocytes in the compact myocardium of control embryos and we found cardiomyocytes dividing in parallel (Figure 17i), obliquely (Figure 17k) and perpendicularly to the ventricular lumen (Figure 17m).

Figure 17. Perpendicular cardiomyocyte division is dramatically reduced after *Nrg1* deletion in the endocardium

a) Simplified model of the cardiomyocyte division orientation. b-n) IF on cryosections of control and *Nrg1^{flox};Tie2^{Cre}* embryos at E8.5 (b-g) and E9.5 (i-n) of SURVIVIN (green), SMA (red) and DAPI (blue). White lines represent the orientation of the basal region of cardiomyocytes towards the lumen. Yellow lines follow the division of one cardiomyocyte into two daughter cells. The angle formed between these two lines represents the orientation of the cardiomyocyte division. E8.5 control embryos (b, d, f) and *Nrg1^{flox};Tie2^{Cre}* (c, e, g) cardiomyocytes. Cardiomyocytes are dividing in parallel (b, c), obliquely (d, e) and perpendicularly (f, g) to the lumen. E9.5 control embryos (i, k, m) and *Nrg1^{flox};Tie2^{Cre}* (j, l, n) cardiomyocytes. Cardiomyocytes are dividing in parallel (i, j), obliquely (k, l) and perpendicularly (m, n) to the lumen. h and o) Quantification of the percentage of each type of division in control and *Nrg1^{flox};Tie2^{Cre}* mutant hearts at E8.5 and E9.5. SMA, smooth muscle actin. Scale bar: 10 μm (b-g, i-n).

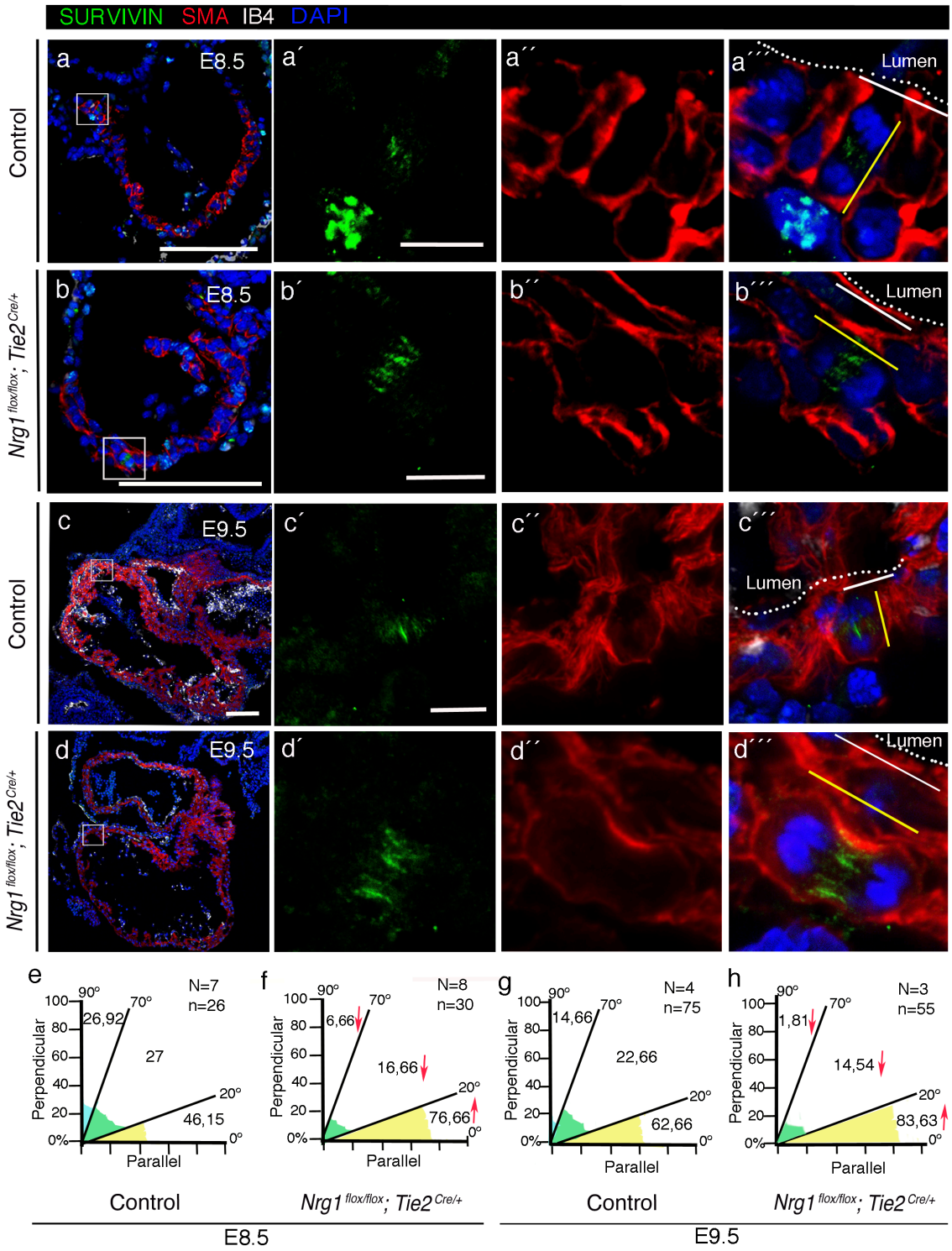

In *Nrg1*^{flox};*Tie2*^{Cre} mutant hearts, we found cardiomyocytes dividing in parallel (Figure 17j), obliquely (Figure 17l), and perpendicularly (Figure 17n). The percentage of parallel cardiomyocyte division was significantly higher in *Nrg1*^{flox};*Tie2*^{Cre} mutants than in control hearts (Figure 17o, light blue bar). Similarly, to what we observed at E8.5, oblique and perpendicular

Figure 18. Parallel cardiomyocyte division is increased after *Nrg1* deletion in the endocardium

a-d) IF on cryosections of control and *Nrg1^{flox};Tie2^{Cre}* hearts at E8.5 (a and b) and E9.5 (c and d). The insets show a cardiomyocyte in a perpendicular division (a, c), and parallel division (b, d). The different channels are shown separately: SURVIVIN (green, a′, b′, c′, d′), SMA (red, a′′, b′′, c′′, d′′) and merge with DAPI (blue, a′′′, b′′′, c′′′, d′′′). White lines represent the orientation of the basal region of cardiomyocytes towards the lumen. Yellow lines follow the division of one cardiomyocyte into two daughter cells. e) Quantification showing that 46,15% of the cardiomyocyte divide in parallel, 27% in oblique and 26,92% perpendicular angles at E8.5 control hearts. Analysis made in 7 embryos and 26 cardiomyocytes in anaphase, telophase or cytokinesis. f) Quantification showing 76,66% of parallel, 16,66% oblique and 6,66% perpendicular divisions at E8.5 mutant hearts. Analysis made in 8 embryos and 30 cardiomyocytes. g) The percentages of the different divisions at E9.5 in control hearts are represented in the graph, 62,66% parallel division, 22,66% oblique division and 14,66% perpendicular division. Analysis was made in 4 embryos and 75 cardiomyocytes. h) Quantification of the different divisions at E9.5 in *Nrg1^{flox};Tie2^{Cre}* mutant hearts, 83,63% parallel, 14,54% oblique and 1,81% perpendicular division. Analysis was made in 3 embryos and 55 cardiomyocytes. SMA, smooth muscle actin; IB4, Isolectin B4. Scale bars: 100µm (a, c, d, g), 10µm (all insets).

cardiomyocyte divisions were reduced in *Nrg1^{flox};Tie2^{Cre}* mutants at E9.5 (Figure 17o, grey and black bars respectively) compared to controls.

We further analysed the most representative type of division in mutant hearts. In the E8.5 control heart (Figure 18a) we observed SURVIVIN staining (Figure 18a′) in a perpendicular cardiomyocyte division in which the nuclei invaded the ventricular lumen (Figure 18a′′, a′′′). At E8.5, quantification was made in 7 different control embryos and the measurement of the angle was done in 26 dividing cardiomyocytes, which showed all types of divisions (Figure 18e). At E8.5, the more frequent division in *Nrg1^{flox};Tie2^{Cre}* heart was parallel to the ventricular lumen (Figure 18b, b′, b′′, and b′′′), in which the nuclei integrated with the compact myocardium. At this stage we quantify 30 cardiomyocytes in 8 *Nrg1^{flox};Tie2^{Cre}* embryos (Figure 18f).

The difference in the percentage of each type of division was even clearer at E9.5, when parallel divisions in *Nrg1^{flox};Tie2^{Cre}* mutant cardiomyocytes (Figure 18d, d′, d′′, and d′′′) were increased compared to control hearts (Figure 18c, c′, c′′, and c′′′), and, consequently, oblique and perpendicular divisions were dramatically reduced in *Nrg1^{flox};Tie2^{Cre}* mutant cardiomyocytes (Figure 18g for controls and h for *Nrg1^{flox};Tie2^{Cre}*). These results confirmed that perpendicular cardiomyocyte division, essential for trabeculae development was severely impaired in *Nrg1^{flox};Tie2^{Cre}* mutant embryos. In addition, increased parallel division appeared to be the cause of the increased compact myocardium thickness in *Nrg1^{flox};Tie2^{Cre}* mutant embryos.

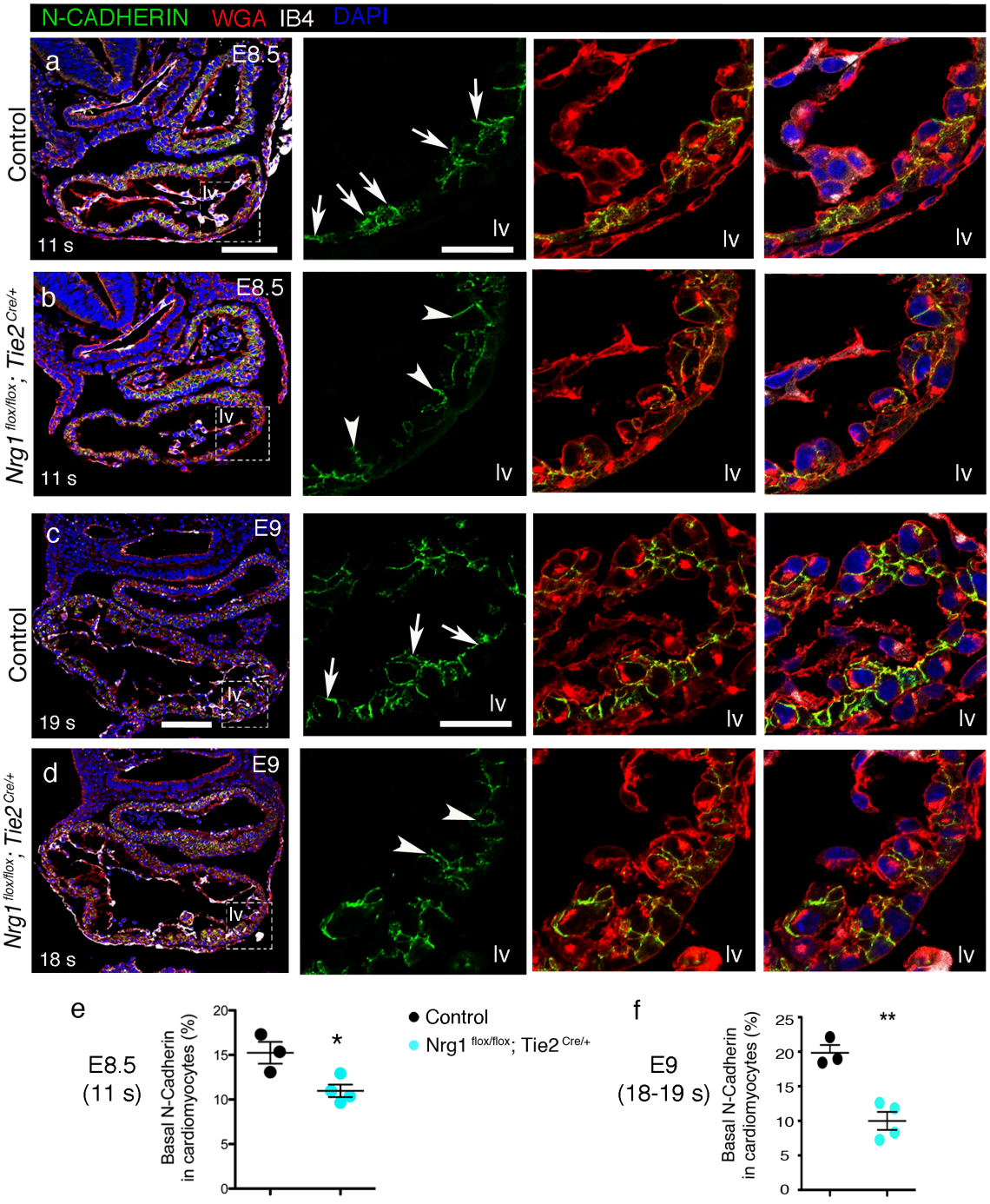

As described in the *Introduction*, functional and imaging studies in zebrafish have shown that during trabeculation n-cadherin undergoes a re-localization, so that prior to cardiomyocyte delamination to the lumen, it is re-distributed from the lateral side of the cardiomyocyte to the basal region, to favour cardiomyocyte delamination. This process is dependent on erbb2 signalling (Cherian *et al.*, 2016).

Figure 19. Latero-basal N-CADHERIN re-distribution in cardiomyocytes is essential for trabeculation and is impaired in *Nrg1^{flox};Tie2^{Cre}* mutant hearts

a-d) IF of N-CADHERIN (green), WGA (red), IB4 (white) and DAPI (blue) in paraffin sections of control and *Nrg1^{flox};Tie2^{Cre}* mutant hearts at E8.5 (11 s) (a and b), and E9.0 (18-19 s) (c and d). Insets are magnifications of lv, and the different channels are shown separately, N-CADHERIN signal, N-CADHERIN and WGA, and merge with DAPI. White arrows indicate basal location of N-CADHERIN and white arrowheads indicate lateral signal of N-CADHERIN in cardiomyocytes. Quantification of the percentage of basal region in cardiomyocyte positive for N-CADHERIN at E8.5 (e) and E9.0 (f). Asterixs indicate significant result (*, P<0.05; **, P<0.01). WGA, Wheat germ agglutinin; IB4, Isolectin B4; s, somites; lv, left ventricle. Scale bars: 100 μm (a, b, c and d), 25 μm (all insets).

We wanted to determine if N-CADHERIN undergoes changes on its localization during trabeculation in mice. We performed N-CADHERIN IF in E8.5 hearts (11 s), when trabeculation has not started yet (Figure 19a-b). Control cardiomyocytes showed N-CADHERIN distribution laterally and basally (Figure 19a and lv insets) but in *Nrg1^{flox};Tie2^{Cre}* mutant hearts, N-CADHERIN distribution persisted in the lateral side of the cardiomyocytes (Figure 19b and lv insets). Basal N-CADHERIN localization was dramatically reduced in *Nrg1^{flox};Tie2^{Cre}* mutants at E8.5 (Figure 19e). This analysis was performed in more advanced embryos (E9.0, 18-21 s), when trabeculation has progressed. We observed the same pattern of N-CADHERIN distribution, with lateral N-CADHERIN in *Nrg1^{flox};Tie2^{Cre}* mutant hearts (Figure 19d and lv insets), unlike the lateral and basal N-CADHERIN distribution in controls (Figure 19c and lv insets). At E9.0, N-CADHERIN localization was almost absent from the basal side of the cardiomyocyte in *Nrg1^{flox};Tie2^{Cre}* mutants embryos (Figure 19f). These results indicate that N-CADHERIN latero-basal re-distribution in cardiomyocytes is relevant for trabeculation in mice, and that this is a conserved process that depends on NRG1-ERBB2,4 signalling.

Nrg1 inactivation in early cardiac mesoderm progenitors disrupts trabeculation

Expression of the MESP1 transcription factor identifies the earliest cardiac mesoderm progenitors in the mouse embryo at E7.5 (Yumiko Saga *et al.*, 1999). To compare the phenotypic severity of *Nrg1^{flox};Tie2^{Cre}* mutants with that of mice with pan-mesodermal deletion of *Nrg1*, we bred *Nrg1^{flox}* mice with the *Mesp1^{Cre}* driver line, to generate *Nrg1^{flox};Mesp1^{Cre}* mutant embryos.

Histological analysis at E9.0 showed defective trabeculation in the *Nrg1^{flox};Mesp1^{Cre}* embryos (Figure 20b and lv inset) compared with the developing trabeculae of control embryos (Figure 20a and lv inset). At E10.5, H&E staining revealed a complex trabecular network in control

embryos (Figure 20c and lv inset), but trabeculae were clearly underdeveloped in *Nrg1*^{flox};*Mesp1*^{Cre} mutant hearts (Figure 20d and lv inset).

To better distinguish the various cardiac tissues, we performed IF for the myocardium (SMA) and for the endocardium (IB4) at E10.5 (Figure 20e-f). SMA-positive trabeculae were very prominent in the control heart (Figure 20e and lv inset) but were reduced in *Nrg1*^{flox};*Mesp1*^{Cre} mutants (Figure 20f and lv inset). In addition, the lethality phase of *Nrg1*^{flox};*Mesp1*^{Cre} mutant embryos was very similar to that of the *Nrg1*^{flox};*Tie2*^{Cre} mutants, with no viable mutant embryos beyond E11.5 (Table 5). Thus, the phenotype of *Nrg1*^{flox};*Mesp1*^{Cre} embryos fully recapitulated the trabeculation defects observed in *Nrg1*^{flox};*Tie2*^{Cre} mice (Figures 7 and 8), suggesting that in both genotypes, the mutant phenotypes represent the complete abrogation of NRG1-ERBB signalling in the heart.

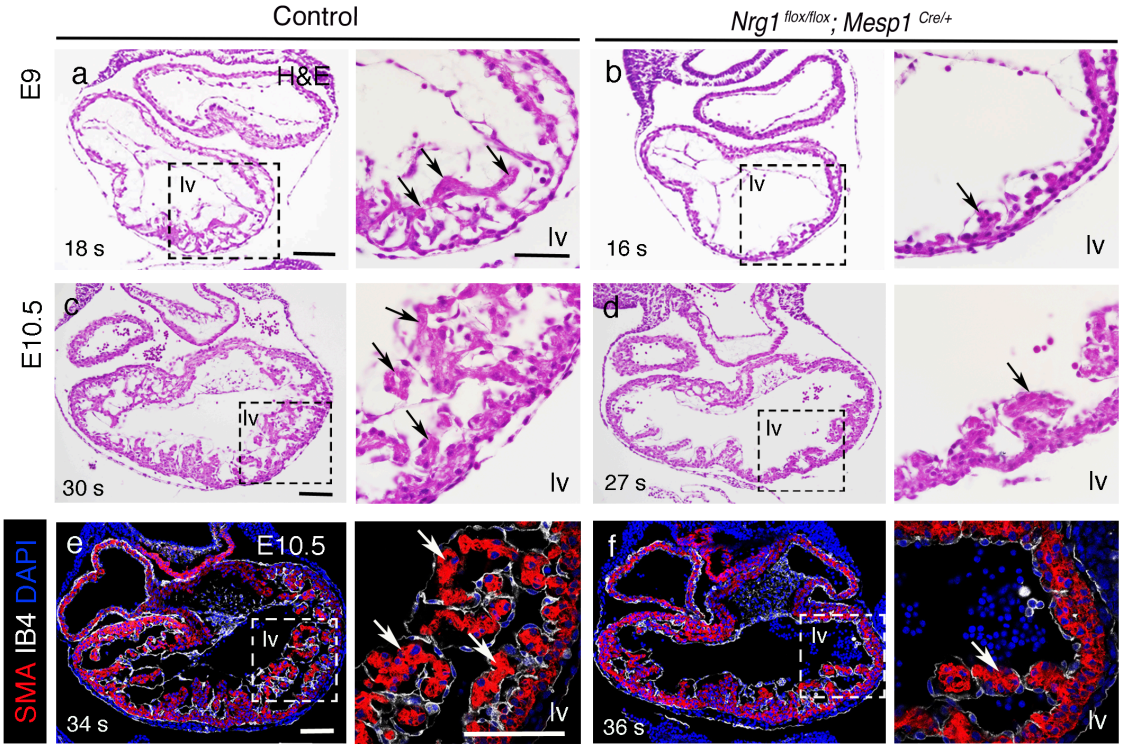

Figure 20. *Nrg1* deletion from early mesoderm causes similar phenotype during trabeculation

a-d) H&E staining in paraffin sections in control and *Nrg1*^{flox};*Mesp1*^{Cre} hearts at E9.0 (a and b) and E10.5 (c and d). Insets show lv magnification and arrows indicate the trabecular region. e and f) E10.5 IF of a control and *Nrg1*^{flox};*Mesp1*^{Cre} mutant heart in paraffin sections with SMA for myocardium (red), IB4 for endocardium (white) and DAPI for nuclei (blue). SMA, smooth muscle actin; IB4, Isolectin B4; s, somites; lv, left ventricle. Scale bars: 100 μm (a, b, c, d, e, f, and insets of e and f), 50 μm (insets of a, b, c and d).

Tamoxifen-induced *Nrg1* deletion in the endothelium leads to defective chamber compaction

To study the role of NRG1-ERBB signalling at later stages of heart development, and prevent the relatively early death caused by *Tie2*^{Cre}-mediated *Nrg1* inactivation, we bred our conditional *Nrg1*^{flox} allele with the endothelial-specific tamoxifen-inducible *Cdh5*^{Cre} line (Luna-zurita *et al.*, 2010; Wang *et al.*, 2010). We carried out two consecutive tamoxifen injections in *Nrg1*^{flox};*Cdh5*^{Cre} females at E10.5 and E11.5 of pregnancy.

To examine the chamber phenotype of mice at the compaction stages, we dissected embryos at E16.5. Upon dissection, hearts did not show any obvious alteration, but histological analysis revealed that while control hearts had trabeculae in the process of compaction and thick ventricular walls (Figure 21a, rv and lv insets), *Nrg1*^{flox};*Cdh5*^{Cre} mutant embryos showed poorly developed trabeculae, thinner compact myocardium and somewhat dilated ventricles and coronary vessels (Figure 21b, rv and lv insets), that leads to postnatal lethality (Table 6).

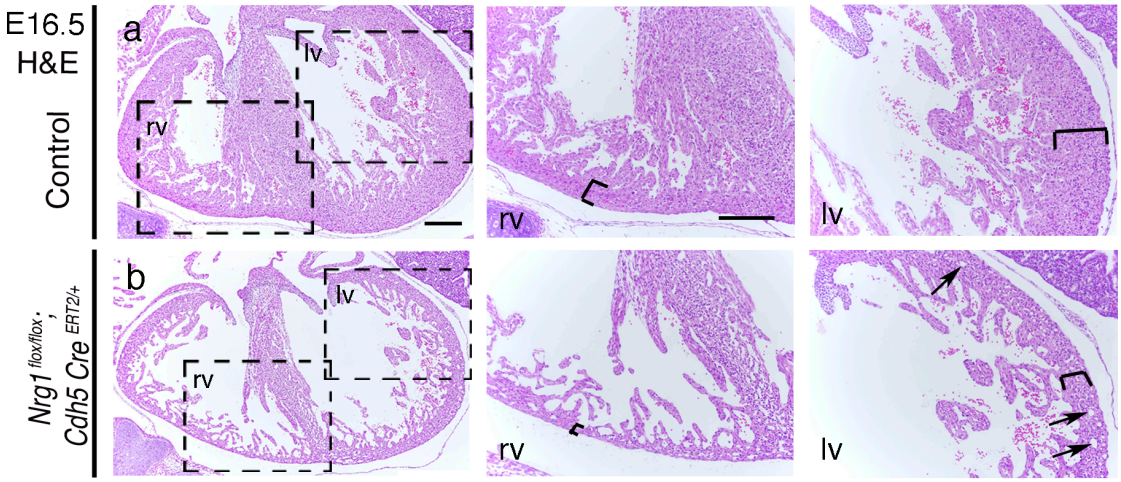

Figure 21. Inducible *Nrg1* deletion disrupts trabecular and compact myocardium

a and b) H&E staining at E16.5 control and *Nrg1*^{flox};*Cdh5*^{Cre} heart. Insets show rv and lv magnification. Black brackets represent CM thickness. Black arrows indicate dilated coronary vessels. rv, right ventricle; lv, left ventricle; H&E, Hematoxylin & Eosin. Scale bars: 100 µm.

To quantify the chamber phenotype of *Nrg1*^{flox};*Cdh5*^{Cre} mutants, we carried out IF for the myocardium marker cardiac TROPONIN T (cTNT) and the endocardial marker ENDOMUCIN, to distinguish well both cell types (Figure 22a, b and insets). In comparison with control hearts (Figure 22a, rv and lv insets), *Nrg1*^{flox};*Cdh5*^{Cre} mutant hearts showed thinner ventricles, and thin trabeculae (Figure 22b, rv and lv insets).

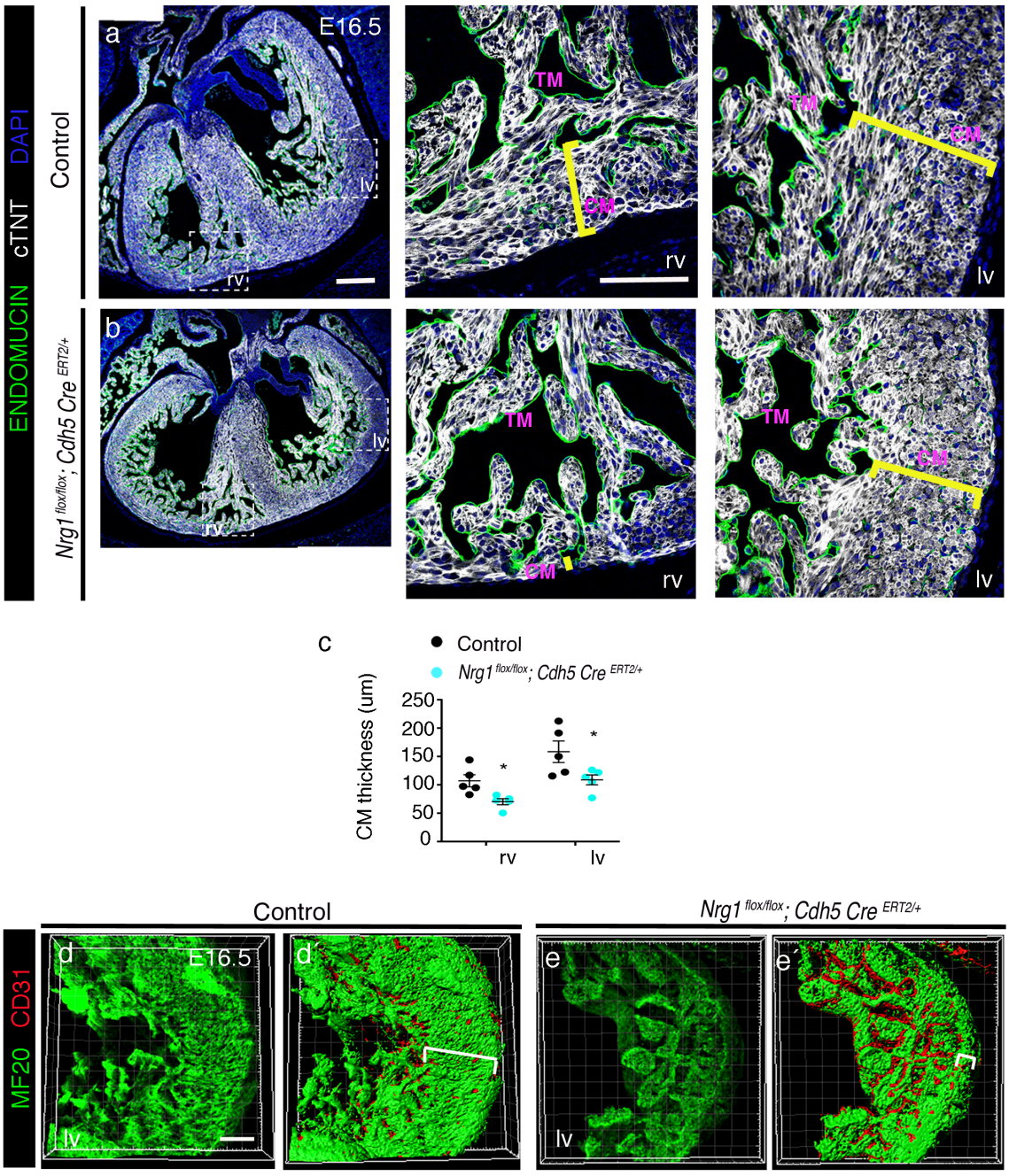

The quantification of the thickness of compact myocardium in both right and left ventricles, showed thinner compact myocardium in *Nrg1^{flox};Cdh5^{Cre}* mutants (Figure 22c).

To better observe the structure of the ventricle, we performed WM staining of the E16.5 heart with MF20 to stain the myocardium, and CD31 for the endothelium (Figure 22d and e). Confocal imaging reconstruction showed that CD31-expressing coronary vessels and endocardium were embedded in the thick ventricular walls and underlying trabeculae of control embryos (Figure 22d´), while CD31-positive cells delineated the thin walls and trabeculae of *Nrg1^{flox};Cdh5^{Cre}* mutant hearts (Figure 22e´).

Figure 22. Inducible *Nrg1* deletion impairs compaction

a-b) IF in paraffin sections of cTNT for the myocardium (white), ENDOMUCIN for the endocardium (green) and DAPI for nuclei (blue) at E16.5 in control (a) and $Nrg1^{flox};Cdh5^{Cre}$ (b) heart sections. Insets show magnifications of the rv and lv. Yellow brackets indicate the CM thickness. c) Quantification of the CM thickness at E16.5 in rv and lv separately. Asterixs indicate significant result (*, P<0.05). d and e) IF in WM E16.5 control (Z-stack=100 µm represented in 3D) and $Nrg1^{flox};Cdh5^{Cre}$ mutant heart (Z-stack=50 µm represented in 3D), with MF20 for myocardium (green) and CD31 for endothelium (red) (e´, f´). Images represent lv magnifications. White brackets indicate CM thickness. cTNT, cardiac Troponin T; rv, right ventricle; lv, left ventricle; CM, compact myocardium; TM, trabecular myocardium; CD31=PECAM, Platelet and Endothelial Cell Adhesion Molecule. Scale bars: 200 µm (a and b) and 100 µm (e, e´, f, f´, and insets of a and b).

Nrg1 deletion disrupts myocardial patterning during compaction

In order to characterize myocardial patterning during compaction in $Nrg1^{flox};Cdh5^{Cre}$mutants, we performed ISH of myocardium markers. We found that in E16.5 control hearts, *Hey2* was expressed in the compact myocardium (Koibuchi and Chin, 2007) (Figure 23a and rv inset), while it was extended to trabecular cardiomyocytes in $Nrg1^{flox};Cdh5^{Cre}$ mutant hearts (Figure 23b and rv inset).

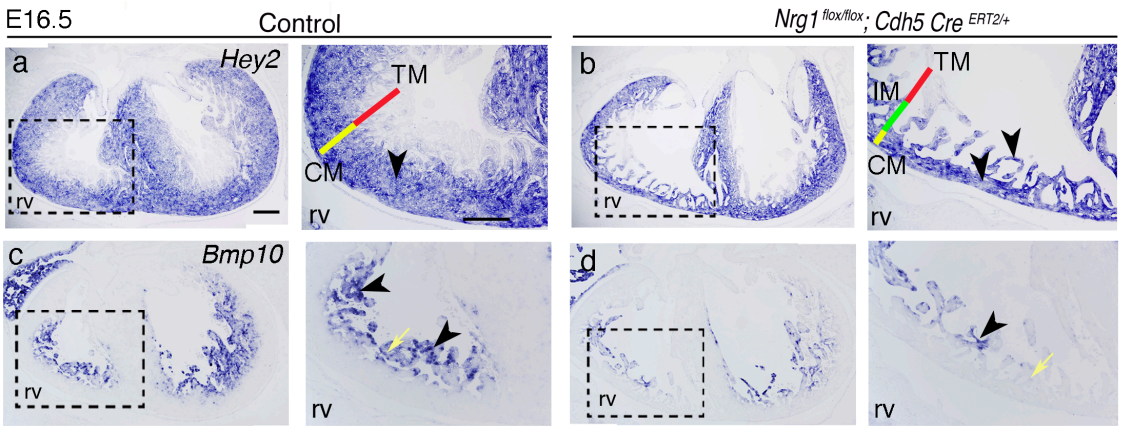

Figure 23. Inducible *Nrg1* deletion affects myocardial patterning during compaction

a-d) ISH at E16.5 in paraffin sections, insets show magnifications of the rv. a) *Hey2* in CM (yellow line) in control heart (rv inset, arrowhead), and in the IM in $Nrg1^{flox};Cdh5^{Cre}$ mutant (b, rv inset, green line, arrowheads). c) *Bmp10* in TM in control (rv inset, black arrowheads and yellow arrow), and in the tip of the trabeculae in $Nrg1^{flox};Cdh5^{Cre}$ mutants (d, rv inset, black arrowhead); yellow arrow shows the IM without *Bmp10* signal in $Nrg1^{flox};Cdh5^{Cre}$ mutants (d, rv inset). rv, right ventricle; CM, compact myocardium; TM, trabecular myocardium; IM, intermediate myocardium. Scale bars: 100 µm.

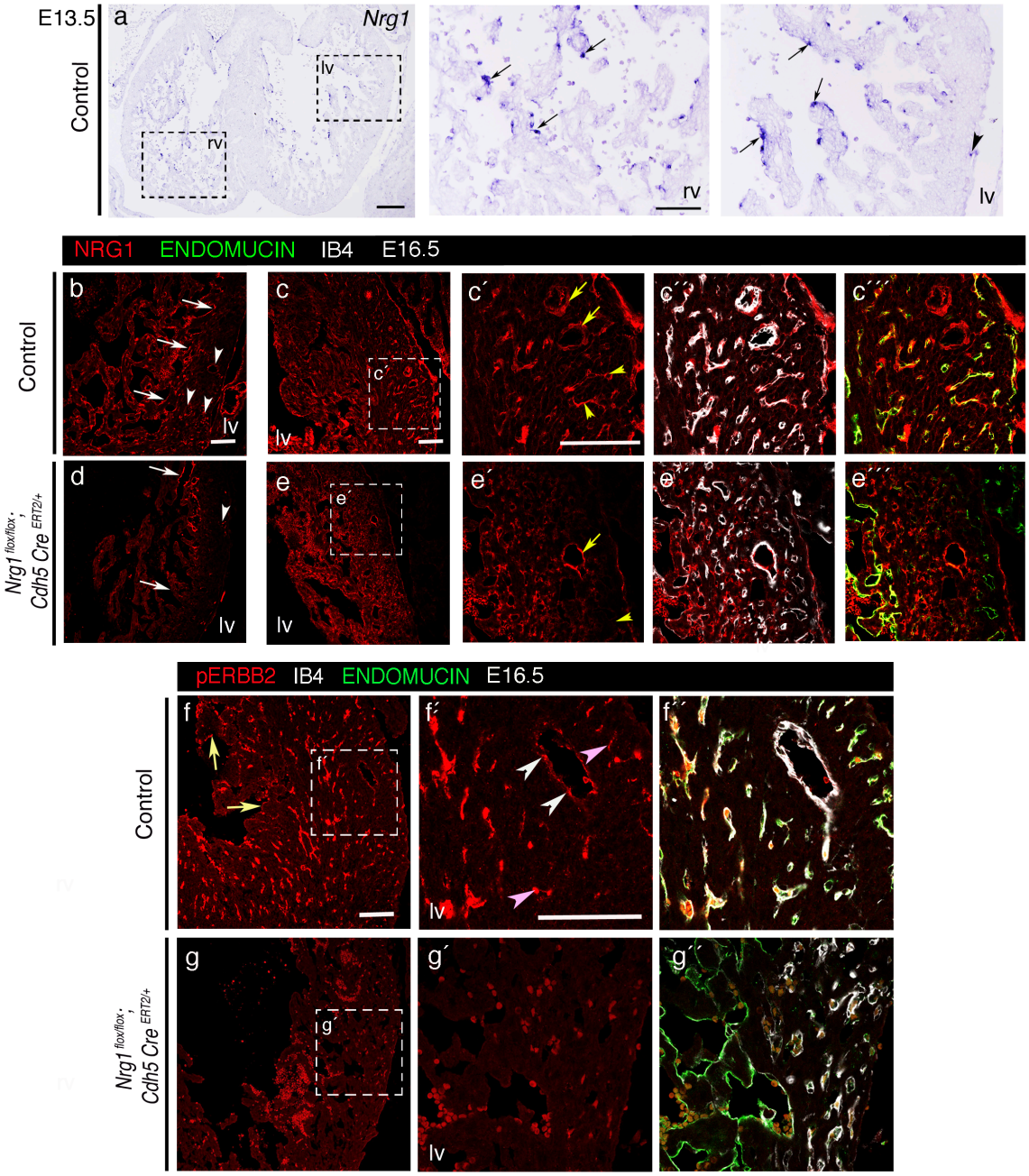

Complementary to that result, *Bmp10*, a trabecular marker (Chen, 2004) (Figure 23c and rv inset), was restricted to the tip of the trabeculae, but was lost in the rest of the trabecular-like myocardium (Figure 23d and rv inset) in $Nrg1^{flox};Cdh5^{Cre}$ embryos. This altered expression pattern of chambers markers was reminiscent of previous results from the laboratory with NOTCH mutants, in which compaction is affected (D'Amato *et al.*, 2016), and suggested that the morphological trabeculae expressing *Hey2* in $Nrg1^{flox};Cdh5^{Cre}$ mutants could be the so called "intermediate myocardium" described in NOTCH mutants (Figure 23b, rv inset). These results show that NRG1 is involved in cardiomyocyte patterning during compaction.

Figure 24. *Nrg1* deletion leads to reduced ERBB2 receptor activation in the endocardium and coronary vessel endothelium

a) *Nrg1* ISH in a E13.5 control heart, insets show magnifications of rv and lv. Black arrows indicate *Nrg1* in the endocardium and black arrowhead in coronary endothelium. b-e) NRG1 IF in E16.5 cryosections. Control (b, c) and $Nrg1^{flox};Cdh5^{Cre}$ (d, e) heart showing lv region. White arrows highlight NRG1 signal in the endocardium and the white arrowheads indicate positive signal in coronary endothelium. Insets show magnifications of the lv. The different channels are shown separately. NRG1 in coronary veins endothelium (yellow arrowheads) and in coronary artery endothelium (yellow arrows) (c´ and e´), IB4 and NRG1 (c´´ and e´´), ENDOMUCIN and NRG1 (c´´´ and e´´´). f and g) pERBB2 IF in E16.5 control and $Nrg1^{flox};Cdh5^{Cre}$ mutant heart sections. Yellow arrows indicate signal in the endocardium. Insets show magnifications of the lv. The different channels are shown separately; NRG1 (f´ and g´), white arrowheads indicate pERBB2 signal in a big coronary artery and pink arrowheads indicate pERBB2 in coronary veins, and pERBB2, IB4 (white) and ENDOMUCIN (green) in control and $Nrg1^{flox};Cdh5^{Cre}$ mutant heart (f´´ and g´´). lv, left ventricle; IB4, Isolectin B4. Scale bars: 100 μm (a, b-g´´), 50 μm (insets of a)

NRG1-ERBB2 pathway activation is impaired in $Nrg1^{flox};Cdh5^{Cre}$ embryos

Nrg1 is expressed in the endocardium and the coronary endothelium in control heart from E13.5 (Figure 24a). In order to examine the extent of $Cdh5^{Cre}$-mediated *Nrg1* deletion in $Nrg1^{flox};Cdh5^{Cre}$ mutant embryos, and to describe NRG1 localization during compaction, we performed NRG1 IF, with ENDOMUCIN to stain endocardium and veins, and IB4 for endothelium at E16.5. NRG1 was expressed in the endocardium and in both coronary arteries and veins in control hearts (Figure 24b-c´´´), and its expression was attenuated in coronary vessels of $Nrg1^{flox};Cdh5^{Cre}$ mutants, especially in veins (Figure 24d-e´´´).

We examined activation of the NRG1-ERBB pathway by IF staining of pERBB2, also with ENDOMUCIN and IB4 antibodies. Figure 24f-f´´shows pERBB2 expression in endocardium and coronary vessels and capillaries. In contrast, a markedly reduced pERBB2 expression was found in endocardium and coronary vessels of $Nrg1^{flox};Cdh5^{Cre}$ mutant hearts (Figure 24g-g´´). These observations suggest that NRG1-ERBB2,4 signalling was impaired in $Nrg1^{flox};Cdh5^{Cre}$ hearts.

Coronary arteries and veins morphology and identity is disrupted in $Nrg1^{flox};Cdh5^{Cre}$ embryos

To better characterize the coronary vessel phenotype observed in the H&E at E16.5 $Nrg1^{flox};Cdh5^{Cre}$ mutant hearts (Figure 21b), we performed *Fabp4 (Fatty acid binding protein)* ISH, a general marker of metabolically active endothelium (Saavedra *et al.*, 2015), to delineate

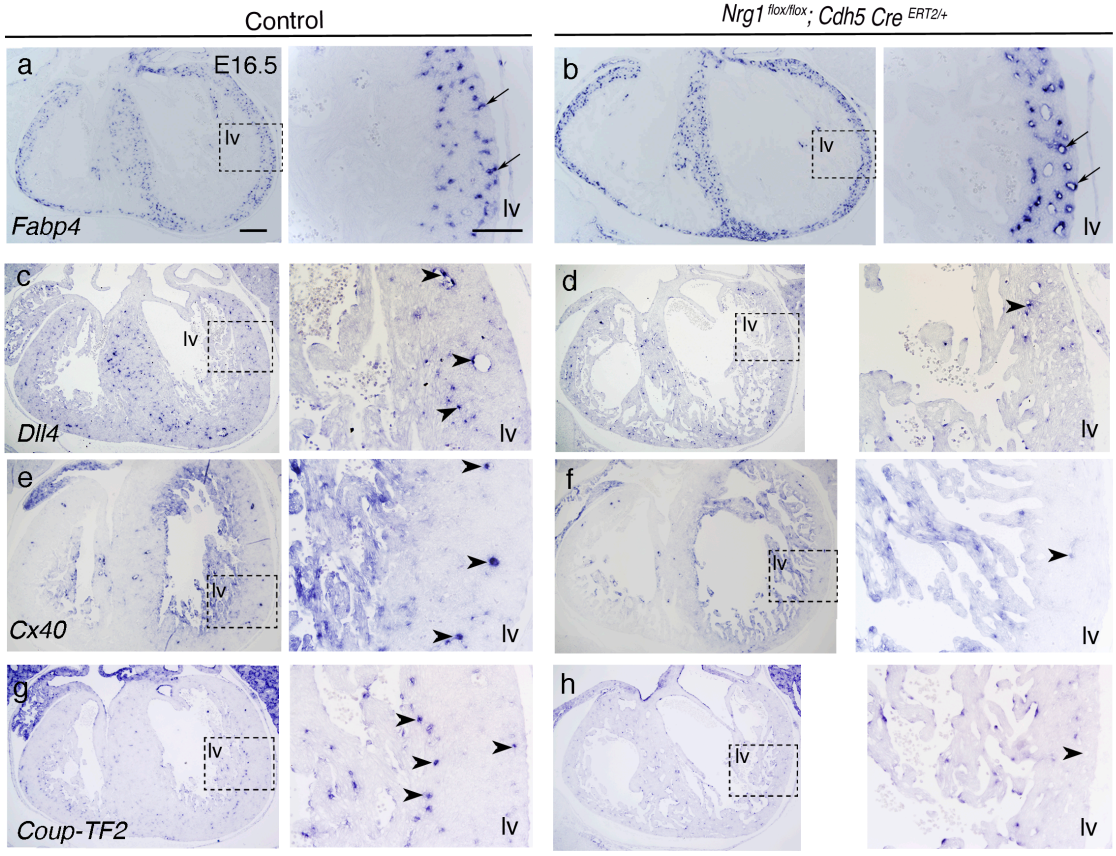

Figure 25. Coronary artery and vein specification is altered in *Nrg1^{flox};Cdh5^{Cre}* mutants

a-h) ISH in E16.5 paraffin sections. Control and *Nrg1^{flox};Cdh5^{Cre}* mutant hearts stained for endothelial *Fapp4* (a and b), arterial *Dll4* (c and d), arterial *Cx40* (e and f) and vein *Couf-TF2* (g and h). Insets represent lv magnification, black arrows or arrowheads indicate positive coronary endothelium. lv, left ventricle. Scale bars: 100 µm (a-h), 50 µm (insets of a-h).

the coronary endothelium. E16.5 control heart sections showed *Fabp4* expression in both coronary arteries and veins (Figure 25a). *Nrg1^{flox};Cdh5^{Cre}* mutants expressed *Fabp4* in coronary vessels that, specially the veins, were dilated (Figure 25b and lv inset). *Dll4* (Duarte *et al.*, 2004) and *Cx40* (Van Kempen and Jongsma, 1999) are specific markers for arteries (Figure 25c and e and lv insets, respectively), and their expression was almost lost in *Nrg1^{flox};Cdh5^{Cre}* mutant ventricles (Figure 25d and f and lv insets, respectively), indicating defective arterial identity after *Nrg1* deletion in the endothelium. We examined whether vein identity was affected using the vein marker *Coup-TF2* (S. Wu *et al.*, 2013). *Coup-TF2* expression was strong in endothelium embedded in the compact myocardium, close to the endocardium in control hearts (Figure 25g and lv inset). In contrast, *Coup-TF2* was reduced across the ventricles of *Nrg1^{flox};Cdh5^{Cre}* mutants (Figure 25h and lv inset). These results suggest that NRG1 signalling is regulating coronary artery and vein identity during compaction.

To better visualize the morphology of coronary vessels in *Nrg1*^{flox};*Cdh5*^{Cre} mutants, we performed WM IF in hearts at E16.5, with ENDOMUCIN to stain veins (Klotz *et al.*, 2015), and IB4 (Laitinen, 1987) as a pan-endothelial marker (Figure 26).

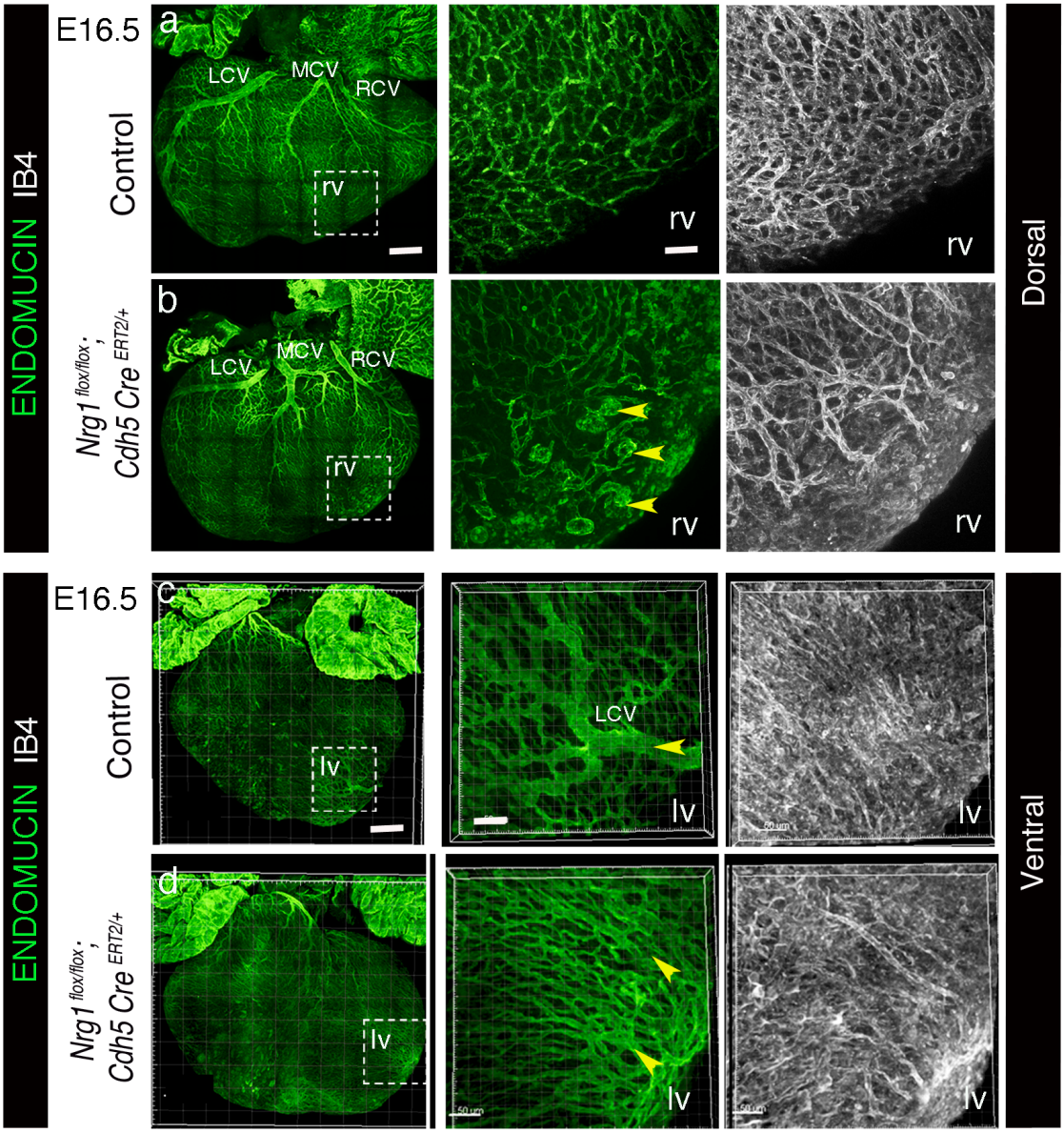

Figure 26. Coronary vessel development is affected in *Nrg1*-inducible mutants

a-d) WM IF for ENDOMUCIN (green) to stain veins and IB4 (white) to stain endothelium at E16.5. Tile scan capture of the heart (a, b, c and d). a and b) Dorsal 3D view of control (Z-projection of 194 µm) and *Nrg1*^{flox};*Cdh5*^{Cre} heart (196 µm). Insets show rv magnification of 66 µm (a) and 73 µm (b). Yellow arrowheads indicate AVM. c and d) Ventral 3D view of control (189 µm) and *Nrg1*^{flox};*Cdh5*^{Cre} mutant (183 µm) hearts. Insets show lv magnification, Z-stack of 41 µm (c) and 42 µm (d). IB4, Isolectin B4; rv, right ventricle; lv, left ventricle; MCV, major caudal cardiac vein; LCV, left cardiac vein; RCV, right cardiac vein. Scale bars: 300 µm (a, b, c and d), 50 µm (all insets).

A dorsal view of the heart showed a nice pattern of major developing coronary veins (Figure 26a), while the *Nrg1^{flox};Cdh5^{Cre}* mutant heart maintained the major veins but had aberrant terminal structures resembling arteriovenous malformations (AVM) (Figure 26b, rv inset of ENDOMUCIN). Arterial ramification (IB4 staining) in compact myocardium showed less branching comparing *Nrg1^{flox};Cdh5^{Cre}* hearts (Figure 26b, rv inset of IB4) with controls (Figure 26a, rv inset of IB4), and we did not observe arteries up to the edge of the ventricular wall in *Nrg1^{flox};Cdh5^{Cre}* hearts (Figure 26b, rv inset of IB4). Vein sprouting reached the ventral side of the heart in control embryos (Figure 26c, lv inset of ENDOMUCIN) but was defective in *Nrg1^{flox};Cdh5^{Cre}* hearts (Figure 26d, lv inset of ENDOMUCIN). These results suggest that NRG1 is required for coronary plexus formation during compaction.

NRG1 regulates cardiomyocytes metabolic homeostasis during compaction

We then examined whether the vascular defects and the thinner compact myocardium observed in *Nrg1^{flox};Cdh5^{Cre}* mutant hearts, were associated with altered myocardial metabolism during compaction.

Glut1, a HIF1 direct target gene, is the main embryonic glucose transporter (Menendez-Montes *et al.*, 2016). GLUT1 was expressed in compact myocardium, and staining was stronger in the right ventricle and interventricular septum in control hearts at E16.5 (Figure 27a, rv and lv insets). In contrast, GLUT1 was strongly expressed in trabecular myocardium in *Nrg1^{flox};Cdh5^{Cre}* mutant hearts which is even clearer in the right ventricle (Figure 27b, rv and lv insets), suggesting that trabecular cardiomyocytes are glycolytically active in *Nrg1^{flox};Cdh5^{Cre}* mutants.

Vegf (Tomanek *et al.*, 1999) was moderately expressed in the trabecular myocardium of the E16.5 control heart (Figure 27c and lv inset), and was upregulated in this tissue in *Nrg1^{flox};Cdh5^{Cre}* mutants (Figure 27d, lv inset). This result suggests an hypoxic environment in the heart of *Nrg1^{flox};Cdh5^{Cre}* mutant hearts, likely due to their defective coronary vessel development.

The glycolytic gene *Pdk1* (*pyruvate dehydrogenase kinase 1*) (Menendez-Montes *et al.*, 2016) was expressed in compact myocardium in control hearts at E16.5 (Figure 27e and lv inset), but its expression was increased and extended to the trabecular region in *Nrg1^{flox};Cdh5^{Cre}* mutants (Figure 27f and lv inset). Together, these results suggest an altered gene expression program of glucose-based metabolism in *Nrg1^{flox};Cdh5^{Cre}* mutant myocardium, likely due to the hypoxia associated to impaired coronaries development.

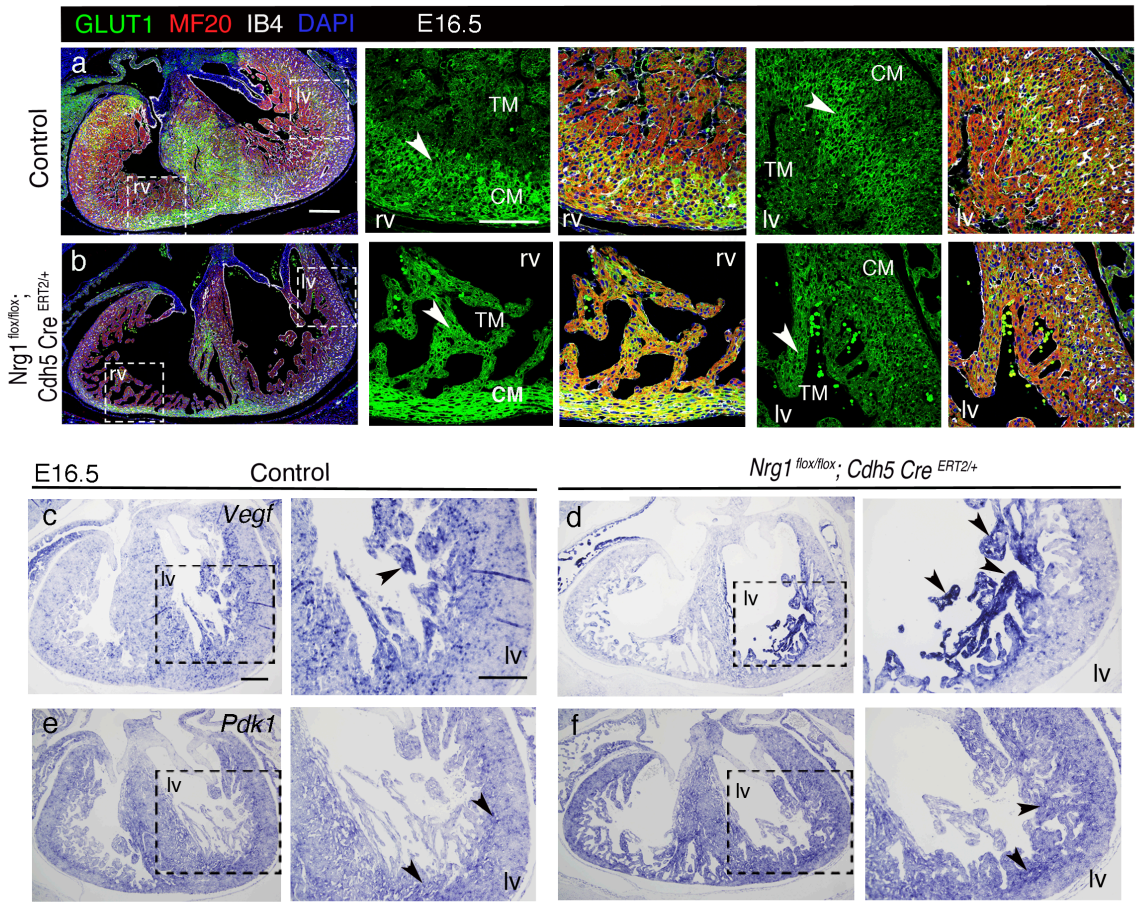

Figure 27. NRG1 regulates cardiomyocyte metabolism during compaction

a and b) GLUT1 IF in paraffin sections at E16.5 control and *Nrg1^{flox};Cdh5^{Cre}* hearts. The different channels are shown separately; GLUT1 signal (green), and merge with MF20 (red) for myocardium, IB4 (white) for endothelium and DAPI (blue) for nuclei. Insets show rv and lv magnifications. White arrowheads indicate GLUT1 in CM in control (a, insets) and in TM in *Nrg1^{flox};Cdh5^{Cre}* mutant (b, insets). c-f) E16.5 ISH in paraffin sections in control and *Nrg1^{flox};Cdh5^{Cre}* mutant heart for *Vegf* (c and d) and for *Pdk1* (e and f). Insets show lv magnifications. Black arrowheads indicate positive signal. IB4, Isolectin B4; rv, right ventricle; lv, left ventricle; CM, compact myocardium; TM, trabecular myocardium. Scale bars: 200 µm (a and b), 100 µm (insets of a and b, c-f and their insets).

Nrg1 overexpression in the endocardium and/or ectopic expression in the myocardium leads to larger valves and chamber defects

We have shown using loss- of function models that NRG1-ERBB signalling is involved in cardiomyocyte proliferation and patterning, polarity and OCD. This pathway is also required for AVC cushion development (Meyer and Birchmeier, 1995; Camenisch *et al.*, 2002), and later for coronary vessel development.

To obtain a complementary view of the function of NRG1-ERBB signalling in heart development, we have generated a transgenic mouse model in which we targeted into the *ROSA26* locus (Soriano, 1999), an expression cassette with *loxP* sites flanking a *PGK-neo-PGK-polyA* sequences followed by three transcriptional STOPS, followed by the *Nrg1* cDNA, and an *IRES-GFP* reporter gene to visualize *Nrg1* expression after CRE recombination (Figure 28).

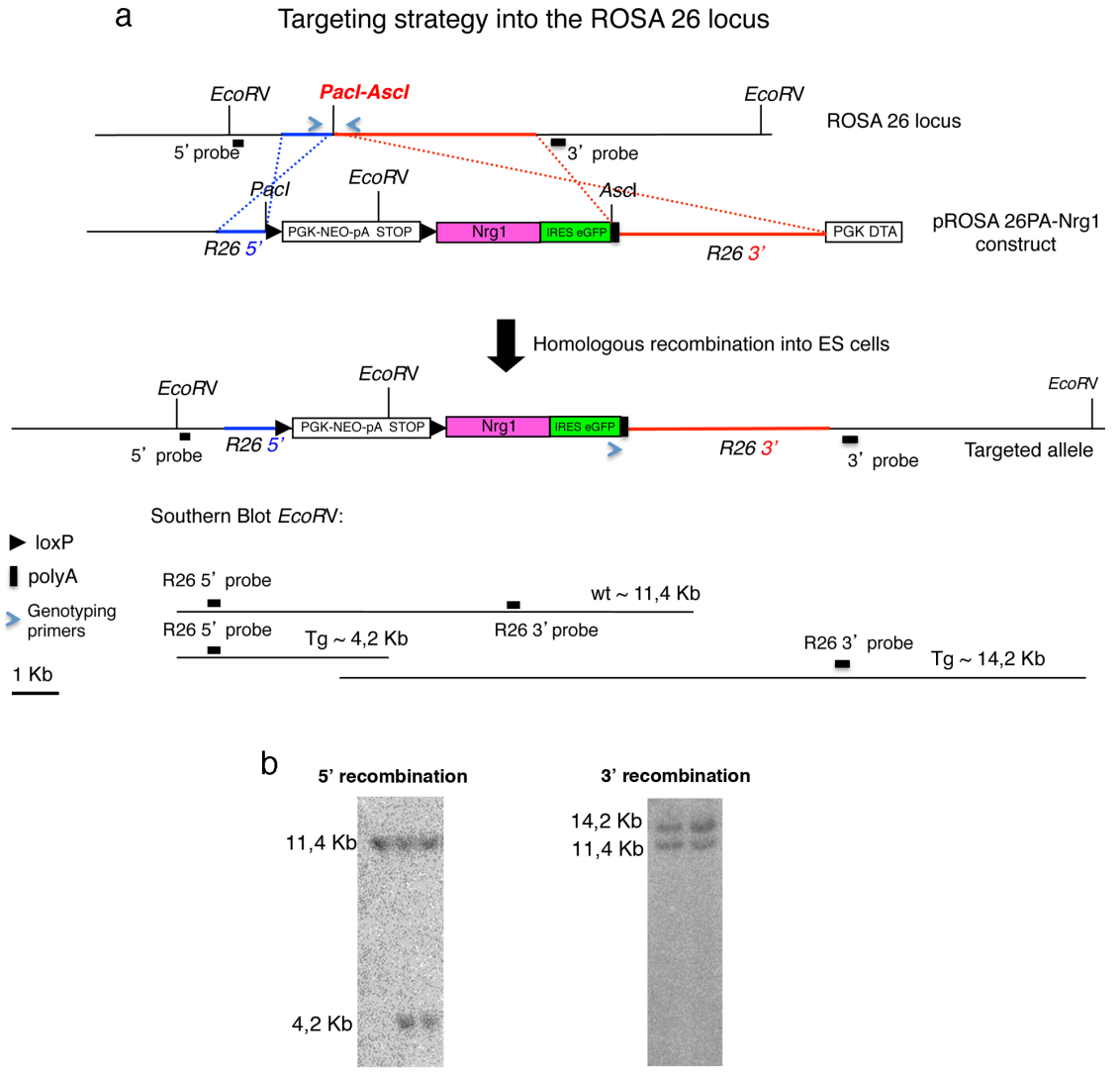

Figure 28. Gene targeting strategy of the *R26Nrg1-iresGFP* mouse line

a) Gene targeting strategy in mouse G4 ESCs. The *floxed PGK-NEO-pA* STOP cassette followed by the *Nrg1* cDNA and an *IRES-eGFP* were targeted into the *ROSA26* locus. The blue arrows indicate the position of the PCR primers used for genotyping. Black arrows indicate flanking *loxP* sites. b) Positive ESC clones analysed by Southern blot of *EcoR*V-digested genomic DNA using 5' and 3' probes that identify a 4.2Kb and a 14.2Kb transgenic bands, respectively.

First, we bred our new mouse line, named *R26Nrg1GFP*, with the endocardium/endothelium *Tie2*^{Cre} driver line (Kisanuki *et al.*, 2001). We analysed GFP expression in E9.5 *R26Nrg1GFP;Tie2*^{Cre} double heterozygous embryos by direct confocal imaging, that showed GFP expression in the endocardium of transgenic hearts (Figure 29b, b´) compare with the lack of GFP in control hearts (Figure 29a, a´).

To analyse the structure of the heart in these embryos, we performed H&E staining at E9.5. *R26Nrg1GFP;Tie2*^{Cre} transgenic embryos showed a prominent trabecular network in the left ventricle (Figure 29d and lv inset), similar to the trabecular myocardium in control embryos (Figure 29c and lv inset). Interestingly, we noticed that the endocardium was distant from the myocardium in the *R26Nrg1GFP;Tie2*^{Cre} transgenic ventricle (Figure 29d and lv inset) compared to control hearts, suggesting increased ECM synthesis in *R26Nrg1GFP;Tie2*^{Cre} transgenic embryos. To examine this possibility, we performed Alcian blue staining at E9.5, and noticed increased ECM secretion, not only in the AVC cushions, but also in the ventricles of *R26Nrg1GFP;Tie2*^{Cre} transgenic embryos (Figure 29f and lv inset). In contrast, the ECM was restricted to the AVC region and lining the trabeculae in control hearts (Figure 29e and lv inset). This increased ECM phenotype was likely due to the overexpression of *Nrg1* in the endocardium of the transgenic heart, and was in agreement with data indicating that NRG1 is involved in ECM synthesis (del Monte-Nieto *et al.*, 2018).

To further confirm NRG1 expression in the endocardium (Figure 29b) we carried out NRG1 IF. We observed NRG1 in the endocardium of control hearts at E10.5 (Figure 29g and g´), and stronger expression in the endocardium of E10.5 *R26Nrg1GFP;Tie2*^{Cre} transgenic hearts (Figure 29h and h´).

We then performed histological analysis in more advanced embryos, to examine their valve and chamber phenotype. Control E12.5 AVC valves (tricuspid and mitral) were nicely delineated (Figure 29i, tv and mv inset), while they were abnormally large in *R26Nrg1GFP;Tie2*^{Cre} embryos at E12.5 (Figure 29j, tv and mv inset). To better appreciate the ECM in the valvular region, we performed Alcian blue staining, that showed enlarged endocardial cushions in E12.5 *R26Nrg1GFP;Tie2*^{Cre} transgenic hearts (compare Figure 29k, l and insets). These results suggest that persistent *Nrg1* expression in the endocardium and cushions leads to thicker valves in *R26Nrg1GFP;Tie2*^{Cre} embryos. Most transgenic embryos do not survive beyond E14.5 (Table 7).

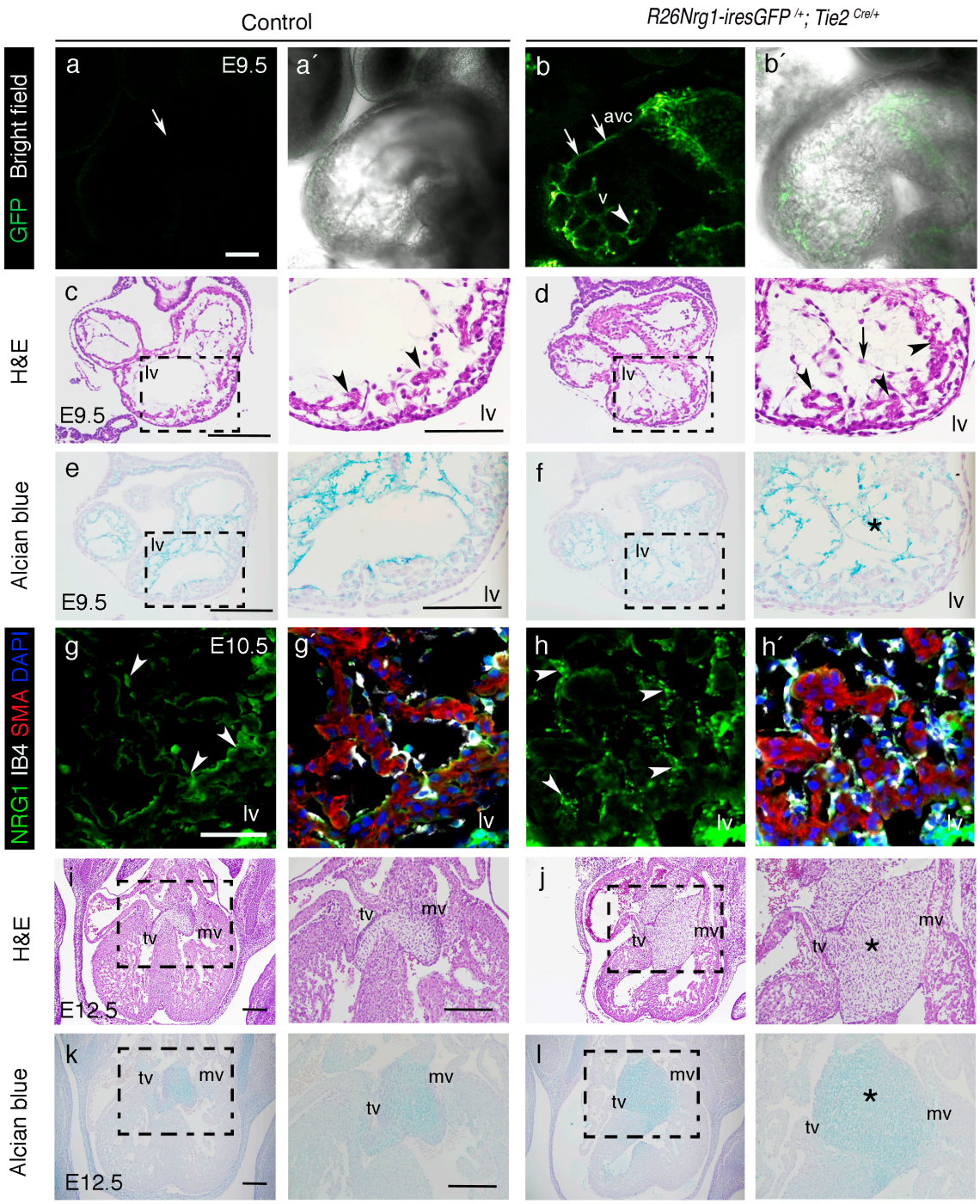
Control
R26Nrg1-iresGFP /+; Tie2 Cre/+
GFP Bright field
H&E
Alcian blue
NRG1 IB4 SMA DAPI
H&E
Alcian blue
a
E9.5
a´
b
avc
v
b´
c
lv
E9.5
d
e
f
g
E10.5
g´
h
h´
i
tv
mv
E12.5
j
k
l

Figure 29. *Nrg1* overexpression in the endocardium leads to thicker valves at E12.5

a and b) Control and *R26Nrg1GFP;Tie2^{Cre}* transgenic littermate WM embryos at E9.5, transgenic GFP signal is shown separately, and colocalizing with the bright field (a´ and b´). White arrows indicate GFP in the avc and white arrowhead in the ventricular endocardium. c and d) H&E in paraffin sections at E9.5 in a control and *R26Nrg1GFP;Tie2^{Cre}* heart. Insets show lv magnification, the black arrowheads indicate TM and black arrow signals the distant between myocardium and endocardium in *R26Nrg1GFP;Tie2^{Cre}* (lv inset). e and f) Alcian blue paraffin staining in a control and *R26Nrg1GFP;Tie2^{Cre}* heart at E9.5. ECM is prominent in the AVC and around trabeculae in control heart (e, lv inset) but extended from the AVC region to the chamber in *R26Nrg1GFP;Tie2^{Cre}* heart (f, asterisk, lv inset). g and h) IF of NRG1 (green) in cryosections at E10.5 control and *R26Nrg1GFP;Tie2^{Cre}* hearts, lv section with positive signal in the endocardium (white arrowheads). Merge with SMA (red) for the myocardium, IB4 (white) for the endocardium and DAPI (blue) (g´, h´). i and j) H&E paraffin staining in E12.5 control and *R26Nrg1GFP;Tie2^{Cre}* heart, the region of the tv and mv is magnified in the insets. Asterisk indicates huge endocardial cushions area in the transgenic. k and l) Alcian blue paraffin staining in E12.5 control and *R26Nrg1GFP;Tie2^{Cre}* heart, the region of the tv and mv is magnified in the insets. Asterisk indicates huge endocardial cushions area in the transgenic. GFP, Green Fluorescence protein; avc, atrioventricular canal; v, ventricle; H&E, Hematoxylin & Eosin; lv, left ventricle; IB4, Isolectin B4; SMA, smooth muscle actin; tv, tricuspid valve; mv, mitral valve. Scale bar: 100 μm.

NRG1-ERBB2,4 signalling pathway is activated in the myocardium during trabeculation (Gassmann *et al.*, 1995; Lee *et al.*, 1995; Meyer and Birchmeier, 1995). Thus, we wanted to study if the ectopic expression of *Nrg1* in embryonic cardiomyocytes disrupts myocardial development. We crossed the *R26Nrg1GFP* mouse line with the *Nkx2.5^{Cre}* line (Stanley *et al.*, 2002) to conditionally overexpress *Nrg1* in endocardial cells, and ectopically in the myocardium.

We analysed GFP expression in E9.5 *R26Nrg1GFP;Nkx2.5^{Cre}* double heterozygous embryos by direct confocal imaging, that showed GFP expression in the myocardium of transgenic hearts (compare Figure 30a, a´ with Figure 30b, b´).

H&E staining at E9.5 showed a developing trabecular meshwork in the ventricle of control embryos (Figure 30c and lv inset), while *R26Nrg1GFP;Nkx2.5^{Cre}* transgenic hearts had a thin compact myocardium and primitive trabeculae (Figure 30d, and lv inset). Alcian blue staining of control and transgenic hearts showed that the ECM was restricted to the endocardial cushions and tightly lining the trabeculae in control hearts (Figure 30e and lv inset), while ECM appeared distant of cardiomyocytes in the ventricles of E9.5 *R26Nrg1GFP;Nkx2.5^{Cre}* transgenic hearts (Figure 30f, and lv inset). This result again supports the implication of NRG1 in ECM secretion during trabeculation (del Monte-Nieto *et al.*, 2018).

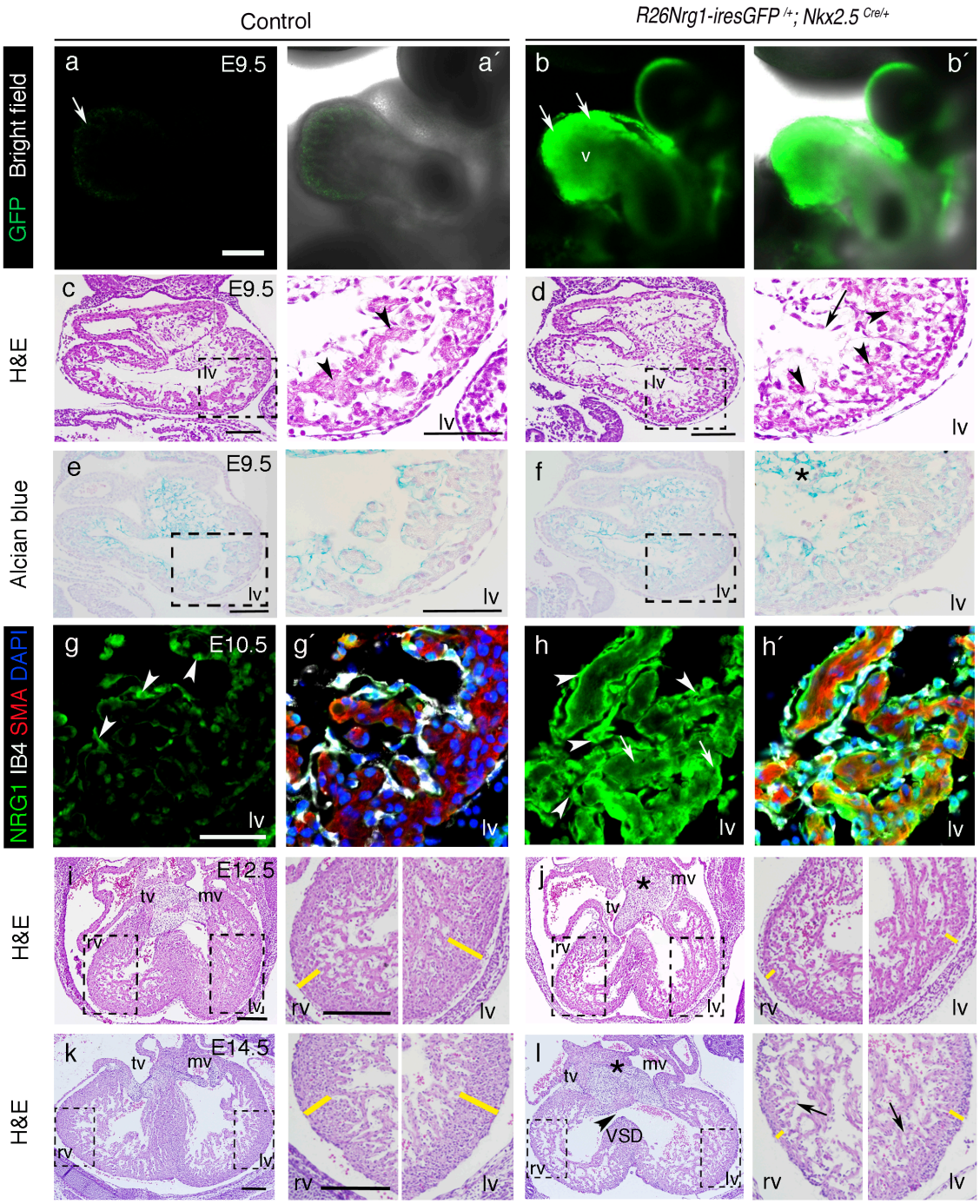
Control
R26Nrg1-iresGFP /+; Nkx2.5 Cre/+
GFP Bright field
H&E
Alcian blue
NRG1 IB4 SMA DAPI
H&E
H&E
a
E9.5
a´
b
b´
v
c
E9.5
d
lv
e
E9.5
f
*
g
E10.5
g´
h
h´
i
E12.5
tv
mv
rv
j
k
E14.5
l
VSD

Figure 30. *Nrg1* overexpression in the endocardium and the myocardium leads to thickened valves and defective myocardium at E14.5

a and b) Control and *R26Nrg1GFP;Nkx2.5^{Cre}* transgenic littermate WM embryos at E9.5, transgenic GFP signal is shown separately, and colocalizing with the bright field (a´ and b´). White arrows indicate GFP in the ventricular myocardium. c and d) H&E paraffin at E9.5 in a control and transgenic heart. Insets show a lv magnification, the black arrowheads indicate TM region, and black arrow signals the distant between myocardium and endocardium. e and f) Alcian blue paraffin staining in a control and *R26Nrg1GFP;Nkx2.5^{Cre}* transgenic heart at E9.5. ECM is extended from the AVC region to the chamber in the transgenic (f, asterisk, lv inset). g and h) IF in cryosections of NRG1 (green) in a E10.5 control and *R26Nrg1GFP;Nkx2.5^{Cre}* heart, lv section with positive signal in the endocardium (g, h, white arrowheads) and in the myocardium (h, white arrows). SMA (red) for myocardium, IB4 (white) for endocardium and DAPI (blue) (g´, h´). i and j) H&E staining at E12.5 in a control and *R26Nrg1GFP;Nkx2.5^{Cre}* transgenic paraffin section, the tv and mv region is increased (asterisk), and rv and lv are magnified (insets). The yellow lines indicate the CM thickness. k and l) H&E staining at E14.5 in a control and *R26Nrg1GFP;Nkx2.5^{Cre}* transgenic paraffin section, rv and lv are magnified (insets). Valves are bigger (l, asterisk) and there is VSD in the *R26Nrg1GFP;Nkx2.5^{Cre}* transgenic ventricles (l, black arrowhead). Black arrows indicate the trabecular region and yellow lines the CM thickness in rv and lv insets. GFP, Green Fluorescence protein; v, ventricle; H&E, Hematoxylin & Eosin; IB4, Isolectin B4; SMA, smooth muscle actin; lv, left ventricle; rv, right ventricle; tv, tricuspid valve; mv, mitral valve; VSD, Ventricular Septal Defect. Scale bar: 100 μm.

We examined by IF NRG1 overexpression and observed normal NRG1 expression in the endocardium of E10.5 control heart (Figure 30g, g´), while NRG1 was strongly expressed in the endocardium and in the myocardium of *R26Nrg1GFP;Nkx2.5^{Cre}* embryos (Figure 30h, h´).

At E12.5, H&E staining showed that the AVC valve region was larger in *R26Nrg1GFP;Nkx2.5^{Cre}* hearts and ventricular walls were less developed (compare Figure 30i with Figure 30j, rv and lv insets). This phenotype was more obvious at E14.5, when *R26Nrg1GFP;Nkx2.5^{Cre}* transgenic embryos showed larger AVC region, ventricular septum defect and thinner compact myocardium (compare Figure 30k with Figure 30l, rv and lv insets). These results indicate that *Nrg1* overexpression in the endocardium and ectopic expression in the myocardium disrupts valve and chamber development in *R26Nrg1GFP;Nkx2.5^{Cre}* transgenic embryos, that do not progress beyond E16.5 (Table 8).

In summary, *Tie2^{Cre}*- and *Nkx2.5^{Cre}*-mediated overexpression of *Nrg1* in the endocardium and/or myocardium impairs valve and chamber development, leading to embryonic lethality between E14.5-16.5.

DISCUSSION

Cardiac development is a fascinating process in which a primitive pumping heart tube undergoes tightly coordinated cellular proliferation, differentiation and morphogenesis, to give rise to the fully functional adult four-chamber heart. The endocardium is a crucial source of signals that guide and pattern the differentiation of the overlying myocardium and coronaries, and there is a close signalling interplay between endocardium and myocardium throughout heart development. In this PhD thesis project, we have used NRG1 loss- and gain-of-function mouse models to study the role of the NRG1-ERBB2,4 signalling pathway in the heart, that connects the endocardium and the myocardium to regulate multiple cardiac development processes.

NRG1 regulates cardiomyocyte polarity and oriented cell division during trabeculation

Previous reports showed that NRG1-ERBB2,4 signalling is required for ventricular chamber development (Gassmann *et al.*, 1995; Lee *et al.*, 1995; Meyer and Birchmeier, 1995). Our data show that conditional inactivation of *Nrg1* with an endothelial driver (or a pan-mesodermal one), severely impairs ventricular trabeculation, without affecting endothelial or myocardial specification, while the compact myocardium appeared thickened, although paradoxically, cardiomyocyte proliferation was significantly reduced.

The PCP pathway is essential for cellular polarity and tissue organization. PCP components are expressed during heart development (Hua *et al.*, 2011). We have found a dysregulation of PCP pathway molecules in the RNA-seq of E9.5 $Nrg1^{flox};Tie2^{Cre}$ mutant embryos. Thus, *Fzd5*, *Vangl1* and *Dvl1* are genes implicated in establishing cell polarity (Henderson and Chaudhry, 2011), and we found them to be upregulated in $Nrg1^{flox};Tie2^{Cre}$ mutants. These changes in gene expression suggests the implication of NRG1-ERBB2,4 signalling in the establishment of the apico-basal polarity of cardiomyocytes, which is essential for trabeculation.

CADHERINS are components of the adherent junctions that allow the organization of cells in tissues and are essential for embryonic development (Stepniak, Radice and Valeri, 1971; Luo and Radice, 2005; J. Li *et al.*, 2016). By RNA-seq we found an upregulation of *Cdh3* and *Cdh13* at E9.5 in $Nrg1^{flox};Tie2^{Cre}$ embryos. CDH3/P-CADHERIN is involved in establishing cell polarity, and favours collective cell migration in tumour cells (Plutoni *et al.*, 2016), while CDH13/T-CADHERIN is also involved in cell polarity and has been related to neural syndromes (Franke, Neale and Faraone, 2009). These results reinforce the idea that cellular polarity is affected in $Nrg1^{flox};Tie2^{Cre}$ mutants.

In vivo imaging experiments in zebrafish have shown that during the onset of trabeculation, n-cadherin redistributes from the lateral to the basal side of cardiomyocytes, to induce the

delamination of the cardiomyocytes to form trabecular-like projections in an erbb2-dependent manner (Cherian *et al.*, 2016). *N-Cadherin* expression was not significantly affected in our RNA-seq, unlike the expression of *Creg1*, which was upregulated. CREG1 binds to N-CADHERIN and localizes in intercalated discs of cardiomyocytes (Liu *et al.*, 2016). The observation that *Creg1* transcription was upregulated in the heart of E9.5 $Nrg1^{flox};Tie2^{Cre}$ mutants, suggests that cardiomyocytes do not progress into a trabecular-like structure because an excessive cell-cell adhesion may prevent their invasion towards the ventricular lumen to form trabeculae. When we analysed N-CADHERIN localization in E8.5 mouse hearts, prior to the onset of trabeculation, we observed that $Nrg1^{flox};Tie2^{Cre}$ mutant embryos persistently maintained N-CADHERIN expression in the lateral side of ventricular cardiomyocytes. This result suggests that similar to the situation in zebrafish (Cherian *et al.*, 2016), N-CADHERIN redistribution from the lateral to the basal side of cardiomyocytes is essential for trabeculation, and that this process is NRG1-ERBB2,4 signalling dependent. Interestingly, the PCP member *Wnt11* knockout mouse embryos show less trabeculation and disturbed patterning of N-CADHERIN and β-CATENIN expression in cardiomyocytes (Nagy *et al.*, 2010). *Wnt11* was downregulated in the RNA-seq of E9.5 $Nrg1^{flox};Tie2^{Cre}$ embryos and may be the cause of the alteration in N-CADHERIN redistribution prior to trabeculation, by affecting cell adhesion between cardiomyocytes. WNT11 controls the directional movements of the maturing cardiomyocytes in the ventricular wall by modulating cell adhesion with changes in the cytoskeleton actin filaments (Nagy *et al.*, 2010; Cherian *et al.*, 2016). These data suggest an implication of WNT11 in cytoskeleton rearrangement during cardiomyocytes migration during trabeculation, being potentially involved in the trabeculation defects of $Nrg1^{flox};Tie2^{Cre}$ mutants.

Thus, our data suggesting that NRG1-ERBB2,4 signalling regulates cardiomyocyte polarity in the mouse heart, is consistent with previous results in the zebrafish heart. Cardiomyocyte apico-basal polarity in the fish is regulated by nrg-erbb signalling and blood flow/cardiac contraction, both being essential for the onset of trabeculation (Jiménez-Amilburu *et al.*, 2016). This result indicates that the role of NRG1-ERBB2,4 signalling in the regulation of cardiomyocyte polarity is conserved during vertebrate evolution.

Cell polarity and mitotic spindle orientation are coupled through the PAR polarity complex, that controls cell polarity necessary for normal tissue generation and morphogenesis (Passer *et al.*, 2016). We observed a downregulation of molecules of the PAR complex (*Prkce* and *Pard3*) in the RNA-seq of E9.5 $Nrg1^{flox};Tie2^{Cre}$ mutant hearts, suggesting that defective polarity may impact on the orientation of the mitotic spindle. The apical localization of prkci has been shown to be essential for trabeculation in zebrafish (Jiménez-Amilburu *et al.*, 2016). Thus, the loss of PRKCi in the apical region of $Nrg1^{flox};Tie2^{Cre}$ mutant ventricles, could contribute to explain the

trabeculation defects of these embryos. Moreover, *Cdc42* expression was downregulated in the RNA-seq of E9.5 in *Nrg1^{flox};Tie2^{Cre}* embryos. CDC42 is involved in the structure and function of the mitotic spindle (Doe and Siller, 2009), suggesting an implication of CDC42 in the alteration of cardiomyocyte OCD in *Nrg1^{flox};Tie2^{Cre}* embryos. The PAR complex member PAR3 (Passer *et al.*, 2016), indirectly controls NuMA, which interacts with the mitotic spindle through DYNEIN to control its orientation, and thus the plane of cell division (Doe and Siller, 2009). Altered PAR complex expression may contribute to the altered pattern of OCD in the E9.5 *Nrg1^{flox};Tie2^{Cre}* mutant trabecular cardiomyocytes. Specifically, the decreased frequency of perpendicular cardiomyocyte division in *Nrg1^{flox};Tie2^{Cre}* mutants could underlie their defective trabeculation, and the increased frequency in parallel cardiomyocyte division may contribute to thickening of the compact myocardium. The increased compact myocardium thickness of *Nrg1^{flox};Tie2^{Cre}* mutants is in concordance with the multi-layered compact myocardium phenotype shown in recent *in vivo* imaging studies in zebrafish, in which the disruption of cardiomyocyte polarity due to mutations in the *adherens* junction protein crb2a, impairs trabeculation and myocardium structure (Jiménez-Amilburu and Stainier, 2019). Interestingly, zebrafish studies show that cardiomyocytes divide predominantly in parallel both in compact and trabecular myocardium, but the division mostly occurs in trabecular cardiomyocytes (Uribe *et al.*, 2018). In contrast, what is described in the mouse model, and we corroborate, is that cardiomyocytes in the compact myocardium divide perpendicularly to the lumen to form trabeculae (J. Li *et al.*, 2016; Jiménez-Amilburu *et al.*, 2016; Passer *et al.*, 2016). Overall, our results suggest that NRG1-ERBB2,4 signalling, orchestrates OCD of cardiomyocytes through PAR complex molecules regulation, which is essential for trabeculation (Figure 31).

LAMININS are components of the basement membrane that contact ECM with cardiomyocyte receptors (Miner and Yurchenco, 2004). We observed a reduction of LAMININ expression in *Nrg1^{flox};Tie2^{Cre}* mutants, both at the RNA and protein levels, suggesting an impaired endocardial-myocardium crosstalk through ECM in *Nrg1^{flox};Tie2^{Cre}* mutant hearts. Constitutively active AKT, activated by receptor tyrosine kinases, induces the synthesis of LAMININ-1 and COLLAGEN IV isotypes, and causes their translocation to the basement membrane (Li *et al.*, 2001). This reduction of LAMININ could be explained because of a severely attenuated NRG1-ERBB-AKT cascade in *Nrg1^{flox};Tie2^{Cre}* mutants.

The receptors for LAMININS in the membrane, the INTEGRINS, mediate cell adhesion, morphology, proliferation, survival, migration, and invasion (Eckert *et al.*, 2009). We analysed the specific ITGα6 distribution in trabecular cardiomyocytes (G. Li *et al.*, 2016b), and observed a reduced myocardial ITGα6 expression in E9.5 *Nrg1^{flox};Tie2^{Cre}* mutants.

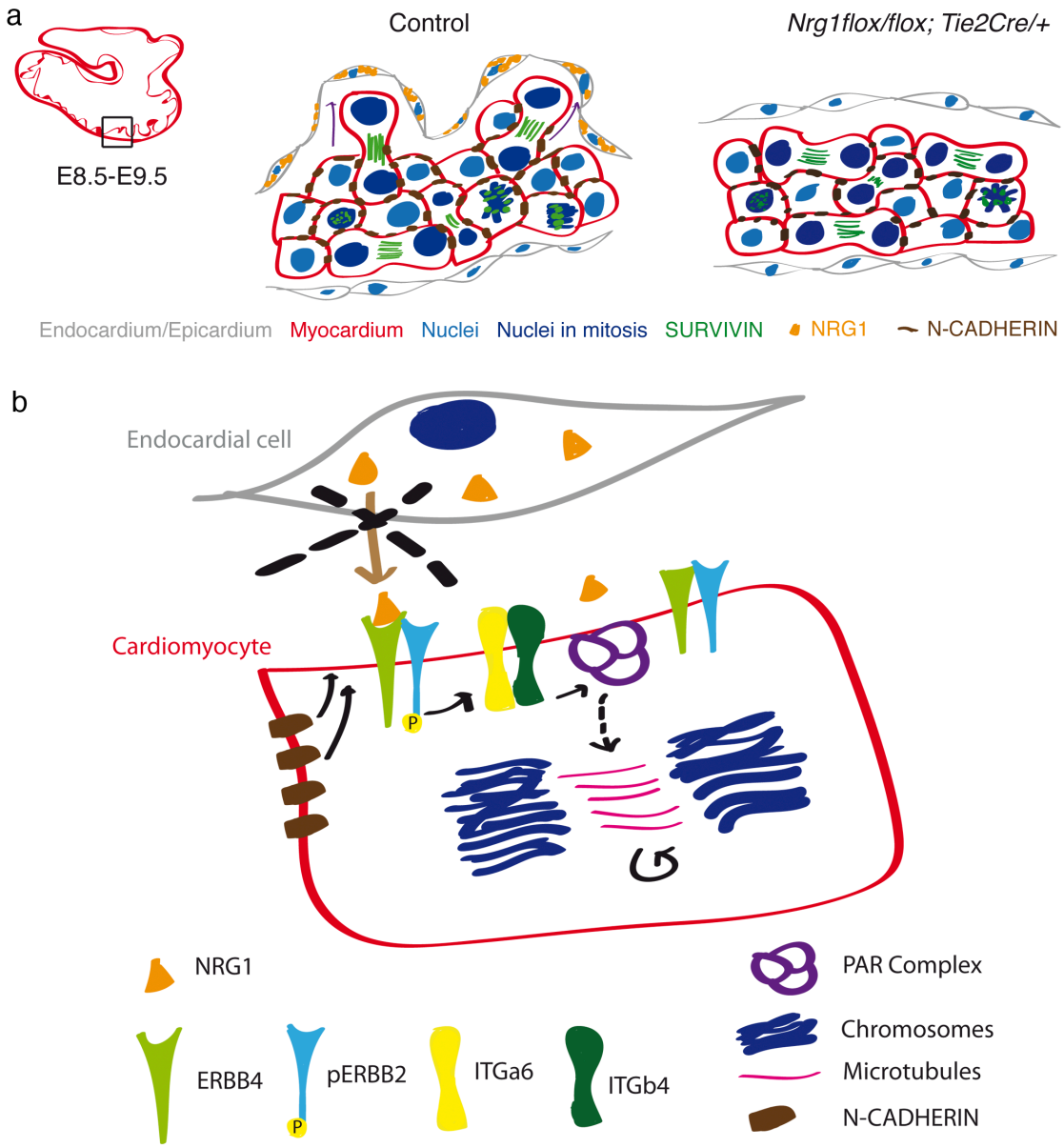

Figure 31. NRG1 signalling cascade controlling orientation of cell division in cardiomyocytes during trabeculation

a) In E8.5-E9.5 control heart, cardiomyocytes (red) divide parallelly, obliquely and perpendicularly towards the lumen. SURVIVIN (green) protein in the mitotic spindle indicates the orientation of the division. N-CADHERIN (brown) is distributed in the lateral and basal side of cardiomyocytes prior to trabeculation (arrow). In $Nrg1^{flox};Tie2^{Cre}$, when NRG1 (orange) is deleted from the endocardium (grey), OCD is mostly parallel and N-CADHERIN maintains its lateral localization. b) NRG1 (orange), from the endocardium, binds to ERBB4 receptor (green) in cardiomyocyte that dimerizes with ERBB2 (blue), which is phosphorylated. This activation regulates INTEGRINS (yellow-green) and PAR complex (purple) signalling, which is going to indirectly regulate the cardiomyocyte OCD. N-CADHERIN from adherent junctions will move from the lateral side to the basal side of cardiomyocytes. All this regulation is abrogated since *Nrg1* is deleted from the endocardium in $Nrg1^{flox};Tie2^{Cre}$ embryos.

ITGα6-ITGβ4 associates with ERBB2 in several breast carcinoma cells (Aplin, Howe and Juliano, 1999), but it is not clear if this is the case in cardiac tissue (Pentassuglia and Sawyer, 2013). Interestingly, we noticed that in E9.5 control hearts, ITGα6 and pERBB2 were co-expressed in regions of trabecular cardiomyocytes, unlike in *Nrg1*^{flox}*;Tie2*^{Cre} mutant hearts. This result suggests that *Nrg1* deletion in the endocardium impairs ITGα6-pERBB2 membrane receptor interaction in cardiomyocytes, disrupting downstream signalling, and impacting on trabeculation.

Phosphorylation of ITGβ4 can be mediated by PKC-α, which induces the interaction with ERBB2 receptors and the regulation of ACTIN filaments during tumour progression (Soung, Clifford and Chung, 2010). Our results suggest that these ERBB-ITGα6-PKC-α interactions can occur in cardiomyocytes to orchestrate cardiomyocyte migration during trabeculation, but these interactions are abrogated in *Nrg1*^{flox}*;Tie2*^{Cre} mutants, inducing trabeculation defects (Figure 31).

Considering our results, we propose a model in which *Nrg1* deletion in the endocardium impairs the activation of ERBB2,4 receptors in cardiomyocytes, so that downstream INTEGRIN signalling is disrupted. Subsequently, the PAR complex is delocalized from the apical side of cardiomyocytes, PKC and PARD3 are downregulated, and are not able to control the mitotic spindle through CDC42 and NuMA, and cardiomyocyte OCD is disrupted. The alteration of OCD, leads to a predominance of parallel cardiomyocyte division, causing an increase in compact myocardium thickness and defective trabeculation in *Nrg1*^{flox}*;Tie2*^{Cre} mutant embryos. As discussed above, after *Nrg1* deletion in the endocardium, N-CADHERIN redistribution from the lateral to the basal side of cardiomyocytes is disrupted. This hypothesis is represented in Figure 31. Both, NRG1 (Gassmann *et al.*, 1995; Lee *et al.*, 1995; Meyer and Birchmeier, 1995) and cell polarity (J. Li *et al.*, 2016; Jiménez-Amilburu *et al.*, 2016; Passer *et al.*, 2016) have been described independently to be crucial for trabeculation. Here, we conclude that NRG1-ERBB2,4 is a key regulator of cardiomyocyte polarity and OCD during trabeculation in mouse heart development.

NRG1 is implicated in ECM secretion, NOTCH signalling and myocardial patterning

The ECM plays a key role in endocardium-myocardium crosstalk during heart development (Sedmera *et al.*, 2000). In particular, ECM remodelling plays a crucial role in trabeculation, where a crosstalk between NOTCH and NRG1-ERBB2,4 signalling, controls the spatio-temporal regulation of ECM secretion and degradation (del Monte-Nieto *et al.*, 2018). NOTCH has been suggested to promote ECM degradation during the formation of endocardial projections that are critical for individualization of trabecular units, whereas NRG1-ERBB2,4 promotes myocardial ECM synthesis, which is necessary for trabecular rearrangement and growth (del Monte-Nieto *et*

al., 2018). We found that *Has2* expression and thus ECM deposition was diminished in *Nrg1^{flox};Tie2^{Cre}* mutant ventricles, which supports the role of NRG1 in promoting ECM secretion. NRG1 has been proposed to regulate N1ICD in the endocardium trough VEGFA, to orchestrate trabecular organization (del Monte-Nieto *et al.*, 2018). In agreement with these findings, we observed a decrease of N1ICD in the endocardium of the *Nrg1^{flox};Tie2^{Cre}* mutant hearts at E9.5, supporting a NRG1-mediated N1ICD regulation. On this regard, NOTCH has been shown to be required for *Nrg1* expression and the cardiac phenotype of cultured NOTCH mutant embryos can be partially rescued adding NRG1 to the media (Grego-Bessa *et al.*, 2007), suggesting that the interplay between NRG1 and NOTCH is complex.

Considering the crosstalk between NRG1 and N1ICD during trabeculation (Grego-Bessa *et al.*, 2007; del Monte-Nieto *et al.*, 2018), we examined whether other molecules related with NOTCH1 were affected, and we found *Jag1* to be downregulated in our E9.5 RNA-seq data of *Nrg1^{flox};Tie2^{Cre}* mutants. Previous work in the laboratory showed that *Gpr126* was downregulated in the endocardium of *Dll4 ^{flox};Tie2^{Cre}* mutant embryos which show severely impaired trabeculation (D'Amato *et al.*, 2016b). It was also shown that *Gpr126* inactivation in mice causes hypotrabeculation and ventricular wall thinning (Waller-Evans *et al.*, 2010). Thus, we tested whether *Gpr126* expression in the endocardium was affected in *Nrg1^{flox};Tie2^{Cre}* mutant hearts. ISH showed that this was indeed the case. These results suggest that NRG1-ERBB2,4 and NOTCH signalling work together to coordinate the expression of genes essential for trabeculation. Interestingly, as NRG1 activates its receptor and signalling in cardiomyocytes, while NOTCH signalling is active in the endocardium, it would be of interest to identify the molecule(-s) besides VEGFA (del Monte-Nieto *et al.*, 2018) that may be connecting both cell types (Figure 32).

Developmental analysis of ventricular myocardium markers showed that both compact (*Hey2*) and trabecular myocardium (*Bmp10*) expression was disrupted in *Nrg1^{flox};Tie2^{Cre}* mutants, indicating loss of ventricular myocardium identity. Additional trabecular markers like *Irx3* and *Semaphorins* (*Sema3a* and *Sema3c*) (Behar *et al.*, 1996; Kim *et al.*, 2012), were downregulated in E9.5 *Nrg1^{flox};Tie2^{Cre}* mutant hearts, both by RNA-seq and by ISH. How these impairments in trabecular patterning relate with the defective OCD leading to severely defective trabeculation, remains to be studied.

These results indicate that NRG1-ERBB2,4 signalling influences N1ICD signalling, ECM secretion and myocardial patterning during trabeculation.

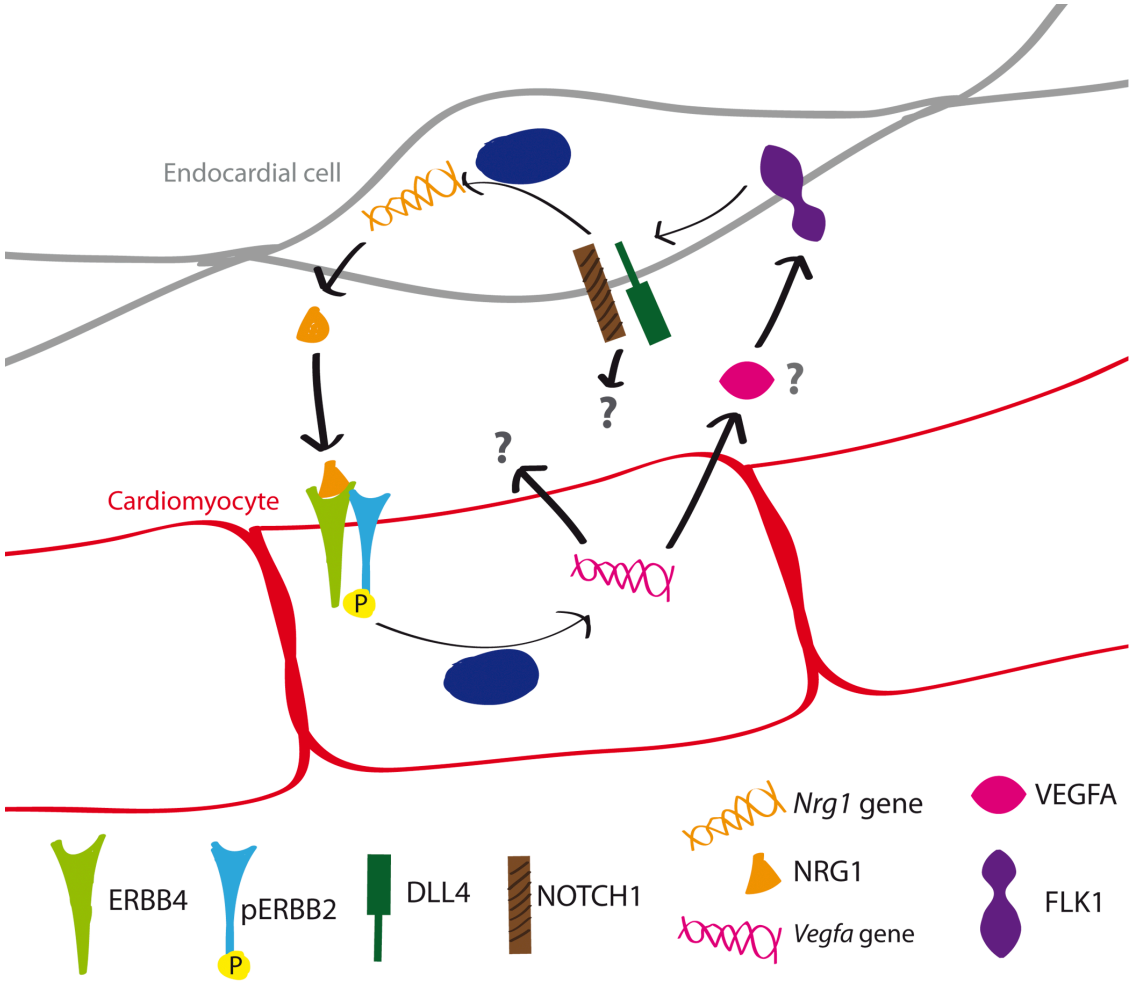

Figure 32. NOTCH1-NRG1-VEGFA interplay between endocardium and myocardium during trabeculation

NRG1 (orange) from the endocardium (grey) binds to the ERBB2,4 receptors (light green and blue) in the myocardium (red) where activates *Vegfa* transcription (pink). Then, VEGFA interacts with its FLK1 (purple) endocardial receptor which regulates NOTCH1(brown) signalling through DLL4 (dark green) that induces NRG1 expression in the endocardium. It is possible that VEGFA and NOTCH1 also regulate other signalling pathways during trabeculation. (modified from Grego-Bessa *et al.*, 2007 and del Monte-Nieto *et al.*, 2018)

NRG1 is required for valve development

The ERBB2,3 is the heterodimeric receptor of NRG1 in the endocardial cushion mesenchyme during formation of the valve primordia (Camenisch *et al.*, 2002). In addition to the defective trabeculation in $Nrg1^{flox};Tie2^{Cre}$ mutant embryos, we observed a reduction of the AVC area in these mutants at E10.5. This result suggests an inactivation of the NRG1-ERBB2,3 signalling in the valve region after *Nrg1* deletion in the $Nrg1^{flox};Tie2^{Cre}$ mutant hearts.

We wanted to analyse if *Nrg1* tissue-specific overexpression would affect heart development. For this purpose, we generated a CRE-*loxP*-based transgenic mouse line in which *Nrg1* expression is under the control of the *ROSA26* promoter (Soriano, 1999). Considering that NRG1 is endogenously expressed in the endocardium (Meyer and Birchmeier, 1995), we conditionally overexpressed *Nrg1* in this tissue under the control of the $Tie2^{Cre}$ driver. We observed normal trabeculation in E9.5 $R26Nrg1GFP;Tie2^{Cre}$ transgenic embryos, but excessive ECM secretion in the AVC and chambers, in agreement with the proposed role of NRG1 in ECM synthesis (del Monte-Nieto *et al.*, 2018). Interestingly, at E12.5, $R26Nrg1GFP;Tie2^{Cre}$ embryos showed thickened AVC valves, suggesting an overactivation of ERBB3 in the mesenchymal region of the endocardial cushions that should be confirmed. Thus, *Nrg1* overexpression in the endocardium induces valve developmental defects that leads to embryonic lethality at E14.5.

As the NRG1-ERBB2,4 signalling pathway is activated in the myocardium of the chambers in early heart development (Lee *et al.*, 1995), we ectopically expressed *Nrg1* in the myocardium and overexpressed it in the endocardium using the $Nkx2.5^{Cre}$ driver. $R26Nrg1GFP;Nkx2.5^{Cre}$ mutant embryos developed primitive trabeculae and increased ECM secretion in AVC cushions and in the chambers at E9.5. We observed thicker AVC valves in $R26Nrg1GFP;Nkx2.5^{Cre}$ embryos at E12.5, but the increased size was not as dramatic as in the $R26Nrg1GFP;Tie2^{Cre}$ embryos, probably because $Nkx2.5^{Cre}$ line (Stanley *et al.*, 2002) is poorly expressed in the AVC endocardium. At E14.5, $R26Nrg1GFP;Nkx2.5^{Cre}$ transgenic embryos developed VSD, associated to mesenchymal alterations. The chambers showed also thinner compact and trabecular myocardium. The severe $R26Nrg1GFP;Nkx2.5^{Cre}$ phenotype leads to embryonic lethality at E16.5, likely due to valve development defects. We obtained similar results in terms of valve and chambers alterations, with the $cTnT^{Cre}$ driver line.

These results suggest that NRG1-ERBB2,3 signalling pathway is involved in the regulation of valve cushion development, in agreement with previous reports (Lee *et al.*, 1995; Meyer and Birchmeier, 1995; Camenisch *et al.*, 2002). The phenotype observed in both transgenic lines ($R26Nrg1GFP;Tie2^{Cre}$ and $R26Nrg1GFP;Nkx2.5^{Cre}$) is similar to the thicker valves and VSD observed after BMP2 overexpression in the myocardium of $R26Bmp2GFP;Nkx2.5^{Cre}$ transgenic embryo (Prados *et al.*, 2018), suggesting that overexpression of signals involved in AVC cushion formation leads to valve malformation and embryonic lethality.

Previous studies have described that excessive NRG1 produce cardiomyocyte hypertrophy and dilated cardiomyopathy (Hertig *et al.*, 1999; Ozcelik *et al.*, 2002; Pimental *et al.*, 2017). Using our new conditional mouse model, we want to analyse in the near future whether myocardial

patterning is altered and whether NRG1 is controlling cardiomyocyte polarity in *R26Nrg1GFP;Tie2*^{Cre} transgenic embryos.

NRG1-ERBB2,4 signalling is required for myocardial patterning and metabolism, and for coronary vessel development during compaction

NRG1 is released from the endocardium into the ECM, and binds to the ERBB2,4 receptors in the myocardium (Falls, 2003; Parodi and Kuhn, 2014). The interplay between endocardium and myocardium is crucial for ventricular chamber development and maturation (Luxán *et al.*, 2016). Endothelial inactivation of NRG1 leads to relatively early embryonic lethality (Meyer and Birchmeier, 1995; Lai *et al.*, 2010; del Monte-Nieto *et al.*, 2018; and this report), so the role of NRG1-ERBB2,4 signalling in late chamber development (compaction) has not been studied before. We found that NRG1 is expressed in the endocardium and in the endothelium of the developing coronary vessels from E13.5 onwards, so that time-controlled *Nrg1* inactivation in the endothelium (*Cdh5*^{Cre}-mediated) would reveal its role at later cardiac development stages. Endothelial *Nrg1* inactivation from E10.5 onwards leads to heart dilation, and thin ventricular walls and trabeculae. Interestingly, patterning of the ventricular myocardium is affected in *Nrg1*^{flox}*;Cdh5*^{Cre} mutants, so that expression of compact myocardium markers (i.e.: *Hey2*) is expanded to the base of the morphological trabeculae, while expression of trabecular markers (*Bmp10*) is confined to the distal tip of trabeculae (Figure 33). This molecular phenotype is similar to that of mice with NOTCH signalling inactivation caused by combined JAG1 and JAG2 ligand abrogation in the myocardium (D'Amato et al., 2016), or by deletion of their upstream regulator MIB1 in this tissue (Luxán *et al.*, 2013). In the report by D'Amato et al., it was suggested that NOTCH inactivation leads to a loss of patterning in trabecular myocardium, so that only the distal/older region of the trabeculae, expressed a trabecular marker, while the adjacent morphological trabecular myocardium has lost patterning, abnormally expressed a compact myocardium marker and was termed intermediate myocardium, while the outer myocardium or compact myocardium, was defined by the normal expression of *Hey2*. In this setting, NOTCH is active in chamber endocardium and may exert a non-cell autonomous patterning effect on chamber myocardium, so that NOTCH inactivation leads to a patterning loss in cardiomyocytes.

In the NRG1-ERBB2,4 situation, inactivation is induced after E10.5, when signalling occurs from endocardium to myocardium and, after E12.5, the pathway is predominantly active in developing coronaries. This suggest that the patterning defects observed in the ventricles of E16.5 *Nrg1*^{flox}*;Cdh5*^{Cre} mutants are likely due to NRG1-ERBB2,4 signalling inactivation in the myocardium, while the defects in coronary vessel development occur later. To support this

hypothesis, it will be important to examine when the loss of chamber myocardium patterning occurs in *Nrg1*^{flox};*Cdh5*^{Cre} mutants, to establish if patterning really depends on myocardial NRG1 signalling.

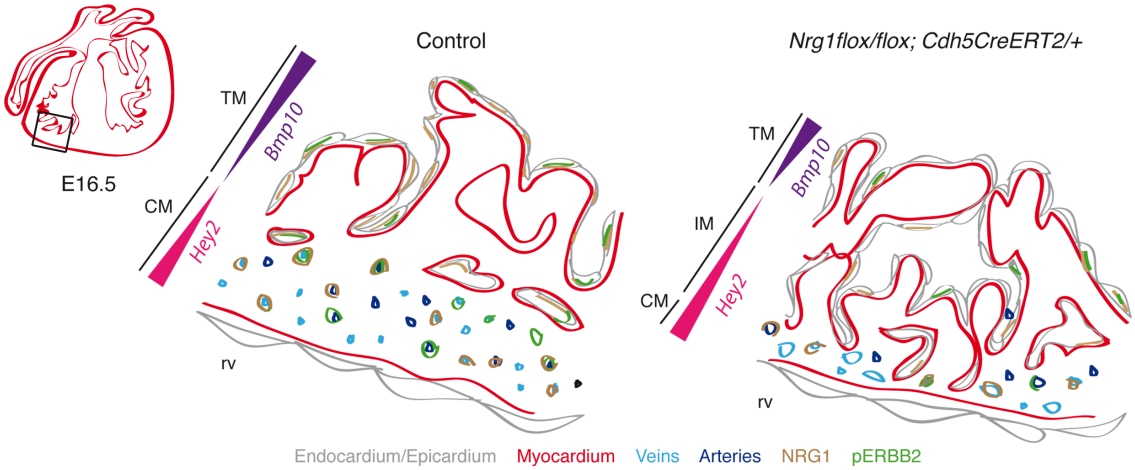

Figure 33. NRG1 is involved in myocardium structure and patterning, and vessel development

In E16.5 control heart, NRG1 (brown) is expressed in the endocardium (grey) and in the coronary endothelium (veins-light blue and arteries-dark blue) where ERBB2 receptor (green) is activated. The ventricle is formed by compact myocardium (CM) that expresses *Hey2* and trabecular myocardium (TM) with *Bmp10* expression. In *Nrg1*^{flox};*Cdh5*^{Cre} heart, NRG1 (brown) deletion form the endothelium (endocardium-grey, coronary veins-light blue and coronary arteries-dark blue) induces reduced phosphorylation of ERBB2 (green) in the endocardium (grey) and in the endothelium of coronary arteries (dark blue) and veins (light blue). This produces a thinner CM and 3 differentiated regions in the ventricular wall: CM and Intermediate myocardium (IM) that show *Hey2* expression, and TM with *Bmp10* expression.

While the ventricular wall is growing and trabeculae mature, more active metabolism is necessary for cardiomyocyte oxygenation and function, thus shifting from glycolysis to respiration. The compact myocardium is characterized by its glycolytic metabolism induced by HIF1α, compared to the mitochondrial switch that occurs in the trabecular region (Menendez-Montes *et al.*, 2016). In agreement with these findings, we observed that in E16.5 *Nrg1*^{flox};*Cdh5*^{Cre} mutant hearts, expression of the glycolytic markers GLUT1 and *Pdk1* was expanded to the trabecular region, suggesting altered cardiomyocyte metabolism, with extended glycolysis to the trabeculae of *Nrg1*^{flox};*Cdh5*^{Cre} mutants. Interestingly, it has been described a crosstalk between the NRG1-ERBB2,4 pathway and metabolism. Thus, in isolated cardiomyocytes, inhibition of glycolysis or mitochondrial respiration causes heat shock protein 90 to rapidly dissociate from ERBB2 (Peng *et al.*, 2005). This, in turn, leads to degradation of ERBB2 and reduced NRG1 activation of

extracellular signal-regulated kinase and AKT signalling. These findings indicate that a crosstalk between NRG1-ERBB2,4 signalling and cardiac metabolism is crucial for adult heart function. *Nrg1^{flox};Cdh5^{Cre}* mutant hearts show strong *Vegfa* upregulation in trabecular myocardium, suggesting that cardiomyocytes are hypoxic, probably due to their defective coronary vessel formation, with impaired arterial and venous development and vascular malformations. Not only vein morphology and identity, with loss of *Couf-TF2* expression, was altered in *Nrg1^{flox};Cdh5^{Cre}* mutants, but also arterial identity, as suggested by the downregulation of *Dll4* (Duarte *et al.*, 2004) and *Cx40* (Van Kempen and Jongsma, 1999). These results indicate that NRG1-ERBB2,4 signalling is implicated in coronary vessels development, and suggest that the defective compaction and thin ventricular walls observed in *Nrg1^{flox};Cdh5^{Cre}* mutants results from the combined effect of endothelial *Nrg1* deletion on chamber cardiomyocyte differentiation and patterning, and in the impaired development of the coronary vessels that should support and nourish the growing ventricular wall. Compaction phenotypes associated to abnormal coronaries development have been previously reported (D'Amato *et al.*, 2016a; Rhee *et al.*, 2018).

We thus can suggest that NRG1-ERBB2,4 signalling during compaction regulates myocardial patterning and metabolism, compact myocardium thickness, and coronary vessel morphology and identity (Figure 33).

On this study we have contributed to understanding the function of NRG1 in heart development, identifying its role in the regulation of cardiomyocyte polarity and oriented cell division during trabeculation. Additionally, we have shown that NRG1 is involved in AVC cushion development and that NRG1-overexpressing transgenic mice cause embryonic lethality associated to severely dysmorphic valves. At later developmental stages, NRG1-ERBB2,4 signalling is required for compaction, regulating cardiomyocyte patterning and metabolism, and coronary vessel development. Overall, these results would allow us to better understand heart development and the possible causes of heart diseases during adulthood after gene regulatory network alteration.

CONCLUSIONS/CONCLUSIONES

1) *Tie2*^{Cre}-mediated NRG1-ERBB2,4 signalling inactivation disrupts trabeculation, induces thickened compact myocardium, and causes embryonic death at E11.5.

2) NRG1-ERBB2,4 signalling is necessary for maintenance of apico-basal cardiomyocyte polarity.

3) NRG1-ERBB2,4 signalling is required for oriented cell division (OCD) of cardiomyocytes during trabeculation.

4) Altered OCD of cardiomyocytes disrupts maintenance of chamber myocardium patterning and growth, but not early endocardial or myocardial differentiation.

5) Early endothelial NRG1 inactivation affects N1ICD signalling and ECM secretion in both chamber and valve tissues.

6) *Cdh5*^{CreERT2}-mediated NRG1-ERBB2,4 signalling inactivation affects compaction and chamber myocardium patterning, leading to early perinatal lethality.

7) Defective compaction is accompanied by defective coronary vasculature development, reduced expression of artery and vein differentiation markers, and vascular malformations.

8) *Cdh5*^{CreERT2}-mediated NRG1-ERBB2,4 signalling inactivation disrupts metabolic progression in the myocardium.

9) *Tie2*^{Cre}-mediated endothelial NRG1 overexpression disrupts endocardial cushion development, and leads to lethality at E14.5.

10) Nkx2.5^{Cre}-mediated endothelial NRG1 overexpression and myocardial ectopic expression disrupts endocardial cushion development, produces VSD, alters ventricular chambers morphology, and leads to embryonic lethality at E16.5.

1) La inactivación de la señalización NRG1-ERBB2,4 mediada por *Tie2*^{Cre} interrumpe la trabeculación, induce un incremento en el grosor del miocardio compacto y causa letalidad embrionaria a E11.5.

2) La señalización NRG1-ERBB2,4 es necesaria para mantener la polaridad ápico-basal de los cardiomiocitos.

3) La señalización NRG1-ERBB2,4 se requiere para la orientación de la división celular de los cardiomiocitos durante la trabeculación.

4) La alteración de la orientación de la división de los cardiomiocitos interrumpe el mantenimiento del patrón y del crecimiento del miocardio de las cámaras, pero no la temprana diferenciación del endocardio o el miocardio.

5) La inactivación temprana de NRG1 en el endotelio afecta a la señalización de N1ICD y a la secreción de matriz extracelular tanto en las cámaras como en el tejido valvular.

6) La inactivación de la señalización NRG1-ERBB2,4 mediada por *Cdh5*^{CreERT2} afecta a la compactación y al patrón del miocardio, induciendo la pronta letalidad perinatal.

7) El defecto en compactación va acompañado de fallos en el desarrollo de la vasculatura coronaria, reducción en la expresión de marcadores de diferenciación arterial y venosa, y malformaciones vasculares.

8) La inactivación de la señalización NRG1-ERBB2,4 mediada por *Cdh5*^{CreERT2} interrumpe la progresión metabólica en el miocardio.

9) La sobreexpresión de NRG1 en el endotelio mediada por *Tie2*^{Cre} afecta al desarrollo de los colchones endocárdicos y produce letalidad embrionaria a E14.5.

10) La sobreexpresión de NRG1 en el endotelio y su expresión ectópica en el miocardio mediada por Nkx2.5^{Cre} afecta al desarrollo de los colchones endocárdicos, produce defectos en el septo interventricular, altera la morfología de las cámaras ventriculares e induce letalidad embrionaria a E16.5.

BIBLIOGRAPHY

Abu-Issa, R. and Kirby, M. L. (2007) 'Heart Field: From Mesoderm to Heart Tube', *Annual Review of Cell and Developmental Biology*, 23(1), pp. 45–68. doi: 10.1146/annurev.cellbio.23.090506.123331.

Aghajanian, H. *et al.* (2016) 'Coronary vasculature patterning requires a novel endothelial ErbB2 holoreceptor', *Nature Communications*. doi: 10.1038/ncomms12038.

Ahmed, N. *et al.* (2005) 'Role of integrin receptors for fibronectin, collagen and laminin in the regulation of ovarian carcinoma functions in response to a matrix microenvironment', *Clinical and Experimental Metastasis*. doi: 10.1007/s10585-005-1262-y.

Aplin, A. E., Howe, A. K. and Juliano, R. L. (1999) 'Cell adhesion molecules, signal transduction and cell growth', *Current Opinion in Cell Biology*. doi: 10.1016/S0955-0674(99)00045-9.

Arnaout, M. A., Mahalingam, B. and Xiong, J.-P. (2005) 'INTEGRIN STRUCTURE, ALLOSTERY, AND BIDIRECTIONAL SIGNALING', *Annual Review of Cell and Developmental Biology*. doi: 10.1146/annurev.cellbio.21.090704.151217.

Bagheri-Yarmand, R. *et al.* (2000) 'Vascular endothelial growth factor up-regulation via p21-activated kinase-1 signaling regulates heregulin-β1-mediated angiogenesis', *Journal of Biological Chemistry*. doi: 10.1074/jbc.M006150200.

Behar, O. *et al.* (1996) 'Semaphorin III is needed for normal patterning and growth of nerves, bones and heart', *Nature*. doi: 10.1038/383525a0.

Caldas, H. *et al.* (2005) 'Survivin splice variants regulate the balance between proliferation and cell death', *Oncogene*, 24(12), pp. 1994–2007. doi: 10.1038/sj.onc.1208350.

Camenisch, T. D. *et al.* (2000) 'Disruption of hyaluronan synthase-2 abrogates normal cardiac morphogenesis and hyaluronan-mediated transformation of epithelium to mesenchyme', *Journal of Clinical Investigation*, 106(3), pp. 349–360. doi: 10.1172/JCI10272.

Camenisch, T. D. *et al.* (2002) 'Heart-valve mesenchyme formation is dependent on hyaluronan-augmented activation of ErbB2-ErbB3 receptors', *Nature Medicine*, 8(8), pp. 850–855. doi: 10.1038/nm742.

Chen, H. (2004) 'BMP10 is essential for maintaining cardiac growth during murine cardiogenesis', *Development*, 131(9), pp. 2219–2231. doi: 10.1242/dev.01094.

Chen, M. S. *et al.* (1994) 'Expression of multiple neuregulin transcripts in postnatal rat brains', *Journal of Comparative Neurology*. doi: 10.1002/cne.903490306.

Cheret, C. *et al.* (2013) 'Bace1 and Neuregulin-1 cooperate to control formation and maintenance of muscle spindles', *EMBO Journal*. doi: 10.1038/emboj.2013.146.

Cherian, A. V. *et al.* (2016) 'N-cadherin relocalization during cardiac trabeculation', *Proceedings of the National Academy of Sciences*, 113(27), pp. 7569–7574. doi: 10.1073/pnas.1606385113.

Chiosis, G. *et al.* (2001) 'A small molecule designed to bind to the adenine nucleotide pocket of Hsp90 causes Her2 degradation and the growth arrest and differentiation of breast cancer cells', *Chemistry and Biology*. doi: 10.1016/S1074-5521(01)00015-1.

Christoffels, V. M. and Moorman, A. F. M. (2009) 'Development of the cardiac conduction system why are some regions of the heart more arrhythmogenic than others?', *Circulation: Arrhythmia and Electrophysiology*, 2(2), pp. 195–207. doi: 10.1161/CIRCEP.108.829341.

Cote, G. M. *et al.* (2005) 'Neuregulin-1α and β isoform expression in cardiac microvascular endothelial cells and function in cardiac myocytes in vitro', *Experimental Cell Research*. doi: 10.1016/j.yexcr.2005.08.017.

Crone, S. A. *et al.* (2002) 'ErbB2 is essential in the prevention of dilated cardiomyopathy', *Nature Medicine*, 8(5), pp. 459–465. doi: 10.1038/nm0502-459.

D'Amato, G. *et al.* (2016) 'Sequential Notch activation regulates ventricular chamber development', *Nature Cell Biology*, 18(1), pp. 7–20. doi: 10.1038/ncb3280.

D'Uva, G. *et al.* (2015) 'ERBB2 triggers mammalian heart regeneration by promoting cardiomyocyte dedifferentiation and proliferation', *Nature Cell Biology*, 17(5), pp. 627–638. doi: 10.1038/ncb3149.

Day, A. J. and Prestwich, G. D. (2002) 'Hyaluronan-binding proteins: Tying up the giant', *Journal of Biological Chemistry*, 277(7), pp. 4585–4588. doi: 10.1074/jbc.R100036200.

Doe, C. Q. and Siller, K. H. (2009) 'Spindle orientation during asymmetric cell division', *Nature cell biology*, 11(4), pp. 365–374. Available at: http://www.nature.com/ncb/journal/v11/n4/abs/ncb0409-365.html.

Duarte, A. *et al.* (2004) 'Dosage-sensitive requirement for mouse Dll4 in artery development', *Genes and Development*, 18(20), pp. 2474–2478. doi: 10.1101/gad.1239004.

Dyer, L. A. and Kirby, M. L. (2009) 'The role of secondary heart field in cardiac development', *Developmental Biology*. Elsevier Inc., 336(2), pp. 137–144. doi: 10.1016/j.ydbio.2009.10.009.

Eckert, J. M. *et al.* (2009) 'Neuregulin-1β and neuregulin-1α differentially affect the migration and invasion of malignant peripheral nerve sheath tumor cells', *GLIA*. doi: 10.1002/glia.20866.

Erickson, S. L. *et al.* (1997) 'ErbB3 is required for normal cerebellar and cardiac development: a comparison with ErbB2-and heregulin-deficient mice.', *Development (Cambridge, England)*, 124, pp. 4999–5011. doi: 10.1002/cne.902310103.

Evans, S. M. *et al.* (2010) 'Myocardial lineage development', *Circulation Research*, 107(12), pp. 1428–1444. doi: 10.1161/CIRCRESAHA.110.227405.

Falls, D. L. (2003) 'Neuregulins: Functions, forms, and signaling strategies', *The EGF Receptor Family: Biologic Mechanisms and Role in Cancer*, 284, pp. 15–31. doi: 10.1016/B978-012160281-9/50003-7.

Fleck, D. *et al.* (2013) 'Dual Cleavage of Neuregulin 1 Type III by BACE1 and ADAM17 Liberates Its EGF-Like Domain and Allows Paracrine Signaling', *Journal of Neuroscience*, 33(18), pp. 7856–7869. doi: 10.1016/j.ajodo.2015.01.022.

Franke, B., Neale, B. M. and Faraone, S. V. (2009) 'Genome-wide association studies in ADHD', *Human Genetics*, 126(1), pp. 13–50. doi: 10.1007/s00439-009-0663-4.

Garcia-Rivello, H. (2005) 'Dilated cardiomyopathy in Erb-b4-deficient ventricular muscle', *AJP: Heart and Circulatory Physiology*. doi: 10.1152/ajpheart.00048.2005.

Le Garrec, J.-F. *et al.* (2013) 'Quantitative analysis of polarity in 3D reveals local cell coordination in the embryonic mouse heart', *Development*, 140(2), pp. 395–404. doi: 10.1242/dev.087940.

Gassmann, M. *et al.* (1995) 'Aberrant neural and cardiac development in mice lacking the ErbB4 neuregulin receptor', *Nature*, 378(6555), pp. 390–394. doi: 10.1038/378390a0.

von Gise, A. (2013) 'Endocardial and epicardial epithelial to mesenchymal transitions in heart development and disease', *Circulation research*, 110(12), pp. 1628–1645. doi: 10.1161/CIRCRESAHA.111.259960.Endocardial.

Grego-Bessa, J. *et al.* (2007) 'Notch Signaling Is Essential for Ventricular Chamber Development', *Developmental Cell*, 12(3), pp. 415–429. doi: 10.1016/j.devcel.2006.12.011.

Grieskamp, T. *et al.* (2011) 'Notch signaling regulates smooth muscle differentiation of epicardium-derived cells', *Circulation Research*, 108(7), pp. 813–823. doi: 10.1161/CIRCRESAHA.110.228809.

Heineke, J. and Molkentin, J. D. (2006) 'Regulation of cardiac hypertrophy by intracellular signalling pathways', *Nature Reviews Molecular Cell Biology*. doi: 10.1038/nrm1983.

Henderson, D. J. and Chaudhry, B. (2011) 'Getting to the heart of planar cell polarity signaling', *Birth Defects Research Part A - Clinical and Molecular Teratology*, 91(6), pp. 460–467. doi: 10.1002/bdra.20792.

Hertig, C. M. *et al.* (1999) 'Synergistic roles of neuregulin-1 and insulin-like growth factor-I in activation of the phosphatidylinositol 3-kinase pathway and cardiac chamber morphogenesis', *Journal of Biological Chemistry*, 274(52), pp. 37362–37369. doi: 10.1074/jbc.274.52.37362.

Holmes, W. E. *et al.* (1992) 'Identification of heregulin, a specific activator of p185erbB2', *Science*. doi: 10.1126/science.256.5060.1205.

Horan, T. *et al.* (1995) 'Binding of neu differentiation factor with the extracellular domain of Her2 and Her3', *Journal of Biological Chemistry*, 270(41), pp. 24604–24608. doi: 10.1074/jbc.270.41.24604.

Hua, Y. *et al.* (2011) 'Planar Cell Polarity Signaling Pathway in Congenital Heart Diseases', *Journal of Biomedicine and Biotechnology*, 2011, pp. 1–8. doi: 10.1155/2011/589414.

Iwamoto, R. and Mekada, E. (2006) 'ErbB and HB-EGF Signaling in Heart Development and Function', *Cell Structure and Function*, 31(1), pp. 1–14. doi: 10.1247/csf.31.1.

Jiménez-Amilburu, V. *et al.* (2016) 'In Vivo Visualization of Cardiomyocyte Apicobasal Polarity Reveals Epithelial to Mesenchymal-like Transition during Cardiac Trabeculation', *Cell Reports*, 17(10), pp. 2687–2699. doi: 10.1016/j.celrep.2016.11.023.

Jiménez-Amilburu, V. and Stainier, D. Y. R. (2019) 'The transmembrane protein Crb2a regulates cardiomyocyte apicobasal polarity and adhesion in zebrafish', *bioRxiv*, 49(0). doi: 10.1242/dev.171207.

Kanzler, B. *et al.* (1998) 'Hoxa-2 restricts the chondrogenic domain and inhibits bone formation during development of the branchial area.', *Development*, 125(14), pp. 2587–97. doi: 10.1002/0471142727.mb1709s32.

Kemi, O. J. *et al.* (2008) 'Activation or inactivation of cardiac Akt/mTOR signaling diverges physiological from pathological hypertrophy', *Journal of Cellular Physiology*. doi: 10.1002/jcp.21197.

Van Kempen, M. J. A. and Jongsma, H. J. (1999) 'Distribution of connexin37, connexin40 and connexin43 in the aorta and coronary artery of several mammals', *Histochemistry and Cell Biology*. doi: 10.1007/s004180050432.

Kim, K. H. *et al.* (2012) 'Iroquois homeodomain transcription factors in heart development and function', *Circulation Research*, 110(11), pp. 1513–1524. doi: 10.1161/CIRCRESAHA.112.265041.

Kisanuki, Y. Y. *et al.* (2001) 'Tie2-Cre transgenic mice: A new model for endothelial cell-lineage analysis in vivo', *Developmental Biology*. doi: 10.1006/dbio.2000.0106.

Klotz, L. *et al.* (2015) 'Cardiac lymphatics are heterogeneous in origin and respond to injury', *Nature*. doi: 10.1038/nature14483.

Koibuchi, N. and Chin, M. T. (2007) 'CHF1/Hey2 plays a pivotal role in left ventricular maturation through suppression of ectopic atrial gene expression', *Circulation Research*. doi: 10.1161/01.RES.0000261693.13269.bf.

Kuramochi, Y., Guo, X. and Sawyer, D. B. (2006) 'Neuregulin activates erbB2-dependent src/FAK

signaling and cytoskeletal remodeling in isolated adult rat cardiac myocytes', *Journal of Molecular and Cellular Cardiology*, 41(2), pp. 228–235. doi: 10.1016/j.yjmcc.2006.04.007.

de la Pompa, J. L. *et al.* (1997) 'Conservation of the Notch signalling pathway in mammalian neurogenesis.', *Development (Cambridge, England)*, 124(6), pp. 1139–48. doi: 10.1049/ip-vis:20041256.

De La Pompa, J. L. *et al.* (1998) 'Role of the NF-ATc transcription factor in morphogenesis of cardiac valves and septum', *Nature*. doi: 10.1038/32419.

Lai, D. *et al.* (2010) 'Neuregulin 1 sustains the gene regulatory network in both trabecular and nontrabecular myocardium', *Circulation Research*, 107(6), pp. 715–727. doi: 10.1161/CIRCRESAHA.110.218693.

Laitinen, L. (1987) 'Griffonia simplicifolia lectins bind specifically to endothelial cells and some epithelial cells in mouse tissues', *The Histochemical Journal*. doi: 10.1007/BF01680633.

Lee, K.-F. *et al.* (1995) 'Requirement for neuregulin receptor erbB2 in neural and cardiac development', *Nature*, 378(6555), pp. 394–398. doi: 10.1038/378394a0.

Lemmens, K. *et al.* (2006) 'Role of neuregulin-1/ErbB2 signaling in endothelium-cardiomyocyte cross-talk', *Journal of Biological Chemistry*, 281(28), pp. 19469–19477. doi: 10.1074/jbc.M600399200.

Lescroart, F. *et al.* (2018) 'Defining the earliest step of cardiovascular lineage segregation by single-cell RNA-seq', *Science*, 359(6380), pp. 1177–1181. doi: 10.1126/science.aao4174.

Leslie, L. K. *et al.* (2012) 'Endocardial Cells Form the Coronary Arteries by Angiogenesis through Myocardial-Endocardial VEGF Signaling', *Cell*, 151(21), pp. 1083–1096. doi: 10.1161/CIRCULATIONAHA.111.087940.The.

Li, B. and Dewey, C. N. (2011) 'RSEM: Accurate transcript quantification from RNA-Seq data with or without a reference genome', *BMC Bioinformatics*, 12. doi: 10.1186/1471-2105-12-323.

Li, G. *et al.* (2016) 'Transcriptomic Profiling Maps Anatomically Patterned Subpopulations among Single Embryonic Cardiac Cells', *Developmental Cell*. Elsevier Inc., 39(4), pp. 491–507. doi: 10.1016/j.devcel.2016.10.014.

Li, J. *et al.* (2016) 'Single-Cell Lineage Tracing Reveals that Oriented Cell Division Contributes to Trabecular Morphogenesis and Regional Specification', *Cell Reports*. The Authors, 15(1), pp. 158–170. doi: 10.1016/j.celrep.2016.03.012.

Li, X. *et al.* (2001) 'Akt/PKB regulates laminin and collagen IV isotypes of the basement membrane', *Proceedings of the National Academy of Sciences*, 98(25), pp. 14416–14421. doi: 10.1073/pnas.251547198.

Liu, J. *et al.* (2010) 'A dual role for ErbB2 signaling in cardiac trabeculation', *Development*, 137(22), pp. 3867–3875. doi: 10.1242/dev.053736.

Liu, J. *et al.* (2016) 'CREG1 Interacts with Sec8 to Promote Cardiomyogenic Differentiation and Cell-Cell Adhesion', *Stem Cells*. doi: 10.1002/stem.2434.

Luna-zurita, L. *et al.* (2010) 'Integration of a Notch-dependent mesenchymal gene program and Bmp2-driven cell invasiveness regulates murine cardiac valve formation Find the latest version : Integration of a Notch-dependent mesenchymal gene program and Bmp2-driven cell invasiveness regu'. doi: 10.1172/JCI42666.transformation.

Luo, Y. and Radice, G. L. (2005) 'N-cadherin acts upstream of VE-cadherin in controlling vascular morphogenesis', *Journal of Cell Biology*, 169(1), pp. 29–34. doi: 10.1083/jcb.200411127.

Luxán, G. *et al.* (2013) 'Mutations in the NOTCH pathway regulator MIB1 cause left ventricular

noncompaction cardiomyopathy', *Nature Medicine*, 19(2), pp. 193–201. doi: 10.1038/nm.3046.

Luxán, G. *et al.* (2016) 'Endocardial Notch Signaling in Cardiac Development and Disease', *Circulation Research*, 118(1), pp. e1–e18. doi: 10.1161/CIRCRESAHA.115.305350.

Macara, I. G. (2004) 'Par proteins: Partners in polarization', *Current Biology*, 14(4), pp. 160–162. doi: 10.1016/S0960-9822(04)00078-8.

MacGrogan, D. *et al.* (2016) 'Sequential Ligand-Dependent Notch Signaling Activation Regulates Valve Primordium Formation and Morphogenesis', *Circulation Research*, 118(10), pp. 1480–1497. doi: 10.1161/CIRCRESAHA.115.308077.

MacGrogan, D., Münch, J. and de la Pompa, J. L. (2018) 'Notch and interacting signalling pathways in cardiac development, disease, and regeneration', *Nature Reviews Cardiology*. Springer US, 15(11), pp. 685–704. doi: 10.1038/s41569-018-0100-2.

Männer, J. (2009) 'The anatomy of cardiac looping: A step towards the understanding of the morphogenesis of several forms of congenital cardiac malformations', *Clinical Anatomy*, 22(1), pp. 21–35. doi: 10.1002/ca.20652.

Martin, M. (2011) 'Cutadapt removes adapter sequences from high-throughput sequencing reads', *EMBnet.journal*. doi: 10.14806/ej.17.1.200.

Meilhac, S. M. (2003) 'A retrospective clonal analysis of the myocardium reveals two phases of clonal growth in the developing mouse heart', *Development*, 130(16), pp. 3877–3889. doi: 10.1242/dev.00580.

Meilhac, S. M. *et al.* (2004) 'Oriented clonal cell growth in the developing mouse myocardium underlies cardiac morphogenesis', *Journal of Cell Biology*, 164(1), pp. 97–109. doi: 10.1109/ISCAS.2008.4541902.

Menendez-Montes, I. *et al.* (2016) 'Myocardial VHL-HIF Signaling Controls an Embryonic Metabolic Switch Essential for Cardiac Maturation', *Developmental Cell*. doi: 10.1016/j.devcel.2016.11.012.

Meyer, D. *et al.* (1997) 'Isoform-specific expression and function of neuregulin', *Cardiovascular Research*, 3586, pp. 3575–3586.

Meyer, D. and Birchmeier, C. (1995) 'Multiple essential functions of neuregulin in development', *Nature*, 378(6555), pp. 386–390. doi: 10.1038/378386a0.

Miner, J. H. and Yurchenco, P. D. (2004) 'LAMININ FUNCTIONS IN TISSUE MORPHOGENESIS', *Annual Review of Cell and Developmental Biology*. doi: 10.1146/annurev.cellbio.20.010403.094555.

Miquerol, L. *et al.* (2010) 'Biphasic development of the mammalian ventricular conduction system', *Circulation Research*, 107(1), pp. 153–161. doi: 10.1161/CIRCRESAHA.110.218156.

Miquerol, L. *et al.* (2013) 'Resolving cell lineage contributions to the ventricular conduction system with a Cx40-GFP allele: A dual contribution of the first and second heart fields', *Developmental Dynamics*, 242(6), pp. 665–677. doi: 10.1002/dvdy.23964.

del Monte-Nieto, G. *et al.* (2018) 'Control of cardiac jelly dynamics by NOTCH1 and NRG1 defines the building plan for trabeculation', *Nature*, 557(7705), pp. 439–445. doi: 10.1038/s41586-018-0110-6.

Del Monte, G. *et al.* (2011) 'Differential notch signaling in the epicardium is required for cardiac inflow development and coronary vessel morphogenesis', *Circulation Research*, 108(7), pp. 824–836. doi: 10.1161/CIRCRESAHA.110.229062.

Moorman, A. F. M. and Christoffels, V. M. (2003) 'Cardiac Chamber Formation: Development, Genes, and Evolution', *Physiological Reviews*, 83(4), pp. 1223–1267. doi: 10.1152/physrev.00006.2003.

Mukouyama, Y. S. *et al.* (2012) 'Whole-mount confocal microscopy for vascular branching morphogenesis', *Methods in Molecular Biology*. doi: 10.1007/978-1-61779-523-7_7.

Nagy, I. I. *et al.* (2010) 'Wnt-11 signalling controls ventricular myocardium development by patterning N-cadherin and β-catenin expression', *Cardiovascular Research*, 85(1), pp. 100–109. doi: 10.1093/cvr/cvp254.

Odiete, O., Hill, M. F. and Sawyer, D. B. (2012) 'Neuregulin in cardiovascular development and disease.', *Circulation research*. doi: 10.1161/CIRCRESAHA.112.267286.

Ozcelik, C. *et al.* (2002) 'Conditional mutation of the ErbB2 (HER2) receptor in cardiomyocytes leads to dilated cardiomyopathy', *Proceedings of the National Academy of Sciences*, 99(13), pp. 8880–8885. doi: 10.1073/pnas.122249299.

Parodi, E. M. and Kuhn, B. (2014) 'Signalling between microvascular endothelium and cardiomyocytes through neuregulin', *Cardiovascular Research*, 102(2), pp. 194–204. doi: 10.1093/cvr/cvu021.

Passer, D. *et al.* (2016) 'Atypical Protein Kinase C-Dependent Polarized Cell Division Is Required for Myocardial Trabeculation', *Cell Reports*. The Authors, 14(7), pp. 1662–1672. doi: 10.1016/j.celrep.2016.01.030.

Patel, R. and Kos, L. (2005) 'Endothelin-1 and neuregulin-1 convert embryonic cardiomyocytes into cells of the conduction system in the mouse', *Developmental Dynamics*. doi: 10.1002/dvdy.20284.

Peng, X. *et al.* (2005) 'Heat shock protein 90 stabilization of ErbB2 expression is disrupted by ATP depletion in myocytes', *Journal of Biological Chemistry*. doi: 10.1074/jbc.M410838200.

Pentassuglia, L. and Sawyer, D. B. (2009) 'The role of Neuregulin-1β/ErbB signaling in the heart', *Experimental Cell Research*. doi: 10.1016/j.yexcr.2008.08.015.

Pentassuglia, L. and Sawyer, D. B. (2013) 'ErbB/integrin signaling interactions in regulation of myocardial cell-cell and cell-matrix interactions', *Biochimica et Biophysica Acta - Molecular Cell Research*. Elsevier B.V., 1833(4), pp. 909–916. doi: 10.1016/j.bbamcr.2012.12.007.

Peshkovsky, C., Totong, R. and Yelon, D. (2011) 'Dependence of cardiac trabeculation on neuregulin signaling and blood flow in zebrafish', *Developmental Dynamics*, 240(2), pp. 446–456. doi: 10.1002/dvdy.22526.

Phillips, H. M. *et al.* (2013) 'Neural crest cells are required for correct positioning of the developing outflow cushions and pattern the arterial valve leaflets', *Cardiovascular Research*, 99(3), pp. 452–460. doi: 10.1093/cvr/cvt132.

Pimental, D. R. *et al.* (2017) 'NRG-1-induced cardiomyocyte hypertrophy. Role of PI-3-kinase, p70 S6K , and MEK-MAPK-RSK ', *American Journal of Physiology-Heart and Circulatory Physiology*, 277(5), pp. H2026–H2037. doi: 10.1152/ajpheart.1999.277.5.h2026.

Plutoni, C. *et al.* (2016) 'P-cadherin promotes collective cell migration via a Cdc42-mediated increase in mechanical forces', *Journal of Cell Biology*, 212(2), pp. 199–217. doi: 10.1083/jcb.201505105.

Prados, B. *et al.* (2018) 'Myocardial Bmp2 gain causes ectopic EMT and promotes cardiomyocyte proliferation and immaturity article', *Cell Death and Disease*. Springer US, 9(3). doi: 10.1038/s41419-018-0442-z.

Qian, L. *et al.* (2015) 'Cardiac contraction activates endocardial Notch signaling to modulate chamber maturation in zebrafish', *Development*. doi: 10.1242/dev.125724.

Ranger, A. M. *et al.* (1998) 'The transcription factor NF-ATc is essential for cardiac valve formation', *Nature*. doi: 10.1038/32426.

Rasouli, S. J. and Stainier, D. Y. R. (2017) 'Regulation of cardiomyocyte behavior in zebrafish trabeculation by Neuregulin 2a signaling', *Nature Communications*, 8(0), p. 15281. doi: 10.1038/ncomms15281.

Red-Horse, K. *et al.* (2010) 'Coronary arteries form by developmental reprogramming of venous cells', *Nature*. Nature Publishing Group, 464(7288), pp. 549–553. doi: 10.1038/nature08873.

Rentschler, S. *et al.* (2001) 'Visualization and functional characterization of the developing murine cardiac conduction system', *Development*, 128, pp. 1785–1792.

Rentschler, S. *et al.* (2002) 'Neuregulin-1 promotes formation of the murine cardiac conduction system', *Proceedings of the National Academy of Sciences*, 99(16), pp. 10464–10469. doi: 10.1073/pnas.162301699.

Rhee, S. *et al.* (2018) 'Endothelial deletion of Ino80 disrupts coronary angiogenesis and causes congenital heart disease', *Nature Communications*. Springer US, 9(1). doi: 10.1038/s41467-017-02796-3.

Riese, D. J. and Stern, D. F. (1998) 'Specificity within the EGF family/ErbB receptor family signaling network', *BioEssays*, 20(1), pp. 41–48. doi: 10.1002/(SICI)1521-1878(199801)20:1<41::AID-BIES7>3.0.CO;2-V.

Robinson, M. D., McCarthy, D. J. and Smyth, G. K. (2009) 'edgeR: A Bioconductor package for differential expression analysis of digital gene expression data', *Bioinformatics*. doi: 10.1093/bioinformatics/btp616.

Rochais, F., Mesbah, K. and Kelly, R. G. (2009) 'Signaling pathways controlling second heart field development', *Circulation Research*, 104(8), pp. 933–942. doi: 10.1161/CIRCRESAHA.109.194464.

Rohrbach, S. *et al.* (1999) 'Neuregulin in cardiac hypertrophy in rats with aortic stenosis: Differential expression of erbB2 and erbB4 receptors', *Circulation*. doi: 10.1161/01.CIR.100.4.407.

Romond, E. H. *et al.* (2005) 'Trastuzumab plus Adjuvant Chemotherapy for Operable HER2-Positive Breast Cancer', *New England Journal of Medicine*. doi: 10.1056/NEJMoa052122.

Saavedra, P. *et al.* (2015) 'Interaction of FABP4 with plasma membrane proteins of endothelial cells', *Clinica e Investigacion en Arteriosclerosis*. doi: 10.1016/j.arteri.2014.05.003.

Saga, Y. *et al.* (1996) 'MesP1: a novel basic helix-loop-helix protein expressed in the nascent mesodermal cells during mouse gastrulation.', *Development*, 122(9), pp. 2769–2778. doi: 10.1016/0169-328x(95)00282-w.

Saga, Y. *et al.* (1999) 'MesP1 is expressed in the heart precursor cells and required for the formation of a single heart tube.', *Development (Cambridge, England)*.

Sanchez-Soria, P. and Camenisch, T. D. (2010) 'ErbB signaling in cardiac development and disease', *Seminars in Cell and Developmental Biology*. doi: 10.1016/j.semcdb.2010.09.011.

Sedmera, D. *et al.* (1997) 'Developmental changes in the myocardial architecture of the chick', *Anatomical Record*, 248(3), pp. 421–432. doi: 10.1002/(SICI)1097-0185(199707)248:3<421::AID-AR15>3.0.CO;2-R.

Sedmera, D. *et al.* (2000) 'Developmental patterning of the myocardium', *Anatomical Record*, 258(4), pp. 319–337. doi: 10.1002/(SICI)1097-0185(20000401)258:4<319::AID-AR1>3.0.CO;2-O.

Sedmera, D. and Thompson, R. P. (2011) 'Myocyte proliferation in the developing heart', *Developmental Dynamics*, 240(6), pp. 1322–1334. doi: 10.1002/dvdy.22650.

Shirai, M. *et al.* (2009) 'T-box 2, a mediator of Bmp-Smad signaling, induced hyaluronan synthase 2 and

Tgf 2 expression and endocardial cushion formation', *Proceedings of the National Academy of Sciences*, 106(44), pp. 18604–18609. doi: 10.1073/pnas.0900635106.

Soriano, P. (1999) 'Generalized lacZ expression with the ROSA26 Cre reporter strain', *Nature Genetics*. Nature America Inc., 21, p. 70. Available at: https://doi.org/10.1038/5007.

Soung, Y. H., Clifford, J. L. and Chung, J. (2010) 'Crosstalk between integrin and receptor tyrosine kinase signaling in breast carcinoma progression', *BMB Reports*, 43(5), pp. 311–318. doi: 10.5483/BMBRep.2010.43.5.311.

Stankunas, K. *et al.* (2008) 'Endocardial Brg1 Represses ADAMTS1 to Maintain the Microenvironment for Myocardial Morphogenesis', *Developmental Cell*. doi: 10.1016/j.devcel.2007.11.018.

Stanley, E. G. *et al.* (2002) 'Efficient cre-mediated deletion in cardiac progenitor cells conferred by a 3′UTR-ires-Cre allele of the homeobox gene Nkx2-5', *International Journal of Developmental Biology*, 46(4 SPEC.), pp. 431–439. doi: 10.1387/IJDB.12141429.

Staudt, D. W. *et al.* (2014) 'High-resolution imaging of cardiomyocyte behavior reveals two distinct steps in ventricular trabeculation', *Development*, 141(3), pp. 585–593. doi: 10.1242/dev.098632.

Stepniak, E., Radice, G. L. and Valeri, V. (1971) 'Adhesive and signalling functions of cadherins in vertabrate development', *Cold harbor perspectives*, 31(5), pp. 515–527. doi: 10.1101/cshperspect.a002949.

Strong Russell, K. *et al.* (1999) 'Neuregulin activation of ErbB receptors in vascular endothelium leads to angiogenesis', *Am J Physiol*.

Taylor, P. *et al.* (2003) 'The Cardiac Valve Interstitial Cell', *International Journal of Biochem Cell Biol*, 35, pp. 113–118.

Tian, X. *et al.* (2013) 'Subepicardial endothelial cells invade the embryonic ventricle wall to form coronary arteries', *Cell Research*. Nature Publishing Group, 23(9), pp. 1075–1090. doi: 10.1038/cr.2013.83.

Tian, X. *et al.* (2014) 'De novo formation of a distinct coronary vascular population in neonatal heart', *Science*, 345(6192), pp. 90–94. doi: 10.1126/science.1251487.

Timmerman, L. A. *et al.* (2008) 'Notch promotes epithelial-mesenchymal transition during cardiac development and oncogenic transformation', *Genes & Development*, 5(C), pp. 99–115. doi: 10.1101/gad.276304.trol.

Tomanek, R. J. *et al.* (1999) 'Vascular endothelial growth factor expression coincides with coronary vasculogenesis and angiogenesis', *Developmental Dynamics*, 215(1), pp. 54–61. doi: 10.1002/(SICI)1097-0177(199905)215:1<54::AID-DVDY6>3.0.CO;2-0.

Ueyama, T. *et al.* (2000) 'Requirement of activation of the extracellular signal-regulated kinase cascade in myocardial cell hypertrophy', *Journal of Molecular and Cellular Cardiology*. doi: 10.1006/jmcc.2000.1135.

Uren, A. G. *et al.* (2000) 'Survivin and the inner centromere protein INCENP show similar cell-cycle localization and gene knockout phenotype', *Current Biology*, 10(21), pp. 1319–1328. doi: 10.1016/S0960-9822(00)00769-7.

Uribe, V. *et al.* (2018) '*In vivo* analysis of cardiomyocyte proliferation during trabeculation', *Development*, 145(14), p. dev164194. doi: 10.1242/dev.164194.

VanDusen, N. J. *et al.* (2014) 'Hand2 Is an Essential Regulator for Two Notch-Dependent Functions within the Embryonic Endocardium', *Cell Reports*, 9(6), pp. 2071–2083. doi: 10.1016/j.celrep.2014.11.021.

Verzi, M. P. *et al.* (2005) 'The right ventricle, outflow tract, and ventricular septum comprise a restricted

expression domain within the secondary/anterior heart field', *Developmental Biology*, 287(1), pp. 134–145. doi: 10.1016/j.ydbio.2005.08.041.

Vintersten, K., Testa, G. and Stewart, A. F. (2004) 'Microinjection of BAC DNA into the pronuclei of fertilized mouse oocytes.', *Methods Mol Biol*, 256, pp. 141–158. doi: 10.1385/1-59259-753-X:141.

Wadugu, B. and Kuhn, B. (2012) 'The role of neuregulin/ErbB2/ErbB4 signaling in the heart with special focus on effects on cardiomyocyte proliferation', *AJP: Heart and Circulatory Physiology*, 302(11), pp. H2139–H2147. doi: 10.1152/ajpheart.00063.2012.

Waller-Evans, H. *et al.* (2010) 'The orphan adhesion-GPCR GPR126 is required for embryonic development in the mouse', *PLoS ONE*. doi: 10.1371/journal.pone.0014047.

Walter, W., Sánchez-Cabo, F. and Ricote, M. (2015) 'GOplot: An R package for visually combining expression data with functional analysis', *Bioinformatics*. doi: 10.1093/bioinformatics/btv300.

Wang, Y. (2007) 'Mitogen-activated protein kinases in heart development and diseases', *Circulation*. doi: 10.1161/CIRCULATIONAHA.106.679589.

Wang, Y. *et al.* (2010) 'Ephrin-B2 controls VEGF-induced angiogenesis and lymphangiogenesis', *Nature*, 465(7297), pp. 483–486. doi: 10.1038/nature09002.

Watts, J. L. *et al.* (1996) 'par-6, a gene involved in the establishment of asymmetry in early C. elegans embryos, mediates the asymmetric localization of PAR-3.', *Development (Cambridge, England)*, 122, pp. 3133–3140.

Weigel, P. H., Hascall, V. C. and Tammi, M. (1997) 'Hyaluronan synthases', *Journal of Biological Chemistry*, 272(22), pp. 13997–14000. doi: 10.1074/jbc.272.22.13997.

Wu, B. *et al.* (2012) 'Endocardial cells form the coronary arteries by angiogenesis through myocardial-endocardial VEGF signaling', *Cell*. Elsevier Inc., 151(5), pp. 1083–1096. doi: 10.1016/j.cell.2012.10.023.

Wu, S. *et al.* (2013) 'Atrial Identity Is Determined by a COUP-TFII Regulatory Network', *Developmental Cell*. Elsevier Inc., 25(4), pp. 417–426. doi: 10.1016/j.devcel.2013.04.017.

Wu, S. P. *et al.* (2013) 'Tbx18 regulates development of the epicardium and coronary vessels', *Developmental Biology*. doi: 10.1016/j.ydbio.2013.08.019.

Zaffran, S. *et al.* (2004) 'Right ventricular myocardium derives from the anterior heart field', *Circulation Research*, 95(3), pp. 261–268. doi: 10.1161/01.RES.0000136815.73623.BE.

Zhang, H. *et al.* (2016) 'Genetic lineage tracing identifies endocardial origin of liver vasculature', *Nature Genetics*, 48(5), pp. 537–543. doi: 10.1038/ng.3536.

Zhou, B. *et al.* (2010) 'Genetic fate mapping demonstrates contribution of epicardium-derived cells to the annulus fibrosis of the mammalian heart', *Developmental Biology*. doi: 10.1016/j.ydbio.2009.12.007.

APPENDIX

Table legends

Red embryonic stages indicate embryonic lethality, the mutant or transgenic NRG1 embryos at these stages which were found necrotic are indicated in brackets.

Table 4. Lethality phase *Nrg1^{flox},Tie2^{Cre}* embryos

Embryonic Stage	Genotype				Extra information		
	Nrg1$^{flox/+}$; +/+	Nrg1$^{flox/flox}$; +/+	Nrg1$^{flox/+}$; Tie2$^{Cre/+}$	Nrg1$^{flox/flox}$; Tie2$^{Cre/+}$	Nº of pups	Resorptions	Nº of litters
E8.5	141	139	136	161	577	14	84
%E8.5	24.44	24.09	23.57	27.9			
E9.5	288	189	165	263	905	59	170
%E9.5	31.82	20.88	18.23	29.06			
E10.5	193	182	153	171	699	19	99
%E10.5	27.61	26.04	21.89	24.46			
E11.5	8	12	10	12 (n=7)	42	4	7
%E11.5	19.05	28.57	23.81	28.57			

Table 5. Lethality phase *Nrg1^{flox},Mesp1^{Cre}* embryos

. Embryonic Stage	Genotype				Extra information		
	Nrg1$^{flox/+}$; +/+	Nrg1$^{flox/flox}$; +/+	Nrg1$^{flox/+}$; Mesp1$^{Cre/+}$	Nrg1$^{flox/flox}$; Mesp1$^{Cre/+}$	Nº of pups	Resorptions	Nº of litters
E8.5	1	2	3	1	7	1	1
%E8.5	14.29	28.57	42.86	14.29			
E9.5	3	6	8	3	20	0	3
%E9.5	15	30	40	15			
E10.5	8	7	10	7	32	5	4
%E10.5	25	21.88	31.25	21.88			
E12.5	9	6	6	5 (n=3)	26	0	3
%E12.5	34.62	23.08	23.08	3.85			

Table 6. Lethality phase *Nrg1^{flox},Cdh5^{Cre}* embryos

Embryonic Stage	Genotype				Extra information		
	Nrg1$^{flox/+}$; +/+	Nrg1$^{flox/flox}$; +/+	Nrg1$^{flox/+}$; Cdh5Cre$^{ERT2/+}$	Nrg1$^{flox/flox}$; Cdh5Cre$^{ERT2/+}$	Nº of pups	Resorptions	Nº of litters
E13.5	4	8	2	5	19	4	4
%E13.5	21.05	42.11	10.53	26.32			
E15.5	34	33	18	31	116	8	18
%E15.5	29.31	28.45	15.52	26.72			
E16.5	40	42	37	32	136	10	23
%E16.5	29.41	30.88	27.21	23.53			
E17.5	3	5	3	4	15	0	2
%E17.5	20	33.33	20	26.67			
E18.5	5	4	3	3	15	6	3
%E18.5	33.33	26.67	20	20			

Table 7. Lethality phase *R26Nrg1GFP,Tie2^{Cre}* embryos

Embryonic Stage	Genotype		Extra information	
	+/+; Tie2$^{Cre/+}$	R26Nrg1-iresGFP/+; Tie2$^{Cre/+}$	Nº of pups	Nº of litters
E9.5	4	2	6	1
%E9.5	66.67	33.33		
E10.5	4	4	8	1
%E10.5	50	50		
E12.5	4	4	8	1
%E12.5	50	50		
E14.5	3	5 (n=3)	8	1
%E14.5	37.5	62.5		

Table 8. Lethality phase *R26Nrg1GFP,Nkx2.5^{Cre}* embryos

Embryonic Stage	Genotype +/+; Nkx2.5$^{Cre/+}$	Genotype R26Nrg1-iresGFP/+; Nkx2.5$^{Cre/+}$	Extra information Nº of pups	Extra information Nº of litters
E9.5	17	18	35	3
%E9.5	48.57	51.43		
E10.5	12	17	29	3
%E10.5	41.38	58.62		
E12.5	15	20	35	4
%E12.5	42.86	57.14		
E14.5	4	7	11	2
%E14.5	36.36	63.64		
E16.5	12	16 (n=4)	28	3
%E16.5	42.86	57.14		

Table 9. RNA-seq data from E9.5 control and *Nrg1^{flox},Tie2^{Cre}* hearts.

KOvsWT original) This sheet contains the original data from the analysis. Up-down significantly changed) This sheet shows the genes that are significantly changed in *Nrg1^{flox},Tie2^{Cre}* mutants order from the most upregulated to the more downregulated. Canonical pathways IPA) This sheet contains the information about the canonical pathways and the genes involved extracted from the IPA software. Diseases and Biofunctions IPA) This sheet shows all the diseases and biofunctions related with the significantly changed genes in *Nrg1^{flox},Tie2^{Cre}* mutants. Yellow cassettes indicate the ones represented in the circular plots.

Video legends

Video 1. WM IF at E10.5 of a control heart representing the lv region. The myocardium is stained in red with SMA and the endocardium in white with IB4. The 3D represents a region of the left ventricle of 204µm and the Z-stack is scanned each 2µm.

Video 2. WM IF at E10.5 of *Nrg1$^{flox/flox}$;Tie2$^{Cre/+}$* heart representing the lv region. The myocardium is stained in red with SMA and the endocardium in white with IB4. The 3D represents a region of the left ventricle of 176µm and the Z-stack is scanned each 2µm.

Video 3. SURVIVIN IF in cryosection in E8.5 heart. The myocardium is stained in red with SMA, nuclei in blue with DAPI and SURVIVIN is stained in green to localize the mitotic spindle. The ventricular myocardium shows dividing cardiomyocyte in prophase, anaphase and telophase. 10µm section.

Video 4. SURVIVIN IF in cryosection in E8.5 heart. The myocardium is stained in red with SMA, nuclei in blue with DAPI and SURVIVIN is stained in green to localize the mitotic spindle. The closer view of the ventricular myocardium shows a cardiomyocyte in parallel division in anaphase. 10 μm section.

Video 5. SURVIVIN IF in cryosection in E8.5 heart. The myocardium is stained in red with SMA, nuclei in blue with DAPI and SURVIVIN is stained in green to localize the mitotic spindle. The closer view of the ventricular myocardium shows a cardiomyocyte in parallel division in anaphase. 10 μm section.

Video 6. SURVIVIN IF in cryosection in E8.5 heart. The myocardium is stained in red with SMA, nuclei in blue with DAPI and SURVIVIN is stained in green to localize the mitotic spindle. The closer view of the ventricular myocardium shows a cardiomyocyte in a perpendicular division in anaphase. 10 μm section.

Video 7. SURVIVIN IF in cryosection in E8.5 heart. The myocardium is stained in red with SMA, nuclei in blue with DAPI and SURVIVIN is stained in green to localize the mitotic spindle. The closer view of the ventricular myocardium shows a cardiomyocyte in a parallel division in cytokinesis. 10 μm section.

Video 8. SURVIVIN IF in cryosection in E8.5 heart. The myocardium is stained in red with SMA, nuclei in blue with DAPI and SURVIVIN is stained in green to localize the mitotic spindle. The closer view of the ventricular myocardium shows a cardiomyocyte in oblique division in telophase. 10 μm section.

Video 9. N-CADHERIN IF in paraffin section in E8.5 heart. The cardiomyocyte membrane is stained in red with WGA, nuclei in blue with DAPI and N-CADHERIN in green. N-CADHERIN shows a punctuate signal in the lateral side of cardiomyocytes in the epithelial myocardium. 7 μm section.

Video 10. N-CADHERIN IF in paraffin section in E8.5 heart. The cardiomyocyte membrane is stained in red with WGA, nuclei in blue with DAPI and N-CADHERIN in green. N-CADHERIN is redistributed to the basal side of the cardiomyocyte previous to the trabecular onset. 7 μm section.

Video 11. N-CADHERIN IF in paraffin section in E8.5 heart. The cardiomyocyte membrane is stained in red with WGA, nuclei in blue with DAPI and N-CADHERIN in green. After the first

cardiomyocyte has invaded the lumen after perpendicular division, N-CADHERIN localizes in the lateral and basal side of the cardiomyocyte. 7 μm section.

Video 12. N-CADHERIN IF in paraffin section in E8.5 heart. The cardiomyocyte membrane is stained in red with WGA, nuclei in blue with DAPI and N-CADHERIN in green. When trabecula is growing, N-CADHERIN localizes in the lateral side of these cardiomyocytes. 7 μm section.

Video 13. WM IF at E16.5 of a control heart representing lv magnification. The myocardium is stained in green with MF20, the endocardium in red with CD31 and the nuclei in blue with DAPI. The 3D represents a region of the left ventricle of 100 μm and the Z-stack is scanned each 1 μm.

Video 14. WM IF at E16.5 of a *Nrg1*^{flox}*;Cdh5*^{Cre} heart representing lv magnification. The myocardium is stained in green with MF20, the endocardium in red with CD31 and the nuclei in blue with DAPI. The 3D represents a region of the left ventricle of 50 μm and the Z-stack is scanned each 1 μm.

Video 15. WM control embryo at E10.5. We have focused on the heart region seen in bright field and no endogenous GFP. The consecutive heart sections show the left ventricle with 120 μm thick and the Z-stack is scanned each 10 μm.

Video 16. WM *R26Nrg1-iresGFP;Tie2*^{Cre} embryo at E10.5. We have focused on the heart region seen in bright field and endogenous GFP in the endocardium that represents NRG1 expression. The consecutive heart sections show the left ventricle with 120 μm thick and the Z-stack is scanned each 10 μm.

Video 17. WM control embryo at E10.5. We have focused on the heart region seen in bright field and no endogenous GFP. The consecutive heart sections show the left ventricle with 90 μm thick and the Z-stack is scanned each 10 μm.

Video 18. WM *R26Nrg1-iresGFP;Nkx2.5*^{Cre} embryo at E10.5. We have focused on the heart region seen in bright field and endogenous GFP in endocardium and myocardium that represents NRG1 expression. The consecutive heart sections show the left ventricle with 90 μm thick and the Z-stack is scanned each 10 μm.

The images of videos 1-2 and 15-18 were captured with the Zeiss 780 confocal microscope fitted with a 20X objective with a dipping lens.

The images of videos 3-12 were captured with the Nikon A1R laser scanning confocal microscope with a 60x objective.

The images of videos 13-14 were captured with the Nikon A1R laser scanning confocal microscope with a 20x objective.

Cover page: Whole mount IF in a E10.5 control embryo showing a magnified region of the left ventricle. The myocardium is stained in red with SMA-Cy3 and the endocardium in white with IB4-647, that allow us to differentiate the trabecular network closely enveloped by the endocardial layer. The images are captured as a Z-stack of 204 μm and are represented in a maximum projection.

Back cover: IF in E9.5 control heart in cryosection. SURVIVIN is stained in green to appreciate the mitotic spindle, the myocardium is stained in red with SMA-Cy3, and the nuclei in blue with DAPI. A cardiomyocyte from the compact myocardium is dividing perpendicularly towards the lumen inducing trabecular growth.